

**Development of a detection system towards a
basophil-microarray for the diagnosis of allergies**

Xiaowei Wang, PhD

Thesis submitted to the University of Nottingham
for the degree of Doctor of Philosophy

April 2014

Abstract

Allergic responses are mainly mediated by immunoglobulin E (IgE) and mast cells or basophils expressing the high-affinity IgE receptor FcεRI. Cross-linking of FcεRI and IgE complexes with allergen induces basophil degranulation and release of inflammatory chemical mediators, leading to clinical symptoms. Common allergy diagnostic tests such as ImmunoCAP, focused on the measurement of specific IgE in patients, commonly lead to misdiagnosis. The allergen-specific IgE in patients' sera might not always lead to FcεRI cross-linking on mast cells or basophils, resulting in no related clinical symptoms, as observed in some food allergies.

In order to mimic the allergic response and generate an *in vitro* diagnostic device to address these issues, a basophil-microarray platform that couples the diversity of a protein array with the biological output of basophilic cells is being developed. This platform allows testing of up to five thousand allergens using a drop of patient's blood. In this study, the optimisation steps and preliminary results are presented.

The platform in development relies upon the use of a humanised rat basophilic leukaemia (RBL) cell line RBL-703/21 and different methods to measure the levels of basophil activation. β-hexosaminidase assay showed that the human FcεRI expressing RBL-703/21 cell line was able to bind human IgE in the presence of anti-IgE/allergens and led to degranulation. Fibronectin has shown to greatly avoid cell losses during experiments, calcium ionophore A23187 is an unsuitable positive control due to a fast down regulation of VLA-4 and subsequent detachment of cells. The commercial Ca²⁺ probe (fluo-4, AM) was shown to efficiently measure the intracellular calcium flux upon activation in the micro-well plate, but due to the lack of a detection system, it can not to be used in the microarray. Two reporter plasmids encoding GFP or DsRed with an NFAT promoter region were transfected into RBL-703/21s and optimised. Both reporter systems were able to detect the presence of functional allergen-specific IgE in the sera of patients, and showed the expected bell-shaped dose response curves. Results correlated with those measured by clinical diagnostic methods. The fluorescence system developed using reporter genes does not need further processing, making it an ideal system for the future development of basophil microarray platforms.

Acknowledgements

My deepest gratitude goes first and foremost to Associate Professor Marcos Alcocer, for his constant guidance and support throughout my studies. I would like to express my sincere appreciation to Associate professor Franco H. Falcone, for his patient advice and great help on the experiments and this thesis. Thanks to the colleagues with whom I have worked in the Division of Nutritional Sciences and School of Pharmacy.

Last but not least, I would like to thank my dearest parents and Xibo, for their unconditional love, support and encouragement throughout my life.

List of Publications

Wang X, Cato P, Lin HC, Li T, Wan D, Alcocer MJ, Falcone FH. (2014). Optimisation and Use of Humanised RBL NF-AT-GFP and NF-AT-DsRed Reporter Cell Lines Suitable for High-Throughput Scale Detection of Allergic Sensitisation in Array Format and Identification of the ECM-Integrin Interaction as Critical Factor. Molecular Biotechnology **56** (2): 136-146.

Wulfert F, Sanyasi G, Tongen L, Watanabe LA, Wang X, Renault NK, Falcone FH, Jacob CM, Alcocer MJ (2012). Prediction of tolerance in children with IgE mediated cow's milk allergy by microarray profiling and chemometric approach. Journal of Immunological Methods **382** (1-2): 48-57.

Abbreviations

ACB	allergen challenge buffer
APC	antigen-presenting cell
Bet v 1,2	birch pollen (<i>Betula verrucosa</i>)
BSA	bovine serum albumin
Ca ²⁺	calcium
CaCl ₂	calcium Chloride
CMP	common myeloid progenitors
CO ₂	carbon dioxide
COL	collagen
CRAC	calcium release-activated calcium
DAG	diacylglycerol
<i>D.F.</i>	<i>D. Farinae</i>
DMEM	dulbecco's modified Eagle's medium
D ₂ O	deuterium dioxide
<i>D.P.</i>	<i>D. Pteronyssinus</i>
ECM	extra cellulose matrix
ERK1/ERK2	extracellular-signal-regulated protein kinase
FCS	fetal calf serum
FN	fibronectin
GADS	GRB2-related adaptor protein
GMP	granulocyte-monocyte progenitor
GRB2	growth-factor-receptor-bound protein
HSC	hematopoietic stem cells
LAT	linker for activation of T cells
Ig's	immunoglobulin
IL-	interleukin
Ionophore	calcium ionophore A23187

IP ₃	inositol 1, 4, 5-trisphosphate
ITAM	immunoreceptor tyrosine-based activation motif
JNK	MAPKs JUN amino-terminal kinase
MAPKS	mitogen-activated protein kinases
MEM	minimum essential medium
ml	millilitre
NaCl	sodium chloride
NFAT	nuclear factor of activated T cells
NFκB	nuclear factor-κB
NLS	nuclear-localization signal
Par j 2	<i>Parietaria judaica</i> pollen
PBS	phosphate buffer saline
Phl p 1,2,6	phleum pollen (<i>phleum pratense</i>)
PIP ₂	phosphatidylinositol 4,5-bisphosphate
PKC	protein kinase C
PMA	phorbol myristate acetate
RAST	radioallegosorbent immunoassay test
RBL	rat basophilic leukaemia
S.C.	<i>secale cereale</i>
S.H.	<i>sorghum halepense</i>
SHC	SH2-domain-containing transforming protein C
SLP76	SH2-domain-containing leukocyte protein of 65kDa
SOS	son of sevenless homologue
SPT	skin prick testing
Syk	spleen tyrosine kinase
TCRs	T-cell antigen receptor
µg	microgram
µl	microlitre

Table of Content

1	Introduction	1
1.1	Immune system	1
1.2	Allergic reactions	2
1.3	Signalling transduction pathways	6
1.4	Past and current diagnosis of allergy	10
1.5	Microarray	11
1.6	Basophil microarray	12
1.7	Aims and objectives	14
2	Optimisation of β-hexosaminidase assay	15
2.1	Introduction	15
2.2	Material and Methods.....	16
2.2.1	Cell line and cell culture	16
2.2.2	Methods for β -hexosaminidase assay	18
2.3	Results	19
2.4	Discussion.....	22
2.5	Conclusion	23
3	Optimisation of the cell adhesion assay	24
3.1	Introduction	24
3.2	Methods	25
3.2.1	Fibronectin -Adhesion assay	25
3.2.2	Immunofluorescence flow cytometry	25
3.3	Results	26
3.3.1	Inclusion of fibronectin increases adhesion	26

3.3.2	VLA-4 is strongly down-regulated by A23187 activation	27
3.3.3	Effects of FN, CO and LA on cell attachment after activation	28
3.4	Discussion.....	29
3.5	Conclusion.....	30
4	Monitoring of degranulation via calcium influx measurements	31
4.1	Introduction	31
4.1.1	Fluo-4, AM.....	32
4.1.2	Premo TM Cameleon calcium sensor	32
4.2	Materials and Methods	33
4.2.1	Equipment	33
4.2.2	Method	33
4.3	Results	36
4.3.1	Fluo-4, AM.....	36
4.3.2	Application of fluo-4 to Microarray	41
4.3.3	PremoCameleon calcium sensor	41
4.4	Discussion.....	42
4.5	Conclusion	43
5	pNFAT-GFP&pNFAT-DsRed reporter systems	44
5.1	Introduction	44
5.2	Materials and methods.....	45
5.2.1	Plasmids	45
5.2.2	Plasmid construction.....	46
5.2.3	Transfection.....	49
5.2.4	Initial optimisation tests	50
5.3	Results	51
5.3.1	Plasmid construction.....	51
5.3.2	Transfection.....	52
5.3.3	Initial optimisation tests	54
5.3.4	Time-lapse of activation of pNFAT-DsRed-RBL-703/21 cells	58

5.4 Discussion.....	60
5.5 Conclusion.....	61
6 Real sera test.....	62
6.1 Introduction	62
6.2 Materials and methods.....	63
6.2.1 Sera characteristics and allergens	63
6.2.2 Methods.....	64
6.3 Results	65
6.3.1 Initial tests	65
6.3.2 Optimisation tests	71
6.3.3 Contrast test.....	79
6.3.4 Time course during cytotoxicity reduction tests.....	81
6.3.5 Preparation of applying the system onto microarray format	82
6.3.6 Zeiss confocal microscope	84
6.4 Discussion.....	86
7 General discussion	88
8 Conclusion.....	92
References	93
Appendix	101

List of Tables

Table 5-1. TR% of pEGFP-Tub transfected into RBL-2H3 cells at different capacitance. ...	52
Table 5-2. TR% of pEGFP-Tub transfected into RBL-2H3 cells at different voltages.	52
Table 6-1. Clinical database data of sera tested.....	63
Table 6-2. Purified recombinant allergens and sources.	63

List of Figures

Figure 1-1. Degranulation of mast cells or basophils by cross-linking of FcεRI- IgE complex when bound to allergen.	4
Figure 1-2. Structure of an IgE molecule.	7
Figure 1-3. FcεRI-mediated Intracellular signalling transduction pathway in mast cell and basophil activation.	9
Figure 1-4. A timeline diagram displays the development of allergy diagnosis	10
Figure 1-5. Principle of a protein microarray.....	11
Figure 1-6. Schematic diagram of basophil-microarray system.	14
Figure 2-1. Morphology of three RBL-2H3 sub-lines: RBL-703/21 and RBL-SX38.	17
Figure 2-2. Sample layout of β-hexosaminidase assay in a Nunclon 96-well plate.	18
Figure 2-3. Titration of human-IgE for β-hexosaminidase assay	20
Figure 2-4. Titration of anti-human IgE for β-hexosaminidase assay	20
Figure 2-5. Comparison of β-hexosaminidase assay between RBL-703/21 and RBL-SX38 cell lines using optimised reagents.	21
Figure 2-6. Comparison of β-hexosaminidase assay between RBL-703/21 and pNFAT-hrGFP-703/21 cells using optimised reagents.....	21
Figure 3-1. Morphology of RBLs.....	24
Figure 3-2. Attachment of RBL-703/21 cells to FN.....	26
Figure 3-3. Time course of VLA-4 Integrin surface expression on RBL-703/21 cells stimulated with anti-IgE or 1 μg/mL A23187	27
Figure 3-4. Attachment of RBL-703/21 cells to FN, type I CO or LA.....	28
Figure 4-1. Schematic of Premo™ Cameleon Calcium Sensor mechanism.	32
Figure 4-2. Settings overview of FLUOstar microplate reader for measuring Ca ²⁺ influx.	33
Figure 4-3. Schematic diagram of spot-printing on glass slide.	35
Figure 4-4. Titration of Fluo-4 AM.	36
Figure 4-5. Comparison of Fluo-4 AM with or without pluronic F-127 for detection Ca ²⁺ flux in RBL 703/21 cells.....	37
Figure 4-6. Calcium titration of Fluo-4 treated RBL-703/21.	38
Figure 4-7. Calcium assay using optimised reaction solution - detection of Ca ²⁺ level in RBL703/21 cells stimulated with ionophore A23187 only or ionophore with PMA	39
Figure 4-8. Detection of intracellular calcium level of RBL703/21 cells using the optimised assay solution.	40
Figure 4-9. Quantitative detection of intracellular calcium influx on glass slide.	41
Figure 4-10. Detection of the intracellular calcium flux by FluoStar in Premo™ Cameleon treated cells within 200 seconds after injection with stimuli.....	42

Figure 5-1. Plasmid map of pNFAT-DsRed (pUB6/V5-His A).....	45
Figure 5-2. Flow diagram showing the cloning strategy and steps for obtaining the NFAT-DsRed plasmid.	48
Figure 5-3. Analysis of ligation products on agarose gel.....	51
Figure 5-4. TR% of pEGFP-Tub plasmid transfected into RBL-2H3 cells at different voltages.	53
Figure 5-5. Transient transfection of RBL-703/21 with pNFAT-hrGFP or pNFAT-DsRed with different stimuli after 48 hours of electroporation.	53
Figure 5-6. Fluorescent intensity of RBL-703/21 and RBL SX38 transfected with NFAT-GFP or NFAT-DsRed after 1 month's antibiotic selection by anti-IgE (2 µg/ml) stimulation..	54
Figure 5-7. Fluorescence intensity time-course of pNFAT-hrGFP-RBL-703/21 cells by different stimulations.	55
Figure 5-8. Calcium titration of pNFAT-hrGFP-RBL-703/21 under different stimulations. Fluorescence intensity detected by Typhoon.	56
Figure 5-9. IgE/anti-IgE titration of pNFAT-hrGFP transfected RBL-703/21 cells after 24 hours stimulation in MR80/20 medium supplemented with 20 mM Ca ²⁺	57
Figure 5-10. Time-lapse of anti-IgE induced pNFAT-DsRed-RBL-703/21 cells.	58
Figure 5-11. Time-lapse of anti-IgE induced pNFAT-DsRed- RBL-703/21 cells.	59
Figure 5-12. Overlay of fluorescent vs. bright field of time-lapse of anti-IgE induced pNFAT-DsRed transfected RBL-703/21 cells by Image J.....	59
Figure 6-1. Fluorescent intensity of serum Arg #19 (1:10 dilution) sensitised pNFAT-hrGFP-RBL-703/21 cells after 24-hour stimulation with Grass pollen.	66
Figure 6-2. β-hexosaminidase assay of serum Arg #19 sensitised pNFAT-hrGFP-RBL-703/21 cells induced by grass pollen.	67
Figure 6-3. Fluorescent and morphology of pNFAT-hrGFP-RBL-703/21 cells with grass pollen extract at 1:5 dilution after 24-hour stimulation	68
Figure 6-4. Fluorescence intensity of FW's serum sensitised pNFAT-hrGFP-RBL-703/21 cells stimulated by 2 µg/ml anti-IgE.....	68
Figure 6-5. Fluorescence intensity of FW's serum (1:40 dilution) sensitised pNFAT-hrGFP-RBL-703/21 cells induced by HDM.....	70
Figure 6-6. β-hexosaminidase assay of FW's serum sensitised pNFAT-hrGFP-RBL-703/21 cells induced by HDM.	70
Figure 6-7. Fluorescence intensity of pNFAT-DsRed-RBL-703/21 cells sensitised by serious dilutions of Adr-Ref serum and stimulated by anti-IgE.....	72
Figure 6-8. β-hexosaminidase assay of pNFAT-DsRed-RBL-703/21 cells..	73

Figure 6-9. Fluorescence intensity of Adr-Rref's serum (1:20) sensitised pNFAT-DsRed-RBL-703/21 cells induced by a series dilution of Par j 2.....	74
Figure 6-10. β -hexosaminidase assay of pNFAT-DsRed-RBL-703/21 cells sensitised by Adr-Ref serum (1:20) and induced by a series dilution of Par j 2.....	75
Figure 6-11. Fluorescent intensity of pNFAT-DsRed- RBL-703/21 cells sensitised with Adr-Ref serum and induced by different allergens.....	76
Figure 6-12. Fluorescent intensity of pNFAT-hr-GFP-RBL-703/21 cells sensitised by Dan #7 and induced with Bet v 1a and Phl p 1.....	77
Figure 6-13. Test of serum Adr #54449 with anti-IgE and recombinant allergens..	79
Figure 6-14. Fluorescent intensity of pNFAT-DsRed-RBL-703/21 cells sensitised by Dan #18 serum and induced by anti-IgE.	80
Figure 6-15. Fluorescent intensity of pNFAT-DsRed-RBL-703/21.....	80
Figure 6-16. Pre-incubation of Dan #19 serum with RBL-2H3 cells before sensitisation pNFAT-DsRed-RBL-703/21cells.	81
Figure 6-17. Anti-IgE titration of the pNFAT-DsRed-RBL-703-21 cells in 384-well plate pre-coated with fn + anti-IgE..	82
Figure 6-18. pNFAT-DsRed RBL 703/21 cell density dilutions in dried 384-well plate.	83
Figure 6-19. Test IgE and patient's serum (FW) sensitised pNFAT-DsRed- RBL-703/21 cells on anti-IgE pre-coated 384-well plate.....	83
Figure 6-20. Relationship between NFAT reporter system and β -hexosaminidase assay.	84
Figure 6-21. Fluorescent intensity of pNFAT-DsRed -RBL-703/21 cells in stimuli-pre-coated 96-well plate.....	85

1 Introduction

1.1 Immune system

Immunity has been understood as a defence against or resistance to contagious (infectious) diseases triggered by viruses, bacteria, fungi, or parasites. Interestingly the mechanisms that confer protection against these diseases also operate when the body mounts a reaction against innocuous substances (Pinchuk, 2002). The immune reaction is complex, involving many different cells, molecules and genes and is aimed at maintaining the genetic integrity of an individual, protecting from the invasion of a wide variety of foreign substances that can bear the imprint of a foreign genetic code. The complex series of responses of the immune system to the introduction of foreign substance is known as immune response (Pinchuk, 2002).

Leukocytes also known as white blood cells, describe a group of well-defined cells that include: phagocytes (macrophages, neutrophils and dendritic cells), mast cells, eosinophils, basophils, natural killer cells and lymphocytes (B cells and T cells). All leukocytes are produced and derived from pluripotent hematopoietic stem cells (HSC) in the bone marrow. A common lymphoid progenitor gives rise to the lymphoid lineage (T, B and NK Cells) and a myeloid progenitor to most of the others (macrophage, neutrophil, dendritic cells, basophil, monocytes, mast cells) (Pinchuk, 2002).

Both B and T cells can recognize antigens by physical contact through antigen receptors. Antibodies (immunoglobulin), the B-cell antigen receptor, are protein molecules synthesized and secreted by plasma cells (B lymphocytes that secrete large volume of antibodies), which recognise the unique part (epitope) of antigens in their native form. Antibody-like molecules expressed on T lymphocytes are T-cell antigen receptor (TCRs), which recognise parts of the antigenic peptides in conjugation with major histocompatibility complex (MHC) molecules, which expressed on host's cell membranes. Only lymphocytes can make antigen receptors, and therefore recognise antigens. T cells not only recognise intracellular antigens, but also regulation and control the function of B cells in most immune responses (Adkinson *et al.*, 2003).

When individual is exposed to a specific antigen (by ingestion, inhalation, injection or direct contact), the antigen is taken up and processed by the antigen-presenting cell (APC) and presented it to T helper cells. T helper cells producing cytokines,

which stimulate B cells to differentiate into either plasma cells (antibody-producing cells) to secrete soluble antibodies, or memory cells that survive in the body for years to allow the immune system to remember the specific antigen and respond faster upon future exposures (Adkinson *et al.*, 2003).

Antibodies that bind to antigens, stimulate the effector functions of immune cells such as phagocytes and other cells by recognizing fragment crystallisable region (Fc region) of antibodies. The specific antibody interacts with the Fc receptor on a particular cell to trigger a particular effector function of that cell, for instance, mast cells and basophils undergo degranulation to release preformed chemical mediators leading to clinical symptoms (Borghesi *et al.*, 2006).

1.2 Allergic reactions

Allergy, a type I hypersensitivity reaction, mainly occurs in atopic individuals when the immune system overreacts to otherwise harmless substances. Allergic reactions are rapid and abnormally vigorous immune responses mediated through immunoglobulin E (IgE), the rarest of the five isotypes of antibody in humans and other mammals. The substances (antigens) that generally trigger an allergic reaction are known as allergens, specific proteins contained for example in plant pollen, dust mite fecal pellets, and animal dander, some dietary substances, found in food such as peanuts, nuts and seafood are the causes of serious allergies in many people. The hypersensitivity reaction occurs during a second and subsequent exposure to an allergen (Debjit *et al.*, 2012).

People can be allergic to different allergens. The sensitivity to different allergens varies widely from individuals, which depends on the nature of the allergens, and the level of the allergen-specific IgE in the individual. Sensitive people can be allergic to a very broad range of substances (Halteren *et al.*, 1997).

The major symptoms of allergy can range from mild, as in hay fever, which is very common in humans, and can cause red eyes, itchiness, or eczema, to extremely serious like asthma and life-threatening anaphylaxis (Ahmed *et al.*, 2013).

The IgE-mediated allergic reaction is a hypersensitivity reaction, meaning that before an allergic response, the individual needs to be sensitised to the allergen by

producing IgE antibody from plasma cells, which is specific for the allergen. The secreted IgE is released and binds to the surface of the granulocytes such as mast cells and basophils via the high-affinity receptor FcεRI in different tissues of the body (Murphy *et al.*, 2008).

Activation of mast cells and basophils by cross-linking of FcεRI-IgE complex result in two phases of effector functions. The early phase involves cell degranulation and release of pre-formed mediators present in the granules (**Figure 1-1**). The activation of cells results in the reorganisation of the cytoskeleton, enabling the movement towards and fusion of the granules with the plasma membrane, and the release of pre-formed chemical mediators into the surrounding tissues, such as histamine, serotonin and degradative enzymes, for instance proteases (chymase, tryptase and carboxypeptidase A). The released mediators can cause a series of acute stages of inflammatory symptoms, such as capillary dilation, airway constriction, itching of skin, mucous secretion, tissue swelling, coughing and vomiting. Severe allergic reactions to some food allergens or medicine can lead to life-threatening anaphylaxis. These reactions occur very quickly – normally within minutes of FcεRI cross-linking (Stoppler *et al.*, 2009).

Histamine, which is a representative of a group of biogenic amines, is non-lipid, low-molecular weight compounds that share an amine group. Histamine is the decarboxylated product of histidine. Histamine exerts its effects upon binding to its receptors (designated H1, H2, H3, H4), expressed differentially on various cells. Binding of histamine to endothelial cells, increases blood vessel permeability and causes the contraction of these cells and leakage of plasma into the tissues, which results in a rapid swelling of tissue, and an increased blood influx through blood vessels that manifests as redness and local hyperthermia. Histamine also causes contraction of intestinal and bronchial smooth muscle, which may result in increased peristalsis and bronchospasms. It also depolarizes nerve endings leading to itching and pain (Pinchuk, 2002).

The late phase involves synthesis and secretion of new mediators such as cytokines, chemokines and prostaglandins, a process which normally takes hours (Blayne A *et al.*, 2008). Interleukins, for instance IL4- and IL-13, are archetypal proallergic cytokines, which are synthesised and secreted to mediate the allergic reactions 4-8

hours later. They increase vascular cells adhesion on the microvascular endothelium and exotoxin synthesis from epithelial cells, supporting leukocyte influx into affected tissues during the development of late-phase responses (Gibbs, 2008).

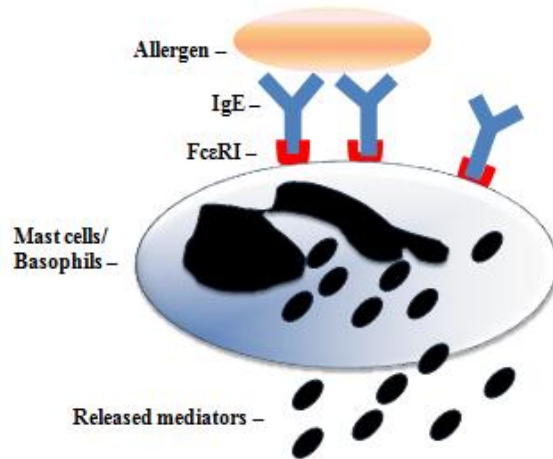


Figure 1-1. Degranulation of mast cells or basophils by cross-linking of FcεRI-IgE complex when bound to allergen. The activation of cells results in the reorganisation of cytoskeleton, enable the movement and fusion of the granules to the plasma membrane, and release the pre-formed chemical mediators such as histamine, serotonin into the surrounding tissues immediately, which cause a series of acute stages of inflammatory symptoms.

1.1 Mast cells and Basophils

All cells of the immune system originate from hematopoietic stem cells (HSC) in the bone marrow. Mast cells and basophils derive from the granulocyte-monocyte progenitor (GMP), a direct descendent of the common myeloid progenitors (CMP), which is derived from the HSC (Iwasaki, 2007).

Mast cells, first described by Paul Ehrlich in 1877, are best known for their important role in the allergic reactions. Mast cells circulate in an immature form and mature in the tissue with the presence of stem cell factor and other cytokines such as the T-cell derived IL-3. Mature human mast cells are usually 9 to 12 μm in diameter and appear as round, spindly or spiderlike cells in tissues. They have numerous granules in the cytoplasm. Mast cells are present in most tissues characteristically surrounding blood vessels and nerves. In humans, there are two types of mast cells termed MC_T and MC_{TC} , named according to the neutral protease

composition. Whereas MC_T cells express tryptase alone, MC_{TC} cells produce tryptase, chymase, mast cell carboxypeptidase and cathepsin. MC_T cells are the predominant mast cells found in normal lung, and in small intestine mucosa. MC_{TC} cells are the predominant type found in normal skin, blood vessels, and gastrointestinal submucosa (Adkinson *et al.*, 2003).

Basophils are basophilic leukocytes, which are susceptible to staining by basic dyes. They leave the bone marrow already mature, and are usually found in the circulation but rarely present in normal tissues. Basophils, containing large cytoplasmic granules, are the least common granulocytes, representing approximately 1% of the circulating blood leukocytes. Basophils express various chemokine receptors and respond to many chemokines and cytokines, which aid their migration (Falcone, 2011). It was reported that, during the allergen-induced asthmatic reactions, basophils were shown to be responsible for the release of 72% of IL-4 protein in the bronchial mucosa (Gibbs, 2008).

Mast cells and basophils, both are originating in the bone marrow and arising from CD34⁺ cells, sharing some similar characteristics, such as the granules content, the expression of the high-affinity IgE receptor, and the ability to release histamine when degranulating upon crosslinking of FcεRI in immediate allergic reactions. However they are not the same, they differ in a number of important aspects regarding their location, their ability to react to various stimuli and the types of mediators they release. Mast cells exit the bone marrow as immature precursors and terminally differentiate only after entering tissues, where they establish long-term residence, and normally do not circulate in the bloodstream. In contrast, basophils enter the circulation fully mature, but maybe recruited to tissues if they are adequately stimulated (Galli *et al.*, 2008).

Mast cells have been long associated with local acute phase reactions that occur within minutes of antigen exposure, due to the location of mast cells in the tissue. In contrast, in terms of cytokine synthesis, human basophils are relatively constrained to generating Th2-like cytokines IL-4 and IL-13 rather than IL-5 or the multitude of proinflammatory cytokines ascribed to mast cells (Gibbs, 2008).

1.3 Signalling transduction pathways

Previous studies have demonstrated that the expression of FcεRI receptors on the surface of mast cells and basophils increases with the concentration of IgE in the serum. IgE concentration is normally low in the bloodstream, but higher levels of IgE capable of causing allergic reactions are commonly seen in atopic patients with enhanced expression of FcεRI on their basophils and mast cells and enhanced response to allergens, because of that, the production of IL-4 and IL-5 in these individuals is enhanced compared to those who are non-atopic (Wedemeyer *et al.*, 2000).

It is well known that the binding of a single epitope of a monovalent allergen with IgE-FcεRI receptor complex results in no cellular responses, whereas crosslinking of IgE by binding to multivalent allergens causes aggregation of FcεRI receptor and initiates the downstream signalling response and activation of effector cells (Wedemeyer *et al.*, 2000).

The allergic reaction is mediated by IgE and the FcεRI receptor. An IgE molecule (**Figure 1-2**) is composed of two sections: the Fab region, which is the specific allergen binding site, and the Fc (constant or crystalline) region, which binds to the FcεRI receptor on the surface of mast cells and basophils (Adkinson *et al.*, 2003).

Like other Immunoglobulins, an IgE molecule consists of four polypeptide chains: two identical heavy chains (50-70kD) and two identical light chains (23kD). Each light chain is attached to a heavy chain through covalent disulfide bonds at the Cε1 domain, the two heavy chains are attached to each other through disulfide linkages and non-covalent interactions at the Cε2 domains. Both heavy chain (H) and light chain (L) can be divided into two regions – variable (V_H and V_L) region and constant (C_H and C_L) region based on variability of amino acid sequences. The unique amino acid sequences in the variable regions make the antibody able to interact with the specific epitope of particular allergen (Adkinson *et al.*, 2003).

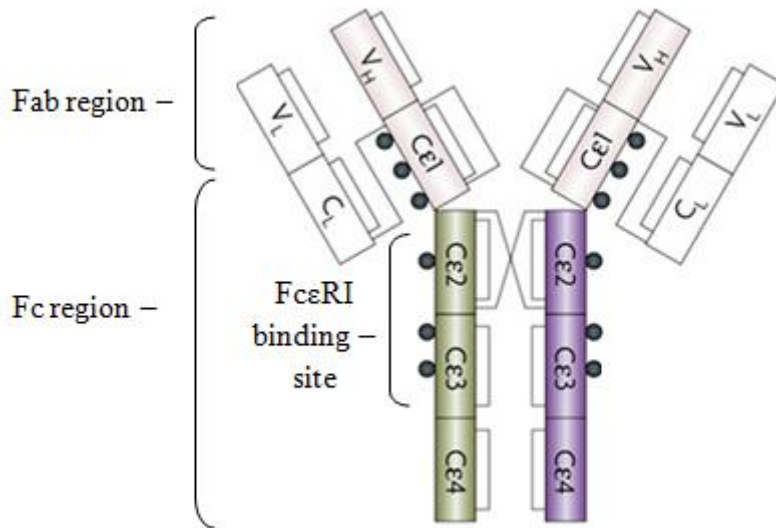


Figure 1-2. Structure of an IgE molecule. Figure adapted from Gould *et al.*, 2008. IgE binds to FcεRI via its Cε2 and Cε3 at the Fc region, and binds allergens via its Fab region.

FcεRI, a tetrameric high affinity IgE receptor, is formed by one FcεRIα, one FcεRIβ, and two FcεRIγ chains. The α-chain binds the constant region (Fc) of IgE at the Cε2 and Cε3 regions at ratio of 1:1; the β-chain is a stabiliser and enhancer of surface expression and signal transduction; the two γ-chains mainly responsible for signal downstream into the cell via its immunoreceptor tyrosine-based activation motif (ITAM), which possess two tyrosine residues separated by 6–8 amino acid residues (Bubnoff *et al.*, 2003).

Aggregation of FcεRI (**Figure 1-3**) results in phosphorylation of the two tyrosine residues within the ITAMs by Lyn, the main SRC-family kinases in basophils. Phosphorylated ITAM provide high-affinity docking site for spleen tyrosine kinase (Syk) binding, and resulting in increases of its catalytic activity (Kopec *et al.*, 2006).

Protein-tyrosine kinase Syk is essential for regulating downstream signalling leading to calcium mobilisation. Activated Syk phosphorylates other proteins, such as linker for activation of T cells (LAT), growth-factor-receptor-bound protein 2 (GRB2), GRB2-related adaptor protein (GADS), SH2-domain-containing transforming protein C (SHC) and SH2-domain-containing leukocyte protein of 65kDa (SLP76). The activation of Syk tyrosine also phosphorylates guanine-nucleotide-exchange factors and adaptors molecules, such as son of sevenless homologue (SOS), and signalling enzymes, such as phospholipase Cγ1 and Cγ2 (PLC). PLC cleaves

phosphatidylinositol 4, 5-bisphosphate (PIP₂) in the plasma membrane and generates diacylglycerol (DAG) and inositol 1, 4, 5-trisphosphate (IP₃) (Siraganian, 2003; Law *et al.*, 2011).

DAG recruits the GEF Ras guanine nucleotide exchange factor (RasGPR), resulting in the activation of protein kinase C (PKC) and a small and transient rise in intracellular calcium (Kopec, 2006; Tomoko *et al.*, 2011).

GEF RasGRP activates Ras, which in turn phosphorylates MEK1, Erk and transcription factor Elk-1. Elk-1 cooperates with a transcription factor called serum response factor to initiate transcription of the Fos gene. Fos combines with Jun to form the Activator protein-1 (Ap-1) complex, which can migrate into the nucleus with other transcription factors to initiate transcription of cytokine genes, such as IL-4 and IL-13 (Siraganian, 2003; Law *et al.*, 2011).

The protein kinase C family activate the small GTPases and lead to phosphorylation and activation of extracellular-signal-regulated protein kinase (ERK1 and ERK 2), mitogen-activated protein kinases (MAPKS), MAPKs JUN amino-terminal kinase (JNK) and p38 MAP kinase pathways. These molecules are important signalling mediators between the cytosol and the nucleus that regulate a variety of transcription factors, such as nuclear factor- κ B (NF κ B). NF κ B is phosphorylated and translocate to the nucleus to initiate transcription of other cytokine genes, such as Tumor-Necrosis Factor-alpha (TNF α) (Tomoko *et al.*, 2011; Gilfillan *et al.*, 2006).

IP₃ binds to the IP₃ receptor in the endoplasmic reticulum and triggers release of Ca²⁺ in the ER into the cytosol, which subsequently opens the channel called calcium release-activated calcium (CRAC) in the plasma membrane, CRAC activates store-operated calcium entry from the extracellular medium via the Stim1 and Orai1 sub-channels. Activation by this later calcium influx is mainly mediated by the transcription factor -nuclear factor of activated T-cells (NFAT). In resting cells, NFAT is kept inactive in the cytoplasm by phosphorylation of multiple serine kinase, while the nuclear localisation sequence (NLS) of NFAT is blocked to prevent it from translocating to the nucleus. Calcium in the cytosol binds to calmodulin (a calcium binding messenger protein) and activates calcium-dependent phosphatase calcineurin,

which dephosphorylates and unmasks the NLS of NFAT, allowing NFAT to enter into the nucleus and interact with the previously mentioned AP-1 to initiate transcription of cytokine genes, such as IL-4 (Gilfillan *et al.*, 2006; Siraganian, 2003 Law *et al.*, 2011; Kraft *et al.*, 2005).

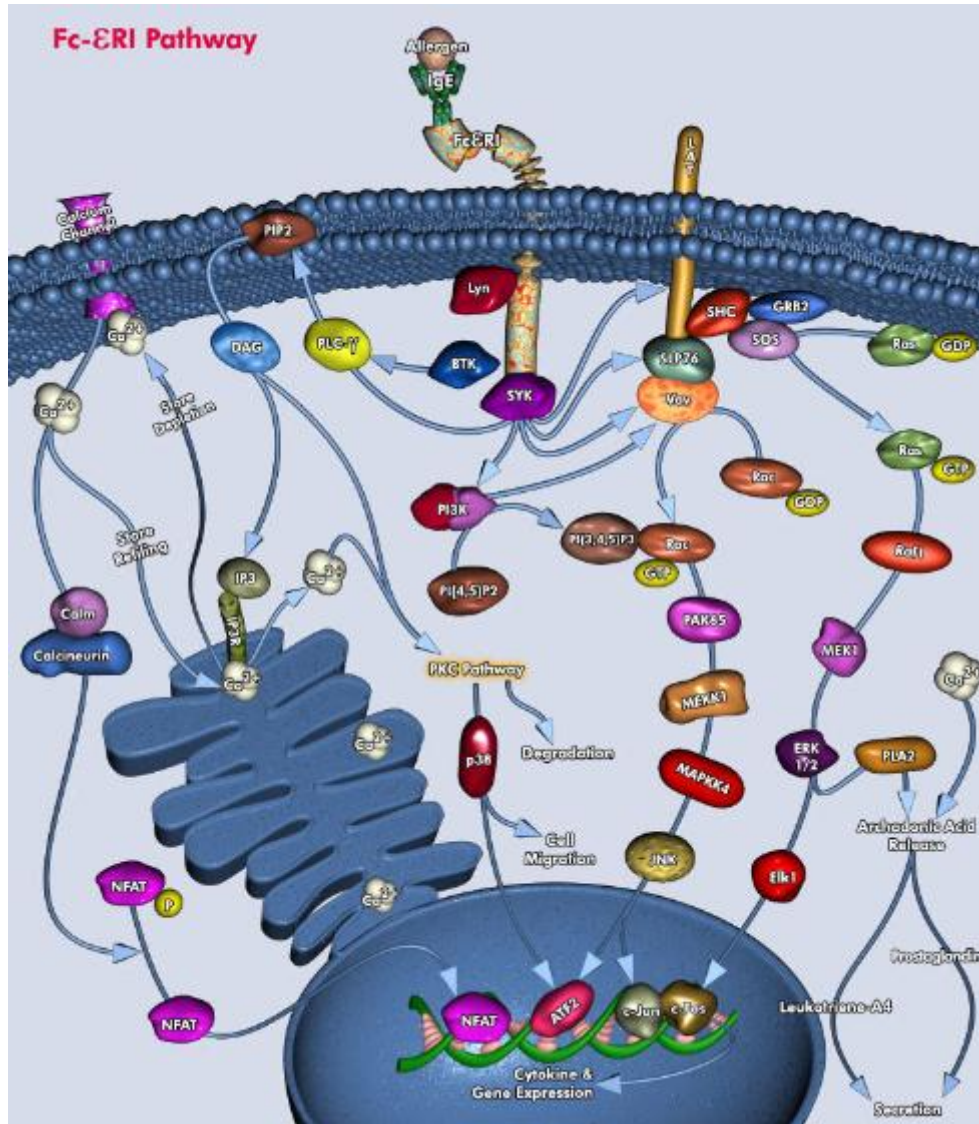


Figure 1-3. FcεRI-mediated Intracellular signalling transduction pathway in mast cell and basophil activation. Figure adapted from (Qiagen.com, with permission). Allergen binds to two or more IgEs and cross-links two FcεRI receptors leading to phosphorylation of the tyrosines in the ITAMs on the β- and γ-chains by Lyn. Syk kinase is recruited and activated by binding to the phosphorylated ITAM of the γ subunit; the activated Syk autophosphorylates and activates downstream signalling which includes phosphorylation of LAT, PLCγ, PI3K and SLP-76. The activated PLCγ hydrolyzes PIP₂ to form DAG and IP₃. The IP₃ activates the IP₃-receptor on the ER releasing calcium, the calcium sensor Stim1 then interacts with the Orai1 membrane protein opening the CRAC channels allowing the increase in intracellular calcium. Calcium binds to calmodulin to activate calcineurin which dephosphorylates and enables NFAT translocation into the nucleus.

1.4 Past and current diagnosis of allergy

Due to the low levels of IgE in peripheral blood, it has taken more than 100 years for the development of allergy diagnosis techniques from skin prick testing in the late 19th century to the modern Allergen Microarrays in the beginning of the 21st century (**Figure 1-4**). The first and still currently used allergy diagnosis technique is known as skin prick testing (SPT) and it was introduced by Charles Blackley in 1880 (Harwanegg *et al.*, 2003). In the 1960s IgE was identified and characterized as the major immunoglobulin response for type I hypersensitivity (Ishizaka and Ishizaka, 1967). The first quantitative radio-labelling technique – radioallergosorbent immunoassay test (RAST) was then developed to enable detection of allergen-specific antibodies (Wide *et al.*, 1967), and its upgraded format using fluorescent labelled markers (Seltzer *et al.*, 1984) is still in use today (Aas *et al.*, 1978).

The introduction of standardisation of allergen extracts was an important advance in allergy diagnosis in the late 1970s. After the first allergen was cloned in the late 1980s (Simpson *et al.*, 1988), the production and tests of purified recombinant allergens of use in allergy diagnosis rather than traditional extracts was taken as priority all through the 1990s (Ferreira *et al.*, 2007). With the advances in microtechnology and the availability of large number of well-purified recombinant proteins, it was then possible to develop multi-allergen microarrays for IgE diagnosis during the early twenties (Harwanegg *et al.*, 2003).

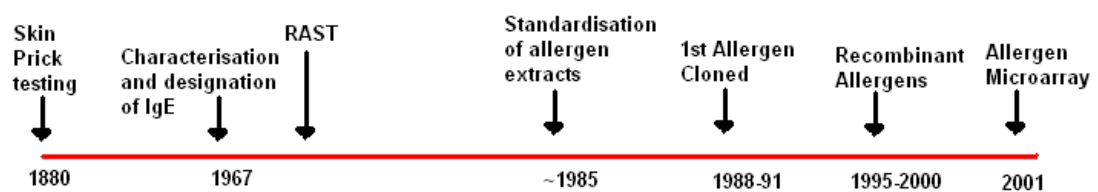


Figure 1-4. A timeline diagram adapted from Harwanegg *et al.*, 2003, displays the development of allergy diagnosis.

1.5 Microarray

Microarray, has been developed for the analysis of thousands of samples in a single experiment under different conditions. The microarray technique was initially a solid-phase media for monitoring of gene expression, but over a short period of time this technique permeated into other areas such as protein and drug discovery arrays (Kukar *et al.*, 2002).

Protein array represents a multi-analyte solid-phase immunoassay, where proteins are immobilised onto the solid surface and incubated with micro-quantities of the serum samples under standard conditions. Allergen-specific antibodies IgE in the patient's serum bind to individual allergen spots on the array. The bound IgE is detected and quantified with a fluorescently labelled anti-isotype antibody and a laser-based scanner. Conventional protein printing robots are now able to deposit 10,000-30,000 spots on a slide of size 75 x 25 mm (Harwanegg *et al.*, 2003).

Renault *et al.*, 2011, from the School of Biosciences (University of Nottingham) reported some improvement on the technique by representing most of the proteins present in the British diet on a microchip device-FAST slide (**Figure 1-5**), which is a glass slide coated with a proprietary nitrocellulose polymer.

With this microchip, it was possible to use single drop of blood from patients and determine within hours the characteristics of the antibodies that the subject was currently producing. The platform allowed quantitative measurements of IgA, IgM, IgE, IgG isotypes or IgG1-4 subclass against common proteins. The preliminary results using this approach have established clear differences between healthy, bacterial infected and IBS patients (Renault *et al.*, 2011).

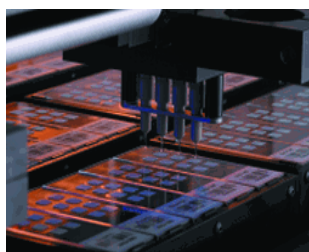


Figure 1-5. A)



Figure 1-5. B)

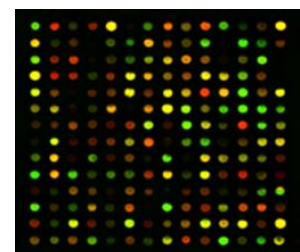


Figure 1-5. C)

Figure 1-5. Principle of a protein microarray (adapted from Renault *et al.*, 2011) A). Protein-spot printing. Purified food proteins are plotted in a FAST slide, at the concentration of 6000spots/slide **B)**. Basic components of a standard protein array. Antibodies from the patient's serum are captured by the immobilised protein molecules on the surface of the

chip, secondary antibodies labelled with fluorescent markers allow the target molecule to be detected and quantified with a laser-based scanner C). Fluorescent labelled antibodies detected by GenePix scanner. Each colour represents a type of antibody. Data were analysed by SQL, Matlab, PCA and ANOVA after normalization extracts and recombinant allergens.

1.6 Basophil microarray

Basophil activation test (BAT) has been developed as a reliable in vitro tool for diagnosis IgE-mediated allergic reactions (Sainte-laudy *et al.*, 2007). Current techniques such as in vitro allergen-specific IgE test such as ImmunoCAP (CAP test), are widely used for the initial screening purposes for responsive allergens. However, results of IgE-detection cannot always be translated into a clear diagnosis, as specific IgE binding to allergens do not always trigger mast cell or basophil activation. Methods based only on IgE detection generate a certain number of false positive results, as they measure both functional IgE (capable of binding to Fcε on mast cells or basophils and activating the cells), and non-functional IgE (Faisal *et al.*, 2012).

BAT tests are thought to minimise false positive results and will not cause potential life-threatening risk as OFC (oral food challenge) to patients with severe allergy. Although BAT could obviate disadvantages of methods based on IgE binding detection, the isolation and purification of primary human mast cells (the main type of cells that involved in mucosal acute allergic reaction) is very difficult and time-consuming, as the mature mast cells are only present in tissues, also they need to be stripped of IgE from the donor that already bound to their receptors before sensitisation with IgE from patients' sera. Current available human mast cell lines are HMC-1, LAD 1 and LAD 2. HMC-1 does not express FcεRI (Nilsson *et al.*, 1994), LAD 1 and LAD 2 cells grow extremely slowly and have unstable FcεRI expression (Laidlaw *et al.*, 2011).

Unlike mast cells, which differentiate and mature in the tissues, mature basophils are found in the circulatory system, but are very rare – less than 1% in total white blood cells (Falcone *et al.*, 2000), also they need to be stripped of IgE from the donor before sensitisation with sera from patients. It was reported that human leukaemia cell lines KU812 and LAMA-84 express low levels of FcεRI (J. M. Reimer *et al.*, 2006).

Based on all these limitations, a variant cell line stably transfected with the human high affinity IgE receptor would be a useful and viable alternative. It was demonstrated that rat basophilic leukemia cell line RBL-703/21, transfected with the alpha chain of human FcεRI could bind specifically and degranulate on the microarray format assay. The activation of human peripheral blood basophils and RBL-703/21 showed comparable results (Lin *et al.*, 2007).

In order to create a more powerful allergy diagnostic technology, the Biosciences and Pharmacy groups at University of Nottingham described a proof of principle for a method based on coupling protein microarray and clinical relevance of cell-based assays. In this method, both human basophils and rat basophilic leukemia cell lines (RBL) were sensitised with patients' sera or monoclonal IgE and incubated with microarray pre-coated with spots of different food allergen extracts to mimic the process of human basophil degranulation. The activation of the cells that were triggered by the crosslinking of FcεRI and IgE-allergen complex could then be measured. The results were very promising and suggested that coupling the diversity of a protein microarray with the potential functionality and biological activity of a cell-based test could be a useful novel tool for improved clinical diagnosis (Lin *et al.*, 2007). The work that follows describes the continuation of this initial development.

1.7 Aims and objectives

Following the work described in Lin *et al.* (2007) and Renault *et al.* (2011), in which the protein microarray platform for diagnosis of allergy was initiated, current work concentrated on the optimisation of the basophil system. Different methods of measuring basophil activation will be developed throughout the project as described below in **Figure 1-6**, and the optimal system will be chosen for use in the microarray format. The main objectives were:

- To introduce a reporter gene (NFAT-GFP and NFAT-DsRed) to RBL cell lines for detecting IgE crosslinking–induced basophil activation
- To address the cell detachment from solid surface problem
- To determine the optimal conditions for maximum cell activation (calcium concentration, allergen/sera dilutions)
- To investigate alternative methods (Fluo-4 and cameleon) for detection of cell activation within a comprehensive microarray background
- To test well characterise allergic sera against allergens using the new reporter system and compare to conventional enzymatic readouts.

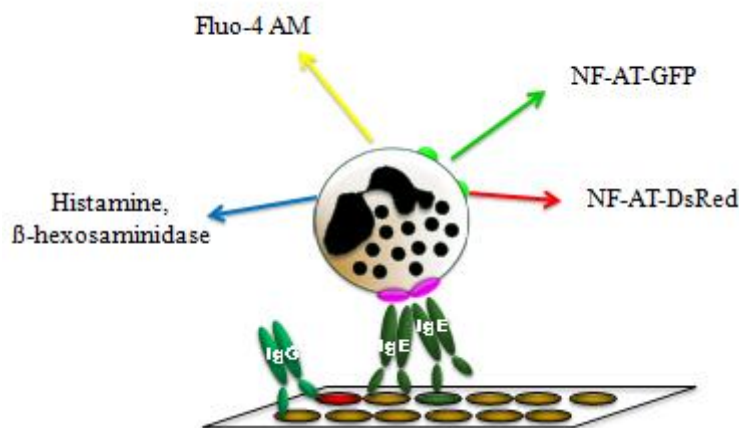


Figure 1-6. Schematic diagram of basophil-microarray system. Purified protein extracts from British diets were printed onto the microarray FAST slide, humanised RBLs sensitised previously with patient's sera were applied on to the slide and incubated for standard conditions. The specific IgE-FcεRI complex bound to allergens, elicited the cells' activation. The cells' degranulation at early stage and fluorescent proteins produced at late stage were detected by different methods

2 Optimisation of β -hexosaminidase assay

2.1 Introduction

As described in Chapter 1 there are many possible ways of measuring significant differences between non-activated and activated RBL cells. Any of the mediators released from degranulated RBLs, such as histamine can report the extent of degranulation and the cross-reactivities between allergens. A well-established assay to measure RBL activation is the β -hexosaminidase assay, which has been chosen as a surrogate marker for histamine in this study. β -hexosaminidase, an enzyme presents in the granules and released together with mediators, is normally used as a surrogate marker for histamine as it can be quantified in a simple and cheap enzymatic reaction (Siraganian *et al.*, 1982). The released β -hexosaminidase hydrolyses the substrate p-nitro-N-acetyl- β -D-glucosaminide to produce N-acetyl- β -D-glucosaminide and a yellow coloured p-nitrophenol that is measured by spectrophotometer. The quantity of p-nitrophenol produced corresponds to the amount of enzyme released and reflects the amount of IgE cross-linking and consequently cells' degranulation.

The biochemical assay adapted from a protocol previously written by Vogel *et al.* (2005) is robust and routinely used as a benchmark to monitor cells' behaviour and function of reagents throughout the project. The optimised method and the results obtained with different cell lines are described here.

2.2 Material and Methods

2.2.1 Cell line and cell culture

The RBL cell lines used throughout the project were the RBL-2H3, RBL-703/21 and RBL-SX38. RBL-2H3, only expressed the endogenous rat FcεRI, which does not bind human IgE, was obtained from ATCC (Manassas, Virginia, USA). RBL-703/21 cells, original RBL-2H3 cells cloned with the genes of the human FcεRI, generated at Paul-Ehrlich-Institut (Langen, Germany) were kindly provided by Lothar Vogel. RBL-SX 38 cells, transfected with genes that encode the three chains of human FcεRI genes, were kindly provided by Dr. Jean-Pierre Kinet (Beth Israel Deaconess Medical Centre, Boston, Massachusetts, USA).

Both RBL-703/21 and RBL-SX38 cells express both rat and human FcεRI proteins, however RBL-703/21 cells express only the α-chain of human FcεRI, whereas RBL-SX38 cells express the α- and γ-chain of the human FcεRI. According to suppliers, both cell lines express human Fcε receptor for years without recognisable decrease, can bind human IgE and have all functional properties of basophils. The cell line that demonstrated higher activation with methods in the following chapters was chosen for final use in the microarray.

All cell culture work was carried out inside class II microbiological safety cabinets, using sterile techniques. RBL cells were cultured in 75 cm² flasks (NUNC, UK) with 0.2 μm vent caps (Corning, USA), at 37 °C in a humidified atmosphere incubator containing 5 % CO₂ (Galaxy S Plus CO₂ incubator, RS Biotech, UK). Each flask was refreshed every three days and passaging was carried out every week.

All cells (**Figure 2-1**) were grown in MR 80/20 medium: 80 % minimal essential medium (MEM; GIBCO, UK) plus 20 % RPMI-1640 medium (Sigma, UK) supplemented with 10 % fetal bovine serum (FBS; Gibco, UK), 2 mM L-glutamine, 50 IU/mL penicillin and 50 mg/mL streptomycin (Invitrogen, UK). 1 mg/ml geneticin sulphate (G-418; Sigma, UK) was used to maintain expression of human FcεRI genes in RBL-703/21 and RBL-SX38 cells.

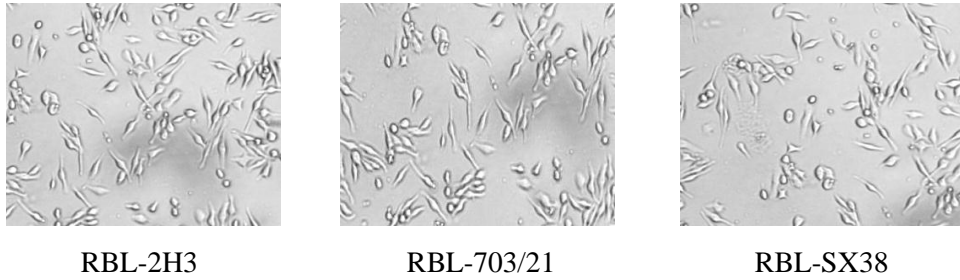


Figure 2-1. Similar morphology of three RBL-2H3 sub-lines: RBL-703/21 and RBL-SX38. Photos were taken at 100x magnification.

Optimised 600 $\mu\text{g/ml}$ hygromycin B (Thermo Scientific, UK) and 20 $\mu\text{g/ml}$ blasticidin S (Invitrogen, California, USA) were separately used to maintain and selection of both RBL-703/21 and RBL-SX 38 cells expressing NFAT-GFP and NFAT-DsRed. Optimisation of antibiotic concentrations was performed in separate experiments (data not shown).

Detachment of cells were carried out by either using cell scrapers (TPP, Switzerland) or incubating 12 ml of medium with 2 ml trypsin-EDTA (Gibco, UK) for 10 minutes following two washes by $\text{Ca}^{2+}/\text{Mg}^{2+}$ - free DPBS (Gibco, UK) and resuspended in fresh medium.

Frozen stocks of cells were prepared in either 90 % MR20/80 medium or FBS plus 10 % DMSO (Sigma, UK). Cells were resuspended in freezing medium to a final concentration of 5×10^6 /ml, 1 ml of each aliquot in a CryoTube vial (Nunc, Denmark), and placed in a polystyrene box at -80 °C for 24 hours before transferring into a liquid nitrogen tank for long term storage.

2.2.2 Methods for β -hexosaminidase assay

Cells (RBL-703/21, RBL-SX38 or pNFAT-hrGFP/pNFAT-DsRed-703/21 cells) were harvested and resuspended in MR80/20 medium to a final concentration of 2×10^6 cells/ml. Cells (100 μ l/well) were transferred to a Nunclon Surface 96-well plate (Nunc, Denmark). Sensitisation (IgE binding to the Fc ϵ receptor) was achieved with human IgE (1 μ g/ml, myeloma, AbD Serotec, UK). All incubations were carried out at 37 $^{\circ}$ C/5 % CO $_2$ in triplicates in a humidified incubator. After 16-hour incubation (optimisation as previously described by Paul Cato, MSc thesis, University of Nottingham), supernatant was twice removed by pipetting and replenished with MR80/20 medium. The stimulation phase (stimuli added) was carried out in Allergen Challenge Buffer (ACB, 100 μ l/well, by mixing 1x Tyrode's Wash Buffer ([Appendix I Table 2](#)) and Deuterium oxide (D $_2$ O) (Acros Organics, Belgium) in a 1:1 ratio). Ca $^{2+}$ concentration was kept at 5 mM (**Figure 2-2**). Total cell lysis was determined with Triton-X100 (1 %, Sigma, UK) and used as a reference positive control (100 % lysis). After 1 hour of stimulation, supernatants (30 μ l/well) were transferred to a new 96 well plate and substrate solution (50 μ l/well, [Appendix I Table 5](#)) was added and further incubated for 1 hour. The reaction was stopped by the addition of stop solution (100 μ l/well, [Appendix I Table 6](#)), the plate was read at 405 nm (reference 590 nm) in a micro-well reader (Model 680 XR, Bio-Rad Laboratories, UK). The average reading from lysed cells was assumed to be 100% of β -hexosaminidase released and all the other readings were taken as percentage of the lysis reading and averaged.

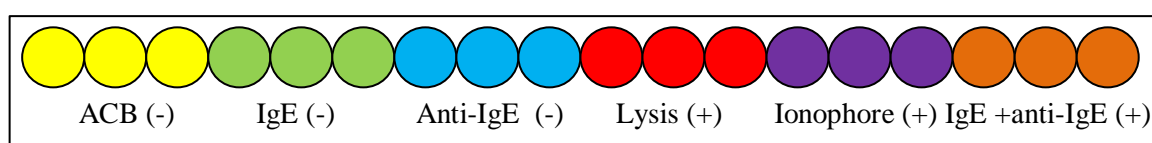


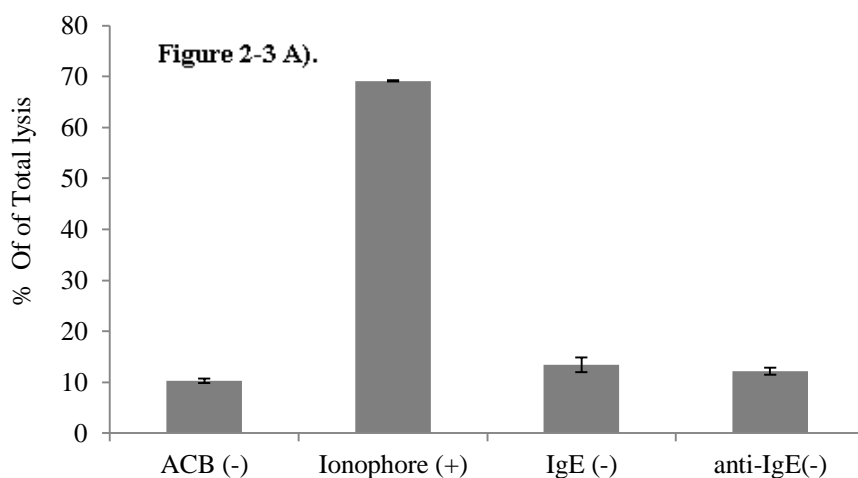
Figure 2-2. Sample layout of β -hexosaminidase assay (triplicates) in a Nunclon 96-well plate. (+) and (-) represent positive and negative controls. *ACB (-)*: non-sensitised cells incubated with ACB buffer only; *IgE (-)*: 1 μ g/ml IgE sensitised cells incubated with ACB buffer, but without addition of stimuli; *Anti-IgE (-)*: non-sensitised cells incubated with 2 μ g/ml anti-human IgE (AbD, Serotech, UK); *Lysis (+)*: non-sensitised cells incubated with lysis buffer alone; *Ionophore (+)*: non-sensitised cells stimulated with 1 μ g/ml calcium ionophore A23187 (Sigma, UK); *IgE + anti-IgE (+)*: 1 μ g/ml IgE sensitised cells incubated with 2 μ g/ml anti-human IgE. All stimuli were diluted in ACB buffer.

2.3 Results

Two stimuli were used as positive controls for the β -hexosaminidase assay: calcium ionophore A23187 and anti-IgE. Ionophore A23187 is lipid soluble molecule, which was previously reported to increase permeability of biological membranes to transfer Ca^{2+} ions across the cell membrane, it was used to activate cells by calcium influx, causing degranulation and release of β -hexosaminidase. Anti-human IgE was used to cross-link human IgE sensitised cells.

As shown in **Figure 2-3 to 2-6** and for all the cell lines, the incubation of the cells with the isotonic buffer ACB containing deuterium water induced a background activation that normally did not exceed 10 % of total activation. Ionophore A23187 at 1 $\mu\text{g}/\text{ml}$ consistently resulted in 60-80 % of the total activation. IgE or anti-human IgE alone induced spontaneous release between 10-20 %. Activation due to IgE and anti-human IgE was generally 3-5 folds higher than the negative controls. As IgE and anti-human IgE were important controls used throughout the project, the optimal concentrations of these two parameters were initially determined.

As shown in **Figure 2-3** the level of cells' degranulation was proportional to the concentration of IgE tested. 1 $\mu\text{g}/\text{ml}$ was the maximum concentration and resulted in approximately 60 % of the total activation. Seven dilutions of anti-human IgE were tested as shown in **Figure 2-4**, though it was not the expected bell-shape curve as the range tested was narrow from 0.1-2 $\mu\text{g}/\text{ml}$, 2 $\mu\text{g}/\text{ml}$ resulted in maximal about 50 % of the total activation was good enough to be used as a proper control for future experiments.



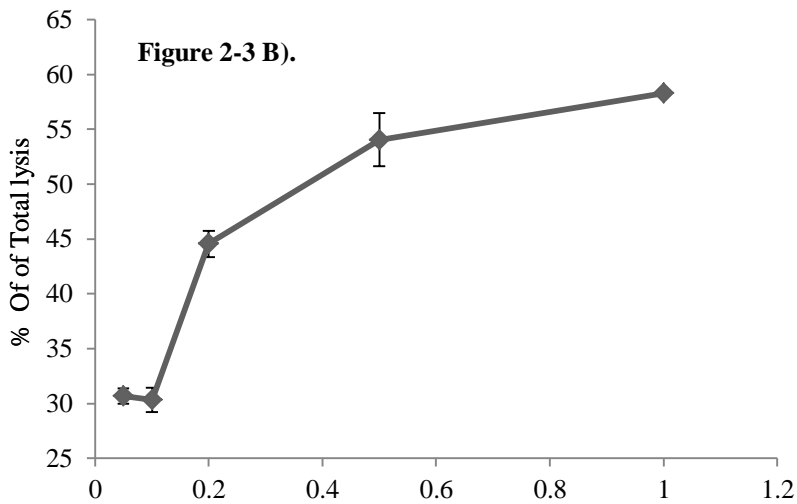


Figure 2-3. Titration of human-IgE for β -hexosaminidase assay. A) Controls. B) Titration of human IgE. RBL-703/21 cell density: 2×10^5 /well, stimuli concentrations: 1 μ g/ml ionophore A23187 and 2 μ g/ml anti- human IgE.

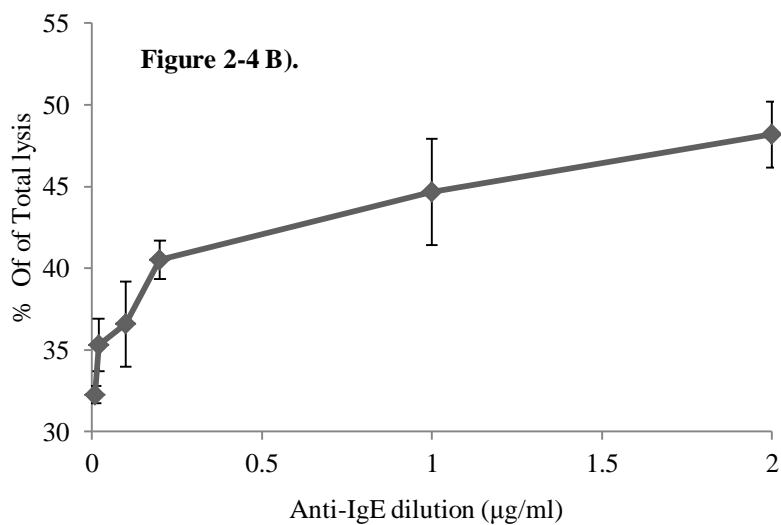
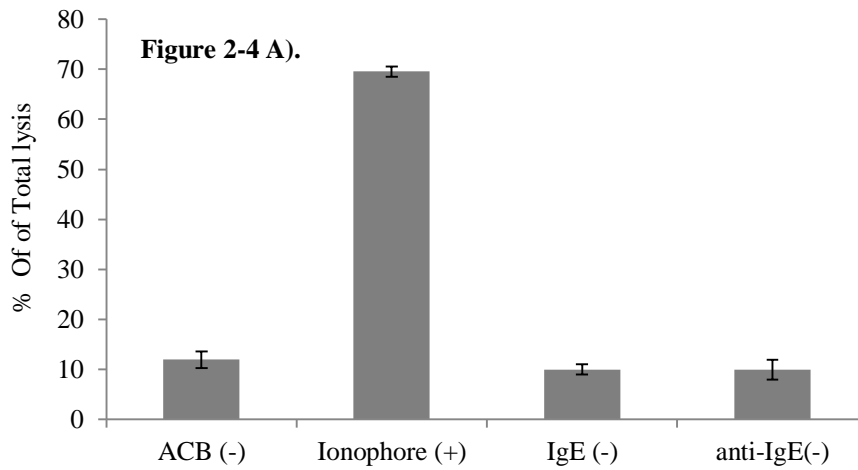


Figure 2-4. Titration of anti-human IgE for β -hexosaminidase assay. A) Controls. B) Titration of anti-human IgE. RBL-703/21 cell density: 1.5×10^5 /well, stimuli concentrations: 1 μ g/ml ionophore A23187 and 1 μ g/ml human IgE.

The optimized conditions were then used to test and compare different cell lines. As shown (**Figure 2-5**), β -hexosaminidase released was similar for RBL-703/21 and RBL-SX38 cells with different stimuli. There was a higher background release in RBL-SX38, which meant that RBL-703/21 cells were more sensitive to stimulations by either ionophore A23187 or (IgE sensitised) anti-human IgE than RBL-SX38.

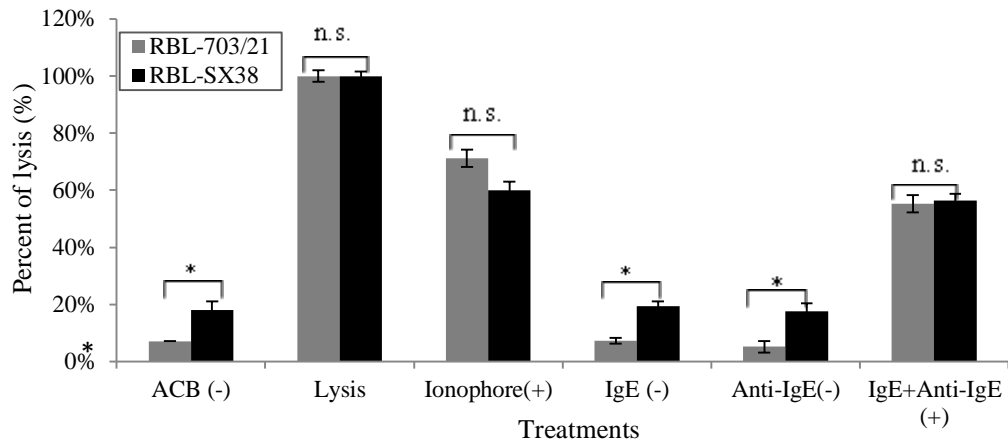


Figure 2-5. Comparison of β -hexosaminidase assay between RBL-703/21 and RBL-SX38 cell lines using optimised reagents. Cell density: 2×10^5 /well, stimuli concentrations: 1 μ g/ml ionophore A23187, 1 μ g/ml human IgE and 2 μ g/ml anti-IgE. Asterisks show results of two-tailed t-test against the negative control (ACB only), n. s.: not significant, * $P < 0.05$, ** $P < 0.01$, *** $P < 0.001$.

The β -hexosaminidase release was also similar for normal and plasmid-transfected RBL-703/21 cells (**Figure 2-6**), a higher spontaneous release was observed from the pNFAT-hr-GFP-703/21 cells as the transfectants were selected from the highest responder clone, and the passage of the transfected cells were higher than the non-transfected cells. Hence overall there was no statistical difference ($p > 0.05$) between the normal and transfected cells.

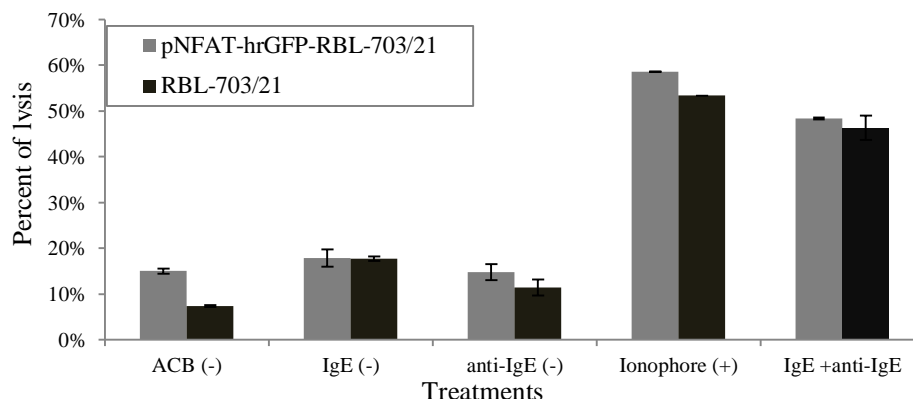


Figure 2-6. Comparison of β -hexosaminidase assay between RBL-703/21 and pNFAT-hrGFP-703/21 cells using optimised reagents. Cell density: 2×10^5 /well, stimuli concentrations: 1 μ g/ml ionophore A23187, 1 μ g/ml human IgE and 2 μ g/ml anti-IgE.

2.4 Discussion

β -hexosaminidase measurement, is a well-established method of determining the degree of degranulation of basophils stimulated by IgE-antigen (Sakai *et al.*, 2009). Microtubules, one of the components of the cytoskeleton, have been recognized as crucial to basophil degranulation. They are important in the maintenance of antigen-induced capacity for Ca^{2+} entry, which is responsible for degranulation and the allergic response (Tatsuya *et al.*, 2005). According to Gillespie *et al.*, 1972, Deuterium oxide (D_2O) seems to stabilize microtubules and thereby favours their formation, enhancing histamine release markedly. The addition of D_2O in ACB buffer accelerates granule translocation and consequently accelerates the overall degranulation. Therefore the reaction medium was made up with 25 % of D_2O (concentration optimised by the previous students).

According to Hoffmann *et al.* (2003), the background release should not be higher than 5 % of the total β -hexosaminidase content. In the experimental conditions in Nottingham, the non-specific release of all the controls were approximately between 5-15 % for different cell lines under different conditions, which was considerably higher than the expected baseline. It was observed that the spontaneous release increased as a function of the passage number, so the number of passages must be critically monitored to control the consistency in the performance of the assay. Also it has been noticed that IgE and anti-human IgE alone can induce degranulation and consequently higher background release than other negative controls (more details in general discussion). The high background observed with the transfected cells might be explained by the selection procedure employed (FACS sorting) where the highest IgE/anti-human-IgE responding clones were favoured (**Figure 2-6**).

As shown in **Figure 2-3&2-4**, the level of degranulation was proportional to the concentration of IgE and anti-human IgE employed. 1 $\mu\text{g}/\text{ml}$ human IgE and 2 $\mu\text{g}/\text{ml}$ anti-human IgE were chosen as the optimal concentration and constantly resulted in approximately 50-60 % of the total activation. It was observed that the intensity of allergic reactions is affected by the level of antigen-specific IgE (Liang *et al.*, 2009). It was reported that, supraoptimal anti-IgE concentrations led to lower mediator release than optimal concentration (Gibbs *et al.*, 2006), according to the previous report from Paul Cato (MSc thesis, University of Nottingham), higher concentrations of IgE/anti-IgE could be supraoptimal and induce inhibitory signalling. A

standardised concentration of 1 µg/ml (1:1000) IgE and 2 µg/ml (1:500) anti-IgE has been used throughout the project to achieve the maximal cell activations.

Interestingly, results of the β-hexosaminidase assay were similar for RBL-703/21 and RBL-SX38 cells, which indicate that both cell lines undergo IgE-mediated degranulation. As described in Chapter 1, RBL-703/21 cells express only the α-chain of human FcεRI whereas RBL-SX38 cells express α and γ chains of human FcεRI. As shown in **Figure 2-5** RBL-703/21 cells were capable of higher level activation by human-IgE cross-linking than RBL-SX38 cells. This is interesting as the expected amplification effect of the accessory chains (RBL-SX38) was not observed. RBL-703/21 and RBL-SX38 cell lines were tested and compared in Chapter 4 by another different method.

Furthermore, as shown in **Figure 2-6**, no statistic difference of β-hexosaminidase release between RBL-703/21 and pNFAT-hrGFP-RBL-703/21 cells was observed, which meant that the transfection did not affect the IgE/anti-IgE-cross-linking triggered degranulation pathway of the RBL-703/21 cells. This an important result as it corroborates the use of the pNFAT-reporter system (Chapter 5) and the enzyme assay as a control in future experiments.

2.5 Conclusion

The results of the β-hexosaminidase assay showed that the human FcεRI expressing rat cell lines were able to bind human IgE and anti-IgE causing degranulation in both normal and transfected RBL-703/21/RBL-SX38 cell lines. The background signals (enzyme released) in the negative controls (ACB, IgE/anti-IgE alone) were acceptable when compared to the ionophore A23187 or IgE/anti-IgE stimulations. This assay in a micro-well format was used routinely to monitor cells' batch-to-batch consistency in all subsequent chapters.

The optimised system was used to test patients' sera against allergens, more results were shown in chapter 6.

3 Optimisation of the cell adhesion assay

3.1 Introduction

During the binding optimisation experiments carried out previously, a severe loss of cells from the solid surface was observed when the cells degranulated. This effect might be due to the well-characterised RBL membrane ruffling effect (**Figure 3-1**) post degranulation as previously reported by Sahara *et al.* 1990. In order to preserve cell binding, the cell adhesion characteristics of different extracellular matrix proteins (ECM) were tested. ECM proteins consist of proteoglycans and glycoproteins including collagen (CO), fibronectin (FN) and laminin (LN).

The adhesion of basophils to ECM proteins has been shown to play an important role in enhancing degranulation of rat

basophil leukemia RBL-2H3 cells (Hamawy *et al.*, 1992; Yasuda *et al.*, 1995). RBL cells normally do not adhere to uncoated surfaces or show any adherence in the absence of Ca^{2+} . RBL adherence to ECM proteins is mediated by specific cell surface receptors that belong to the integrin family (Yasuda *et al.*, 1995). Many integrins bind the tripeptide Arg-Gly-Asp (RGD) sequence present on ECM proteins, originally described on FN (Pierschbacher *et al.*, 1984). The $\beta 1$ integrin subfamily in particular includes receptors that bind to the ECM proteins FN, CO and LN, and have been designed VLA (very late antigen) (Springer, 1990). VLA-4 and VLA-5 have been shown to mediate RBL-2H3 cell adhesion to FN (Yasuda *et al.*, 1995). VLA-4 recognizes the CS-1 sequence present in the type III connecting segment (IIICS) of the cell-binding domain of FN, while VLA-5 recognizes the RGD sequences (Springer, 1990).



Figure 3-1. Morphology of RBLs. (Adapted from Sahara *et al.*, 1990)

3.2 Methods

3.2.1 Fibronectin -Adhesion assay

Fibronectin from bovine plasma (Sigma, UK) was coated at concentrations ranging from 0.625 µg/ml to 20 µg/ml in a Maxi-Sorp 96-well ELISA plate (Nunc, UK), with bovine serum albumin (0.5 % w/v, BSA, Millipore, UK) coated (negative control) and uncoated wells (blank control) at 4 °C overnight prior the assay. RBL-703/21 cells were sensitised with human IgE (1 µg/ml, monoclonal, AbD Serotec, UK) overnight at 37 °C/5 % CO₂. After 16 hours, un-sensitised and IgE sensitised cells were re-suspended in serum-free MR80/20 medium to a final concentration of 1×10⁶ cells/ml. The pre-coated ECM plate was blocked with BSA (0.5 % w/v) at room temperature for 1 hour. One group of the un-sensitised cells and the human-IgE sensitised cells were induced with either calcium ionophore A23187 (1 µg/ml, Sigma, UK) or anti-human IgE (2 µg/ml, AbD Serotech, UK). Cell suspensions (100 µl) were immediately added to each well of the plate, each condition in triplicates, and incubated for 2 hours. After incubation, the unattached cells were removed by pipetting and replenished with MR80/20 medium three times. The bound cells were stained with crystal violet (0.1 % m/v, Millipore, UK) for 10 minutes, lysed with acetic acid (10 % v/v, Fisher, UK) and read by Bio-Rad micro-well reader at 550 nm.

3.2.2 Immunofluorescence flow cytometry

The surface expression of VLA-4 integrin was analysed by flow cytometry. Normal and IgE-sensitised cells were harvested and resuspended as described above. After washing, cells were incubated in the absence or presence of calcium ionophore A23187 (1 µg/ml, Sigma, UK) or anti-human IgE (2 µg/ml, AbD Serotech, UK) at 37 °C/5 % CO₂ for 0, 5, 30, 60, 120, 180 and 240 minutes, then incubated with fluorescein isothiocyanate (FITC)-conjugated anti-human VLA-4 integrin antibody (2.5 µg/ml, Novus, UK) at for 1 hour. After two washes, cells were fixed with formaldehyde (0.5 % v/v, Sigma, UK) in PBS on ice, and analysed in a FACScan flow cytometer (Beckman-Coulter, USA), data were processed and analysed by Weasel software (WEHI, Australia).

3.3 Results

3.3.1 Inclusion of fibronectin increases adhesion

IgE-sensitised RBL-703/21 cells bound to FN in a dose-dependent manner (**Figure 3-2A**), with highest binding at a concentration of 20 $\mu\text{g}/\text{mL}$. Activation with anti-human IgE antibody enhanced cell adhesion compared with IgE alone (control, **Figure 3-2B & 3-2C**) at suboptimal FN concentrations (0.625-10 $\mu\text{g}/\text{mL}$, **Figure 3-2A**). Addition of calcium ionophore A23187 caused marked cell detachment from FN within the 2-hour incubation period (**Figure 3-2D**), even with the highest used FN concentration. Detachment of cells after activation in the absence of FN was also seen in anti-IgE stimulated cells (**Figure 3-2E**), about less pronounced than with the calcium ionophore.

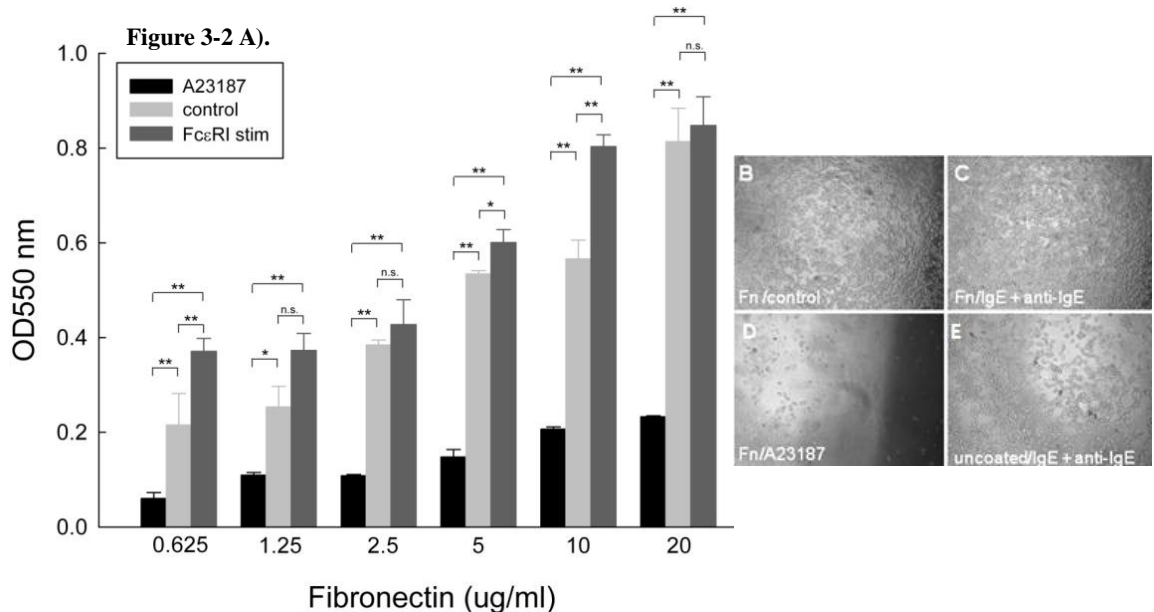


Figure 3-2. Attachment of RBL-703/21 cells to FN. A). Different concentrations of FN (0.625-20 $\mu\text{g}/\text{mL}$) were used for coating, cells were activated with 1 $\mu\text{g}/\text{mL}$ A23187, 2 $\mu\text{g}/\text{mL}$ anti-IgE, or left untreated (control). 120 minutes after activation, cells were washed three times and the amount of adherent cells quantified by a colorimetric assay using crystal violet. Data expressed are mean \pm s.d. from triplicate determinations. Representative of three independent experiments with comparable results. Asterisks show results of two-tailed t-test, n. s.: not significant, * $P < 0.05$, ** $P < 0.01$, *** $P < 0.001$. **B-E).** 50x Light microscopy magnification of RBL 703-21 cells, after 2 hours binding to 20 $\mu\text{g}/\text{mL}$ FN without stimulation **B**), activation with 2 $\mu\text{g}/\text{mL}$ anti-IgE with FN **C**), or activation with 1 $\mu\text{g}/\text{mL}$ A23187 with FN **D**), or activated with 2 $\mu\text{g}/\text{mL}$ anti-IgE without FN coating (**E**).

3.3.2 VLA-4 is strongly down-regulated by A23187 activation

Due to the strong detachment observed after A23187 stimulation, even in the presence of 20 $\mu\text{g/mL}$ FN as coating agent, the surface expression of VLA-4, the main FN receptor on RBL cells was then assessed. As shown in **Figure 3-3**, flow cytometric analysis of surface VLA-4 expression clearly demonstrated a fast down-regulation of the integrin already measurable 15 minutes after addition of A23187, reaching a maximum after 2-hour incubation, then recovering steadily in the next two hours. In contrast, IgE-dependent activation did not result in measurable changes in surface VLA-4 levels, and was very similar to sensitised, non-stimulated cells.

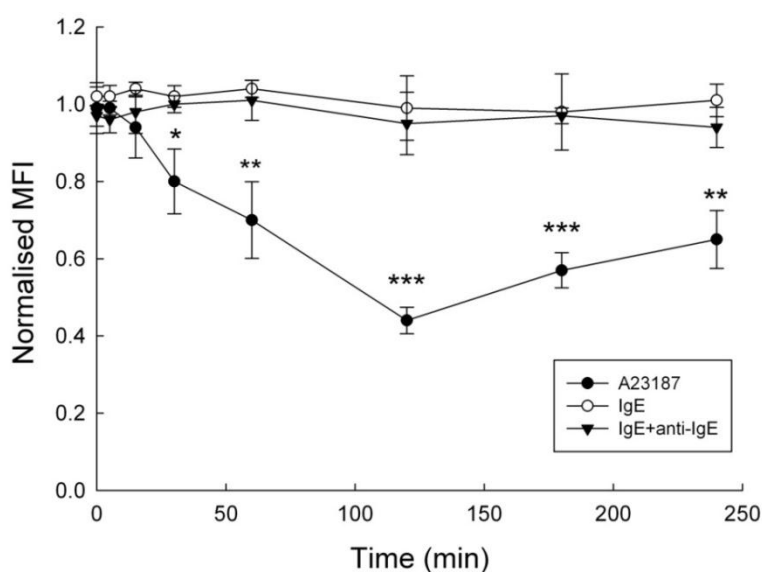


Figure 3-3. Time course of VLA-4 Integrin surface expression on RBL-703/21 cells stimulated with anti-IgE or 1 $\mu\text{g/mL}$ A23187. Data are expressed as mean \pm s.d. from three independent experiments. MFI values were normalised to 100% for the unstimulated, unsensitised cells within each experiment. Asterisks show results of two-tailed t-test, * $p < 0.05$, ** $p < 0.01$, *** $p < 0.001$ of A23187 vs. IgE + anti-IgE treatment for each time point.

The strong, progressive down-regulation of VLA-4 after A23187, but not anti-IgE stimulation, may explain the stronger and almost complete detachment of cells seen with ionophore stimulation. To the best of our knowledge, this is the first report of a differential VLA-4 integrin down regulation on RBL cells upon receptor-mediated vs. non receptor-mediated stimulation.

3.3.3 Effects of FN, CO and LA on cell attachment after activation

The effect of different ECM proteins on RBL-703/21 attachment during activation were then assessed. All three ECM were used at 20 $\mu\text{g}/\text{mL}$, which had shown the highest cell binding capability for FN. As shown in **Figure 3-4**, receptor-independent stimulation with A23187 led to more than 60 % cell detachment during washes in the presence of FN or type I CO but only approximately 25 % with LA. Fc ϵ RI-dependent stimulation appeared to lead to increased binding for FN, although this did not achieve statistical significance, but not for CO and LA. In the latter case, ionophore or Fc ϵ RI-dependent resulted in a similar loss of cells after activation despite the presence of LA; however cell detachment was less pronounced than with FN or CO. Furthermore, human with bovine FN were also compared but no difference between the two was observed (data not shown).

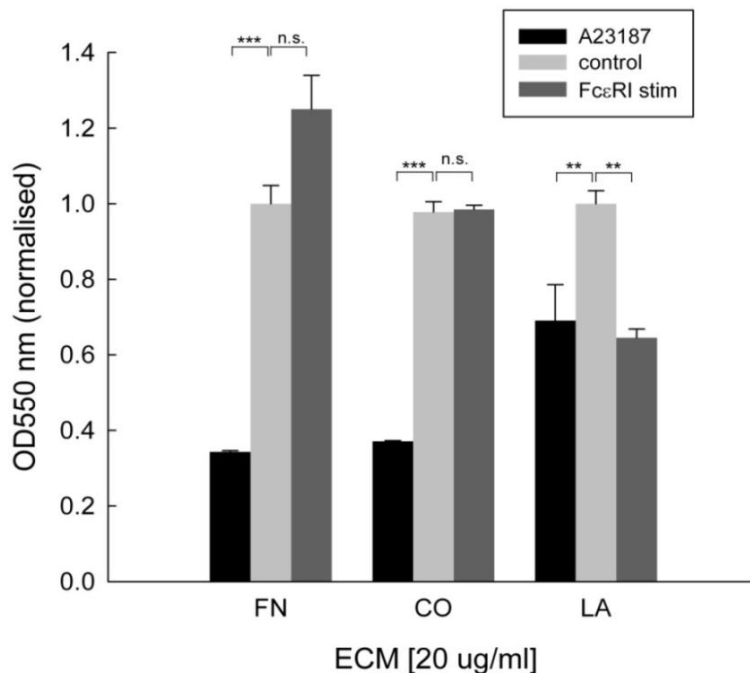


Figure 3-4. Attachment of RBL-703/21 cells to FN, type I CO or LA. 20 $\mu\text{g}/\text{mL}$ of each ECM protein was used for coating; cells were activated with 1 $\mu\text{g}/\text{mL}$ A23187, via crosslinking of Fc ϵ RI bound IgE, or left untreated (control). 120 minutes after activation, cells were washed and the amount of adherent cells quantified by a colorimetric assay using crystal violet. Data expressed are mean \pm s.d. from triplicate determinations. Asterisks show results of unpaired t-test; n.s.: not significant, ** p < 0.01, *** p < 0.001. Data were normalized for OD 550 nm of control unstimulated cells.

3.4 Discussion

In many cells, stress fibers emanate from distinct areas of the plasma membrane known as focal adhesions, where clusters of integrin receptors bind to ECM proteins. Focal adhesion proteins at the intracellular surface of the plasma membrane include vinculin, paxillin and talin, which are known to link F-actin with integrins (Krüger-Krasagakes *et al.*, 1996). Adherence to ECM-coated surfaces results in cell spreading, reorganization of cytoskeletal F-actin and the formation of surface ruffles (Hamawy *et al.*, 1992).

It was reported that treatment of RBL-2H3 cells with Ca^{2+} ionophore A23187 or anti-human IgE leads to redistribution of vinculin to the cytoskeletal fraction (Kawasugi *et al.*, 1995). Although both anti-human IgE and Ca^{2+} ionophore can lead to changes of the cell surface morphology, our adhesion experiment results showed that the surface levels of the integrin VLA-4 behave very differently between the receptor and non-receptor mediated activation pathways. As a result, while inclusion of FN in the array is important in reducing cell losses during the washing steps, A23187 but not anti-IgE stimulation leads to a pronounced RBL cell detachment after activation even in the presence of FN. Therefore, A23187 is clearly not a suitable positive control for our RBL array.

There are several reports describing an increased attachment of mast cells and basophils (Thompson *et al.*, 1990; Dastyh *et al.*, 2001) to ECM proteins after activation. In such reports, attachment of primary mast cells to ECM proteins was found to depend on pre-activation, as in the case of bone marrow-derived murine or peritoneal rat mast cells, via PMA (Dastyh *et al.*, 1991). However, such pre-activation is not necessary for RBL (Hamawy *et al.*, 1992) or MCP-5 cells (Dastyh *et al.*, 1991), which are able to attach spontaneously. Thompson *et al.* (1990) assessed that attachment of A23187 or antigen stimulated mast cells to laminin and found that approximately 20% of mast cells attached to LA. However, they did not study the detachment of previously attached cells after stimulation. Thus the apparent discrepancies between reports in the literature describing increased attachment to ECM after activation and our own, which clearly demonstrate pronounced detachment after stimulation with A23187, are due to differences in the protocol. Another, perhaps unexpected, result was the ability of CO and LA to bind the RBL

cells and prevent losses during the washing step. Ra *et al.* (1994) have found that while RBL-2H3 bound to VN and FN, they did not bind to CO and LA. However binding of RBL-2H3 cells to type I CO and LA, although less pronounced than to FN, has been described by other authors (Sarratt *et al.*, 2004). Interestingly, none of the three ECM proteins appeared to increase cell attachment after IgE dependent activation. Cell loss of CO-attached cells after A23187 treatment was very similar to FN, however cell loss with LA was far less pronounced. This suggests that the corresponding integrins, which partially overlap between CO and LA but not with FN, are also differentially regulated by A23187 activation in RBL cells.

3.5 Conclusion

In summary, the cell adhesion characteristics of different extracellular matrix proteins were assessed and showed that the inclusion of FN will greatly reduce cell losses during the washing steps. Calcium ionophore A23187 is an unsuitable positive control due to a fast down-regulation of surface expression of VLA-4 and subsequent detachment of cells. The optimised conditions will be applied for the use of humanised RBL cells in array format.

4 Monitoring of degranulation via Calcium influx measurements

4.1 Introduction

Calcium plays a central role in the modulation of basophil degranulation and cytokine synthesis triggered by the cross-linking of FcεRI and IgE complexed with allergen.

As described in chapter 1, in response to cellular processes a very small transient intracellular calcium increase is produced by binding of DAG and IP₃ to the ligand-gated channel in the endoplasmic reticulum where calcium ions are stored. This binding causes a subsequent release of calcium ions into the cytoplasm and leads to activation of the cells. The observed transient increase in Ca²⁺ concentration is not sufficient for most cellular responses but it opens calcium channels in the plasma membrane to facilitate further Ca²⁺ influx by CRAC (store-operated calcium entry) from the extracellular medium (Law *et al.*, 2011).

The rise in cytosolic Ca²⁺ is essential for regulating the activities of transcription factors (e.g. NFAT) and synthesis of cytokines. Calcium in the cytosol binds to calmodulin and activates calcineurin, which induces NFAT dephosphorylation and translocation to the nucleus and interact with AP-1 to initiate transcription of cytokine (IL-4, IL-13) gene expression (Vinita *et al.*, 2004). Moreover, calcium mobilisation is central for driving the degranulation of histamine-containing vesicles and de novo synthesis of lipid mediators (M. Law *et al.*, 2011). Therefore, the intracellular calcium measurement is critical for biological investigation of basophil degranulation and its signal transduction pathways.

Currently available Ca²⁺ probes are commercial fluorescent indicators developed in the 1980s. These fluorescein-based Ca²⁺ reagents show spectral responses upon binding Ca²⁺ and can be detected by fluorescence instruments e.g. microscopy, flow cytometry, spectroscope and microplate readers (Takahashi *et al.*, 1999).

In this chapter Fluo-4 (AM) and Premo™ Cameleon were used to detect intracellular fluctuations of calcium during RBL degranulation.

4.1.1 Fluo-4, AM

Fluo-4 AM (Invitrogen, UK) is a commercial fluorescent indicator supplied as AM (acetoxymethyl) ester that gives bright images of intracellular calcium dynamics. The indicator is essentially nonfluorescent unless bound to calcium. The most important property of Fluo-4 in cellular applications is a large fluorescence intensity increase in response to Ca^{2+} binding. The particular use of the AM ester derivative aims to help the permeability of the fluorescent dye into live cell non-invasively. Once internalised, the ester is cleaved for the release of the free acid by intracellular esterases. Pluronic F-127, a non-ionic surfactant relatively non-toxic to cells at low concentration is normally used to improve the water solubility of AM esters.

4.1.2 Premo™ Cameleon calcium sensor

Premo™ Cameleon is a commercially well-established calcium sensor system that consists of two fluorescent proteins CFP (cyan) and YFP (yellow) linked by a calmodulin binding peptide (**Figure 4-1**) and delivered by a baculovirus (BacMam) system. The system was engineered to detect calcium level by FRET (fluorescence resonance energy transfer) immediately after addition of the stimulus. The expression levels can be maintained for several days, enabling iterative assays to be run. It is supposed to be a versatile and sensitive fluorescent indicator to be used in array.

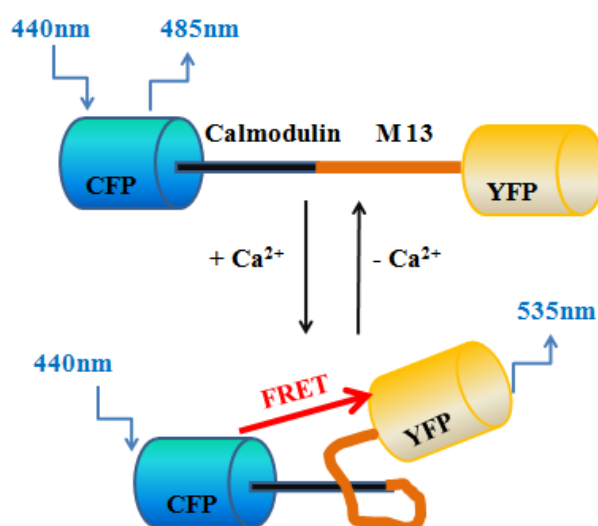


Figure 4-1. Schematic of Premo™ Cameleon Calcium Sensor mechanism. Upon binding of four Ca^{2+} ions the calmodulin-M13 moiety undergoes a marked conformational change that brings the fluorescent protein-domains into close proximity, allowing fluorescence resonance energy transfer (FRET) to occur.

4.2 Materials and Methods

4.2.1 Equipment

Unless otherwise stated, most of the readouts from this chapter were carried out using FLUOstar Optima microplate reader (BMG LAB, UK) integrated with an injection system that start the measurement immediately after injection (speed: 100 $\mu\text{l}/\text{second}$) of stimuli (**Figure 4-2**).

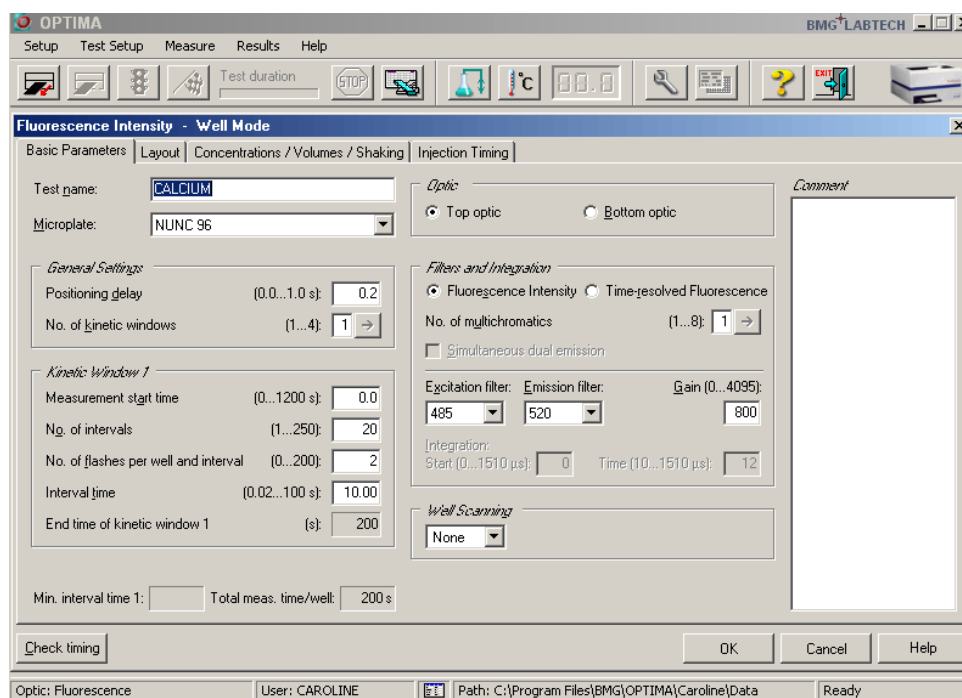


Figure 4-2. Settings overview of FLUOstar microplate reader for measuring Ca^{2+} influx.

4.2.2 Method

4.2.2.1 Fluo-4, AM

RBL-703/21 cells (2 ml of 1.5×10^6 /ml) were incubated with Fluo-4 AM (8 μM) supplemented with 15 % (v/v) pluronic F-127 for 1 hour. After two washings with MR80/20 medium, cells were re-suspended in ACB buffer (supplemented with 1.5 mM Ca^{2+}) to a final concentration of 5×10^6 /ml. Cells (100 $\mu\text{l}/\text{well}$) were loaded into a 96-well white plate (Sigma, UK). The measurement started immediately after addition of the stimuli in order to detect the very initial peak signal. Details of the optimisation of this assay are described below.

Initial step I – Titration of Fluo-4 AM

Different concentrations of Fluo-4 AM (0, 1, 2, 4, 5, 8 and 10 μM) were prepared by incubation with cells (1.5×10^6 /ml, 500 μl /well) separately in a 12-well plate for 1 hour. After two washes, cells were re-suspended in ACB buffer (supplemented with 1.5 mM Ca^{2+}) and set ready to be injected with ionophore A23187 (1 $\mu\text{g}/\text{ml}$, Sigma, UK).

Initial step II – Comparison of Fluo-4 AM with and without pluronic F-127

RBL-703/21 (1.5×10^6 /ml) cells were sensitised with human IgE (1 $\mu\text{g}/\text{ml}$, Abd Serotec, UK) overnight. Next day, the same quantity of un-sensitised and sensitised cells were incubated with Fluo-4 (8 μM) alone and Fluo-4 supplemented with 15 % pluronic F-127 separately for 1 hour. After two washes, cells were re-suspended in ACB buffer (containing 1.5 mM Ca^{2+}) to a final concentration of 1.5×10^6 cell/ml and loaded into each well of a 96-well white plate (100 μl). Stimuli solutions were prepared at the same time – calcium ionophore A23187 (1 $\mu\text{g}/\text{ml}$, Sigma, UK), phorbol myristate acetate (PMA, 10 μM , Sigma, UK), anti-human IgE (2 $\mu\text{g}/\text{ml}$, Abd Serotec, UK) before detection, then the programme was run with different stimuli injected separately.

Initial step III Calcium titration of Fluo-4 assay

RBL-703/21 cells (1.5×10^6 /ml) were incubated with Fluo4 (8 μM , supplemented with 15 % pluronic F-127) for 1 hour, then re-suspended in ACB buffer with different concentration of calcium (0, 0.5, 1, 2.5, 5, 8 and 10 mM) before adding stimuli.

4.2.2.2 Application of fluo-4 to Microarray

The optimised Fluo-4 system was then applied to a microarray-like format. Un-sensitised/IgE-sensitised cells (with Fluo-4, AM) (5×10^6 /ml) were manually loaded to FN/stimuli-pre-coated microarray slide (**Figure 4-3**) and immediately scanned by

Typhoon Trio scanner (Amersham Bioscience, Sweden). Photos were taken every 5 minutes, the fluorescence of each dot was quantitatively analysed by Image Quant software (Gel life science, USA).

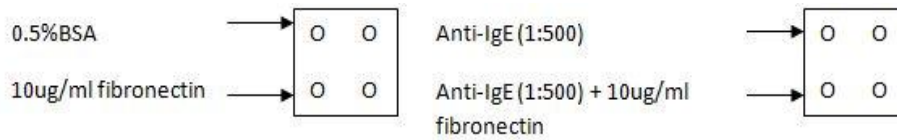


Figure 4-3. Schematic diagram of spot-printing on glass slide. 0.5 μ l of cell re-suspension was added on top of each spot just before scanning.

4.2.2.3 Premo™ Cameleon Calcium Sensor

RBL-703/21 cells (5ml/dish of 1.5×10^6 /ml) were seeded into two 10 cm petri dishes (Sigma, UK), after 4-h incubation, the supernatants were removed by pipetting and replaced by 5.5 ml/dish Cameleon Calcium Sensor (2 ml diluted in 3.5 ml D-PBS w/o Ca^{2+} / Mg^{2+}) and incubated for 4 hours with gentle rotation at room temperature. Then supernatant containing the calcium sensor was aspirated, 5 ml/dish MR80/20 medium containing 5 μ l enhancer (1000x stock in DMSO) supplied with the kit was added and incubated for 2 hours. Supernatant, containing enhancer, were then aspirated, and 5 ml/dish MR80/20 medium was added and incubated overnight. Cells in dish 2 were sensitised with 1 μ g/ml IgE. After 16-hour incubation, non-sensitised and sensitised cells were re-suspended in MR80/20 medium (without phenol red) to a final conc. of 5×10^6 /ml, then cells (100 μ l/well) were loaded into a white NUNC 96-well plate (Sigma, UK), and injected with different stimuli, signals were measured by FLUOstar every 15 seconds after injection.

4.3 Results

4.3.1 Fluo-4, AM

Initial step I – Titration of Fluo-4 AM

As shown in **Figure 4-4** the fluorescence response at 520 nm was proportional to the concentration of Fluo-4 used. Although the background increased proportionately to the quantity of Fluo-4, the calcium binding in the presence of the ionophore A23187 induced a significant signal ($p=0.015$) compared to non-stimulated cells. Later assays were fixed on a Fluo-4 at the concentration of 8 μM .

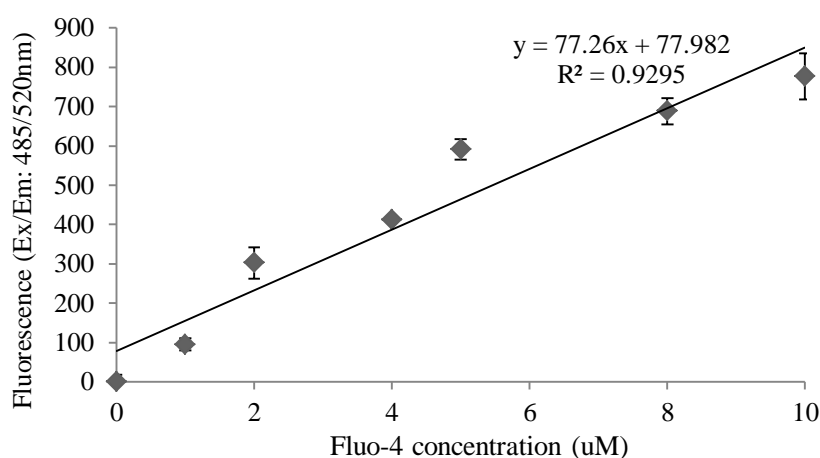


Figure 4-4. Titration of Fluo-4 AM (background subtracted). RBL-703/21 cell density: 2×10^5 /well (NUNC MaxiSorp 96-well white plate), Ca^{2+} concentration 1.5 mM.

Initial step II – Comparison of Fluo-4 AM with and without pluronic F-127

The detergent pluronic F-127 has been widely used as an aid for the Fluo-4 cellular integration (Takahashi *et al.*, 1999). In order to assess its contribution in the humanised RBL-703/21 system, different dilutions of pluronic F-127 were tested. The results (**Figure 4-5**) showed that the presence of pluronic F-127 produced an increase in the overall fluorescence for most of the conditions when compared with Fluo-4 alone. Statistically significant differences were only obtained in cells sensitised with IgE or sensitised and stimulated with anti-IgE. Hence F-127 helped to increase the aqueous solubility of the dye, therefore the mixed solution was used for all the following experiments.

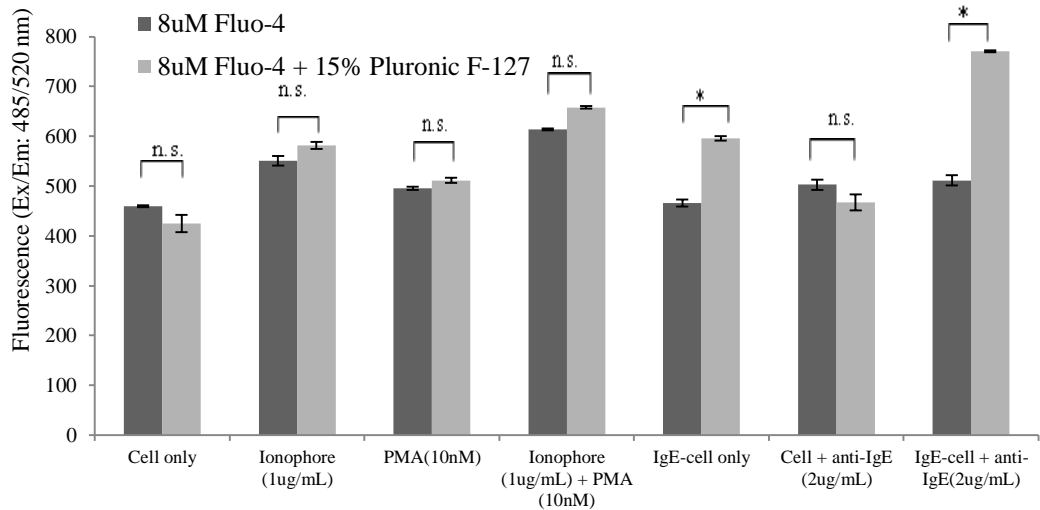


Figure 4-5. Comparison of Fluo-4 AM with or without pluronic F-127 for detection Ca^{2+} flux in RBL 703/21 cells. Cell density 1.5×10^5 /well (NUNC MaxiSorp 96-well plate), Ca^{2+} concentration 1.5 mM.

Initial step III - Calcium titration of Fluo-4 assay

In order to assess the influence of different calcium concentrations in the reaction medium (ACB buffer), a titration experiment was set up. As shown in **Figure 4-6** the signal peaked in the medium containing 0.5 mM calcium. As previous tests were all performed using 1.5mM calcium all the future tests were adjusted to use 1mM instead.

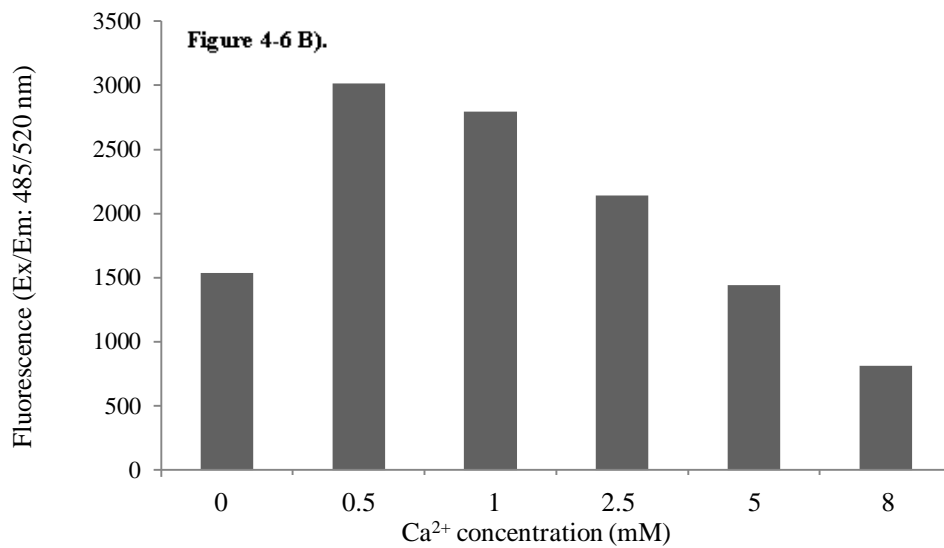
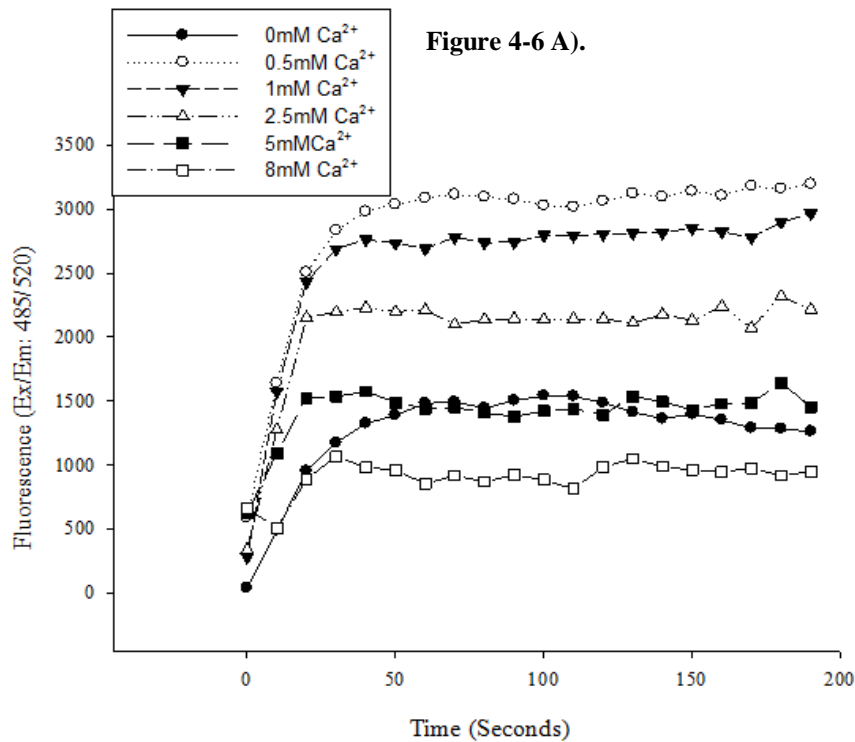


Figure 4-6. Calcium titration of Fluo-4 treated RBL-703/21. A) Fluorescence intensity of Fluo-4 treated RBL-703/21 cell within 200 seconds measurement after adding of stimuli. Cell density 2.5×10^5 /well (NUNC MaxiSorp 96-well plate). **B)** Fluorescence intensity of Fluo-4 treated RBL-703/21 cell with different Ca²⁺ concentrations at 100 seconds after injection (background subtracted).

After the initial optimization steps, several experiments were carried out in order to detect the Ca²⁺ influx of the degranulated RBL-703/21 cells by using different stimuli such as ionophore, IgE and anti-human IgE. As shown in **Figure 4-7 and 4-8** RBL703/21 cells stimulated with 1 μ g/ml ionophore A23187 produced greater signal

than the non-stimulated ones, while the presence of PMA increased the cell activation than ionophore alone (**Figure 4-7**). 1 µg/ml IgE-sensitised cells activated by 2 µg/ml anti-IgE showed significantly higher fluorescence intensity than non-sensitised and the control cells (**Figure 4-8 A**). The transient signal occurred at the very beginning of the activation – about 250 seconds, and after that the signal dropped back to half of the peak and increased steadily (**Figure 4-8 B**).

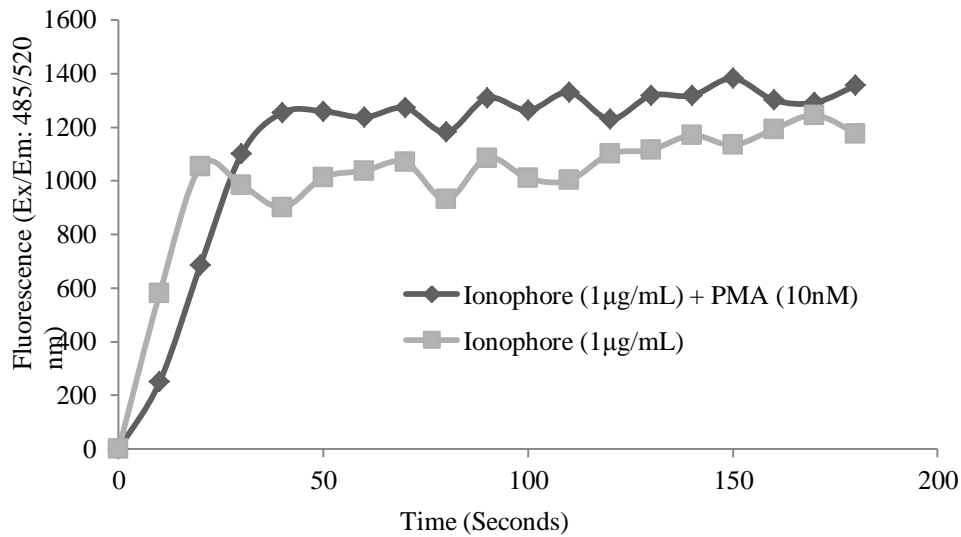


Figure 4-7. Calcium assay using optimised reaction solution - detection of Ca²⁺ level in RBL703/21 cells stimulated with ionophore A23187 only or ionophore with PMA (subtracted background, both in 1mM Ca²⁺ ACB buffer). RBL-703/21 cell concentration 4x10⁵/well (NUNC 96-well white plate).

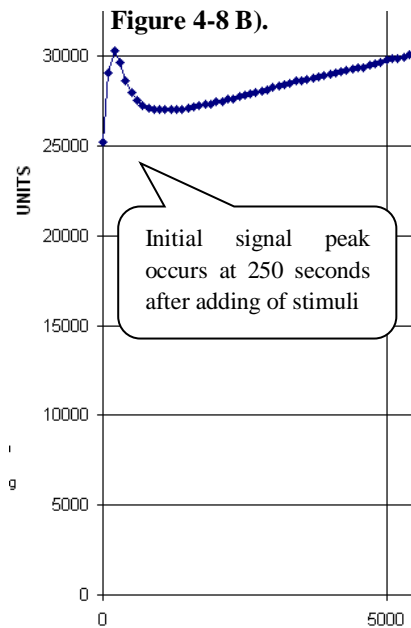
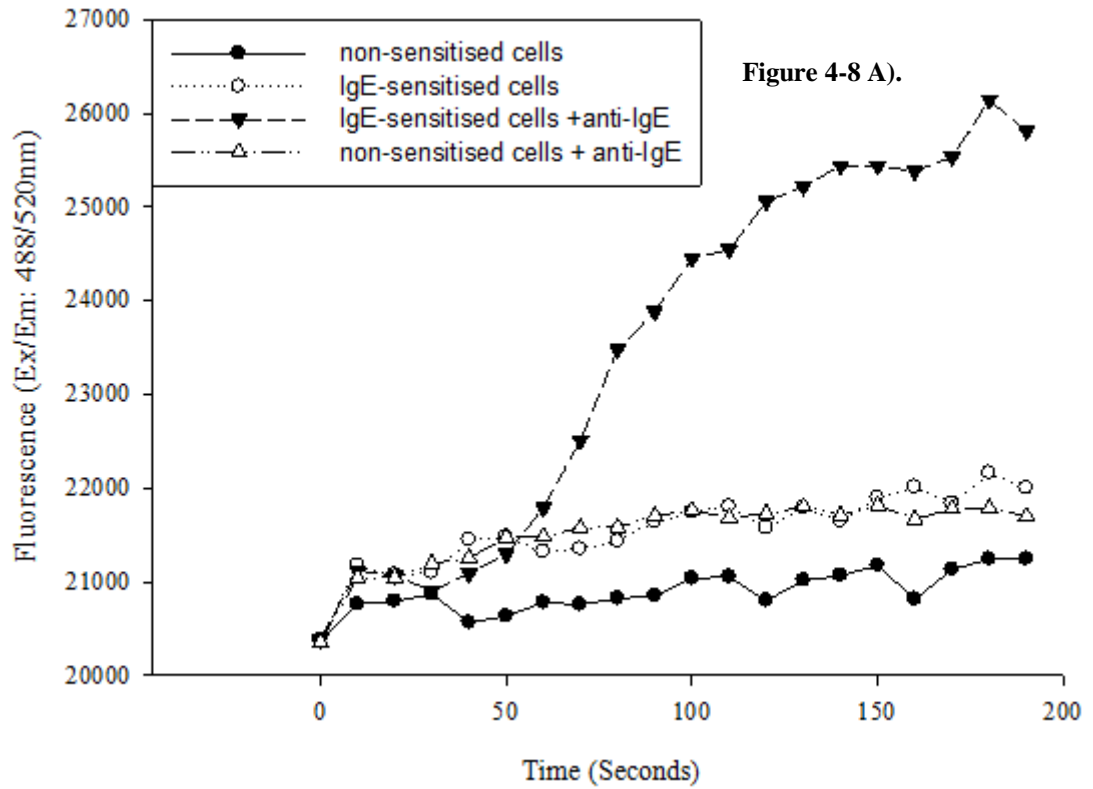


Figure 4-8. Detection of intracellular calcium level of RBL703/21 cells using the optimised assay solution. A) Within 200 seconds after injection. Cell density: 1.5×10^6 /well (NUNC 96-well white plate), Ca^{2+} conc. 1mM. **B)** Extension of measurement time to 500 seconds to monitor the intracellular calcium dynamic after cells activated by anti-human IgE (Screen print from the software).

4.3.2 Application of fluo-4 to Microarray

In order to assess whether the cells would show similar activities on array, the optimised Fluo-4 system was applied to a microarray-like format. Experiments showed that the signal stays up from the beginning to the end of the measurement (0-20 minutes) (**Figure 4-9**). Dried cells were observed after 15 minutes of scanning. There was a difference of fluorescence intensity between negative controls (0.5% BSA, IgE cells only) and the stimulated cells (anti-IgE, with or without FN).

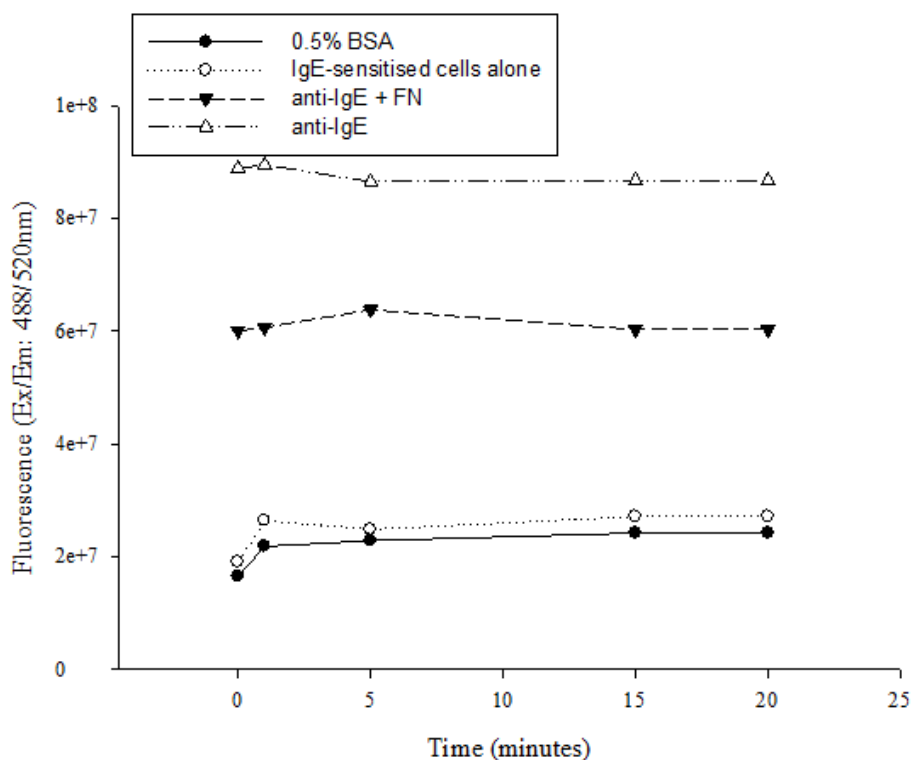


Figure 4-9. Quantitative detection of intracellular calcium influx on glass slide.

4.3.3 PremoCameleon calcium sensor

A different system using the commercially available Premo™ Cameleon was tested after Fluo-4. As expression levels can be maintained for several days, made it to be used on the microarray format. As shown in **Figure 4-10** Premo™ Cameleon treated cells stimulated with ionophore A23187 produced strong signals about 30 seconds after stimulation. Although clear positive signals could be easily detected at early time points, no activation of the sensitised RBL-703 cells (IgE/anti-human IgE stimulated cells) was observed. The signals were not different from the negative controls (non-sensitised cells) at various concentrations (results not shown).

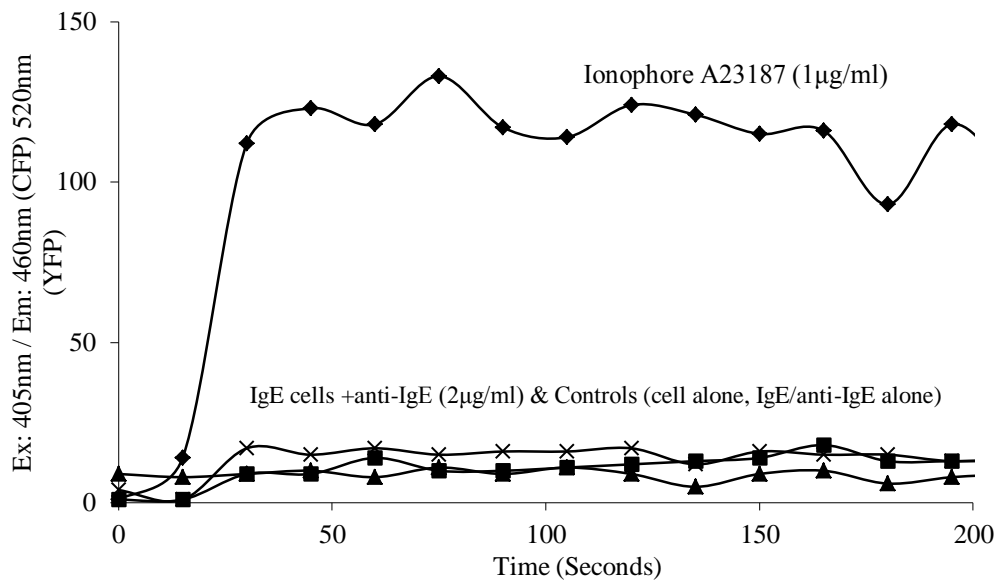


Figure 4-10. Detection of the intracellular calcium flux by FluoStar in Premo™ Cameleon treated cells within 200 seconds after injection with stimuli.

4.4 Discussion

Fluo-4 AM (or Fluo-3) has been widely used to measure calcium mobilisation in RBL-2H3 cells (Shota *et al.*, 2009). The results shown here demonstrated that Fluo-4 AM was an effective marker of calcium mobilisation for the humanised RBL-703/21 cells under different stimulations. The results are in agreement with general observation that the IgE-mediated basophil activation triggered by FcεRI causes a rapid transition to a higher cytosolic calcium level (Donald *et al.*, 2001) that is followed by a subsequent increase of calcium concentration. Several authors (Kenneth *et al.*, 2000, Ishihara *et al.*, 2006) reported that the addition of calcium ionophore together with PMA strongly enhanced the degranulation of basophils and histamine release. Our results from **Figure 4-7** clearly showed that, in the presence of PMA, the humanised RBL activation was not significantly increased when compared with ionophore alone.

The microarray results did not show the similar calcium dynamic as seen in micro-well format. The dynamic of the scanner system used in these experiments was identified as the main stumbling block for the procedure. The transient calcium activation occurs very rapidly peaking at about 200 seconds after adding the stimulus,

while the initialisation of the machine takes about 3 minutes at high resolution and the whole pad scanning time took over 5 minutes. Therefore the observed signals of the activated cells by anti-IgE did not show any change from the starting point to 20 minutes until the cells dried (after 15-minute scanning), the machine was too slow to catch the initial signal increase. This approach has been abandoned at this stage, a much higher speed system would be needed to perform these measurements.

More tests were performed on both RBL-703/21 and RBL-SX38 cell lines by using different reaction media, changing calcium concentrations, changing stimuli/calcium sensor concentrations and extending measurement times (data not shown), but in all conditions both cell lines induced with anti-human IgE did not show any difference from the negative controls. Although it was a priori an attractive system, as the calcium sensor was very effective in detecting the large intracellular influx induced by ionophore A23187, it was totally insensitive to receptor mediated activation via FcεRI and IgE. Thus the cameleon calcium sensor cannot be employed to detect intracellular fluctuations of calcium during RBL degranulation.

4.5 Conclusion

Using Fluo-4 AM can efficiently detect the intracellular calcium flux for both ionophore A23187 and anti-IgE activated basophil degranulation, but the optimised system cannot be applied properly onto microarray format currently, due to the lack of suitable equipment.

5 pNFAT-GFP&pNFAT-DsRed reporter systems

5.1 Introduction

As described in Chapter 1, crosslinking of FcεRI on mast cells and basophils induces marked gene expression of chemokines, cytokines, and other proteins (Nakamura *et al.*, 2002). A number of transcription factors participate in such responses and it has been demonstrated that nuclear factor of activated T-cells (NFAT) plays an important role in FcεRI crosslinking– induced gene expression in RBL-2H3 cells (Teshima *et al.*, 2000).

Four NFAT isoforms are reported, which are designated as NFAT1, NFAT2, NFAT3 and NFAT4 (Masuda *et al.*, 1998) and their transcriptional activity is modulated by cytoplasmic calcium levels. The crosslinking of FcεRI and IgE complex with antigen inducing basophil degranulation is known to increase intracellular calcium concentration and activation of the Ca²⁺ dependent serine phosphatase calcineurin. Active calcineurin dephosphorylates cytoplasmic NFAT which exposes NFAT nuclear-localisation signals (Siraganian *et al.*, 2003; Law *et al.*, 2006). NFATs then migrate to the nucleus where they bind to the DNA major and minor groves of many chemokines and cytokines genes at the 5' and 3' canonical recognition sequence GGAAAA of the promoter region of these genes helping the initiation of transcription (Masuda *et al.*, 1998).

As one of the main aims of this project was to produce a reporter gene system that would allow humanised basophils to respond to IgE crosslinking signals, in this chapter the design, construction and initial testing of commercial and in-house constructed NFAT-responsive fluorescent reporter genes are described.

5.2 Materials and methods

5.2.1 Plasmids

Five plasmids either purchased from commercial companies or constructed in our lab were used to develop the fluorescence system, details are described below.

pEGFP-Tub (Stratagene, USA, plasmid map in [Appendix II](#)) a commercial plasmid encoding a fusion protein - a derivative of the GFP mut1 variant consisting of the red-shifted, human codon-optimized green fluorescent protein (EGFP), which encodes human α -tubulin. This plasmid possesses the constitutive CMV promoter and was used as a control to optimise the transfection settings and the green fluorescence system at the initial stage. pNFAT-hrGFP (Stratagene, USA, plasmid map in [Appendix II](#)), a commercial plasmid encodes a humanised *Renilla* green fluorescence protein (hrGFP) reporter gene that is terminated by a SV40 poly A signal gene. The reporter gene expression is driven by a human NFAT promoter region. This vector was used as a source of the NFAT enhancer element. pDsRed-Express 2-1 (Clontech, USA, plasmid map in [Appendix II](#)), a vector encoding the constitutive expression of DsRed-Express2 and was used as a control for the red fluorescence system. pUB6/V5-His A (Invitrogen, UK, plasmid map in [Appendix II](#)), plasmid encodes blasticidin S resistance was used as a base vector for the construction of new plasmid.

pNFAT-DsRed (pUB6/V5-His A, **Figure 5-1**). Following the diagram shown in **Figure 5-2** the pNFAT-DsRed was generated by removing and replacing the BglIII/EcoRI and EcoRI/XhoI of the pUB6/V5-His with NFAT promoter sequence (996bp) from pNFAT-hrGFP and DsRed reporter region from pDsRed-Express2-1 (678bp) (Sequences see [Appendix II](#)).

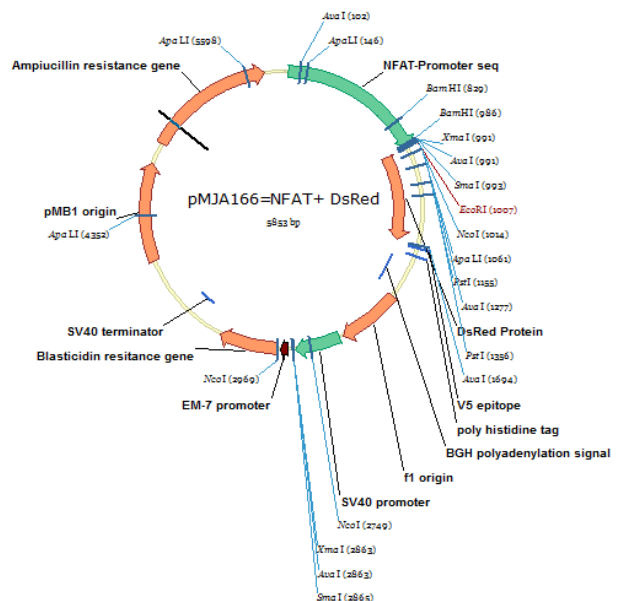


Figure 5-1. Plasmid map of pNFAT-DsRed (pUB6/V5-His A).

5.2.2 Plasmid construction

The whole processes were shown as flow diagram in **Figure 5-2**.

Oligonucleotides primers were ordered from Sigma Genosys UK (Table 7, [Appendix III](#)). Dried DNA oligos were resuspended in sterile water (RNase/Dnase free) to make a final concentration of 10 μ M and kept at -20 °C.

PCR reactions (100 μ l) were set up (Table 8, [Appendix III](#)) in 0.2 ml thin walled PCR tubes (Starlab, UK) in a GeneAmp PCR system 9700 Thermal Cycler (Life technologies, USA). The $MgCl_2$ concentration was optimised to 4.5 mM and annealing temperature was experimentally adjusted to 61 °C. A reaction programme would have 94 °C/1 minute, annealing/1minute and 72 °C/1minute for 35 cycles, using plasmid pDsRed-Express2-1 as template (0.04 μ g) and primers DsRed + **EcoRI** (Forward) ATATAATAGAATTCAACCATGGATAGCACTGGAACGTCATCAAG and DsRed + **XhoI** (Reverse) ATATTTAATCTCGAGCTACTGGAACAGGTGGTGGCGG produced a 678bp fragment; using pNFAT-hrGFP as template (0.024 μ g) and primers NFAT + **BglIII** (Forward) ATAATTAAAGATCTGCAGAACTGTGAATGCGCAAACC and NFAT + **EcoRI** (Reverse) ATAATTAATGAATTCGAGCTCGGTACC CGG produced a 996bp fragment.

For detection, the amplified fragments (5 μ l) were mixed with 1x blue loading buffer (7 μ l) and run alongside 1kb DNA Ladders (Promega, UK) in 1.5 % agarose gels with 1.6 μ g/ml ethidium bromide (Sigma, UK) in 1xTAE buffer (Fisher, UK) at 100 V for 90 minutes then imaged by Gel doc 2000 (Bio-Rad, UK).

The (678 and 996 bp) PCR products were purified using QIAquick PCR Purification Kit (Qiagen, Germany) before setting up the restriction digest with BglIII/EcoRI and EcoRI/XhoI (All from Promega, UK) separately at 37 °C for 3 hours (Table 9, [Appendix III](#)), then enzymes were heat inactivated at 65 °C for 20 minutes. pUB6/V5-His A was double digested using BglIII and EcoRI at 37 °C for 3 hours. The restricted plasmid fragments (1300 and 4163 bp) were isolated in agarose gels, cut off, purified and extracted using QIAquick Gel Extraction Kit (Qiagen, Germany).

Ligation of NFAT+BglIII/EcoRI and the digested pUB6/V5-His A were carried out in a 3 insert: 1vector molar ratio at 25 °C for 1 hour and incubating overnight at 12 °C

(Table 10, [Appendix III](#)). The ligated product was transformed by either electroporation into (50 µl) JM109E. coli (Invitrogen, UK) in 1 mm cuvette by a MicroPulser electroporator (Bio-Rad, UK) or heat shocking into TOP10 Eco.li (Invitrogen, USA) in PCR tubes. Positive colonies were screened directly by PCR using primers NFAT+BglIII/EcoRI at the same conditions as described above. Colonies containing the 996 bp fragments were grown in larger flasks and plasmid DNA extracted and purified using Maxiprep DNA extraction kit (Qiagen, Germany) in order to make large frozen stocks.

The NFAT- pUB6/V5-His A was digested again by EcoRI and XhoI and ligated with DsRed +EcoRI/XhoI (Table 11 and 12, [Appendix III](#)). The ligated product was transformed and the positive colonies were purified by MaxiSorp same as described above.

Glycerol stocks were made by inoculating single colonies with LB medium with appropriate antibiotics and growing at 37 °C with 220 rpm overnight, then mixed with sterile glycerol (Thermo Scientific, UK) to make a final concentration of 30 % v/v glycerol, and flash frozen in CryoTube vials (Nunc, Denmark) by liquid nitrogen and long-term stored at -80 °C.

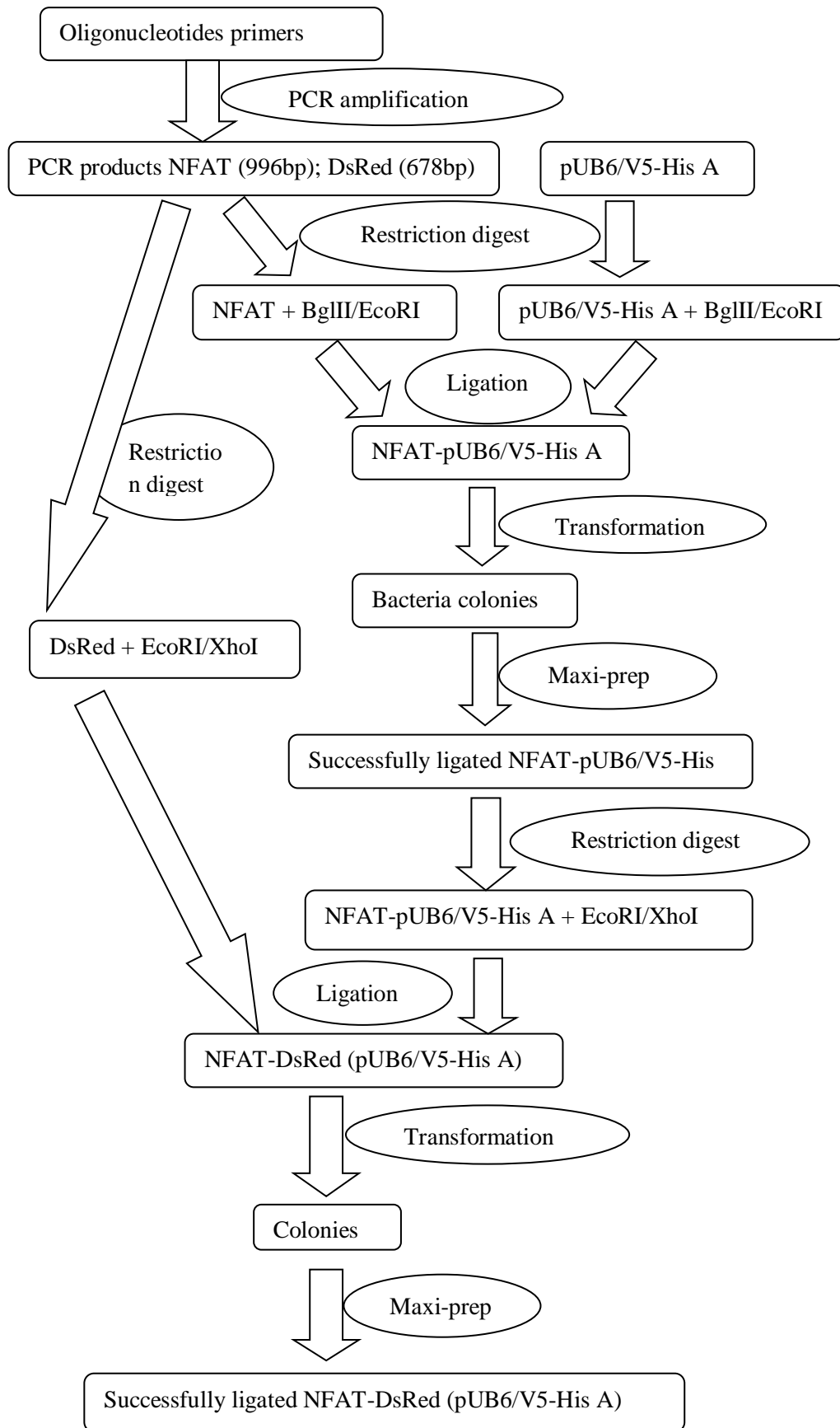


Figure 5-2. Flow diagram showing the cloning strategy and steps for obtaining the NFAT-DsRed plasmid.

5.2.3 Transfection

Frozen *E. coli* glycerol stocks of successfully transformed bacteria were inoculated into 150 ml LB medium with appropriate antibiotics, and grown at 37 °C with 225 rpm overnight. After harvesting (6000 g/15 minutes centrifugation), the plasmid DNA was purified by QIAGEN Plasmid Maxi-Prep Kit (QIAGEN, Germany) following the manufacturer's protocol. Plasmid concentrations were measured by NanoDrop (Thermo Scientific, UK).

RBL-703/21 (and RBL-SX38) cells were harvested and resuspended in Dulbecco's modified Eagle's medium with L-glutamine (DMEM; Sigma, UK) containing 10 % FBS (GIBCO,UK), 100 I.U./ml penicillin, 100 µg/ml streptomycin and 1 mM sodium pyruvate (Sigma, UK) at concentration of 4×10^7 cells/ml. 4×10^6 cells (100 µl) were mixed with 15 µg of plasmid and electroporated in a 0.4 cm cuvette (Bio-Rad, USA) at 250 V and 250 µF capacitance (Gene Pulser Xcell, Bio-Rad, USA). The transfected cells were immediately transferred into 12-well plates with pre-warmed antibiotic-free MR80/20 medium and kept in a 37 °C/5 % CO₂ humidified cell incubator.

For analysis of transient transfection, transfected cells were stimulated with either 1 µg/ml calcium ionophore A23187 (Sigma, UK) or 2 µg/ml anti-human IgE antibody (AbD Serotech, UK) after 24 hours of electroporation. Photos of fluorescent cells were taken by microscope Leica DFC420 (Leica Microsystems, Switzerland) at 100x magnification.

To obtain stable transfected pNFAT-GFP and pNFAT-DsRed cells were selected in, previously optimised 600 µg/ml hygromycin B (Thermo Scientific, UK) and 20 µg/ml blasticidin S (Invitrogen, Canada) respectively. After 4-weeks of antibiotic selection (**Figure 5-5**) the stably transfected cells were sensitised with 1 µg/ml human IgE (AbD Serotech, UK) and induced with 2 µg/ml anti-human-IgE antibody (AbD Serotech, UK). The highest responder clones (between 7 % - 15 % of total clones) were sorted out by Coulter Altra Flow Cytometer and MoFlo Cell Sorter (both Beckman Coulter, USA). The latter equipment was capable of sorting out single cells into each well of a 96-well plate with medium. The sorted stable transfectants were used in the following experiments.

5.2.4 Initial optimisation tests

Preliminary test I – Time course

Non-sensitised and human-IgE sensitised pNFAT-hrGFP-RBL703/21 cells (96-well plate, 3×10^4 cell/well) were stimulated by ionophore A23187 (1 μ g/ml) and anti-IgE (2 μ g/ml) separately for 30 hours in MR80/20 (80 % MEM, 20 % RPMI-1640, phenol red-free) medium supplemented with 1.5 mM Ca^{2+} . Photos were taken for every 2 hours for up to 30 hours and fluorescence intensities were measured by FluoStar micro-well reader at excitation/emission of 485/520 nm (BMG, UK).

Preliminary test II – Calcium

As the extracellular calcium level is essential for the activation of basophils, a series titration of calcium concentrations in reaction medium was tested. Briefly, non-sensitised pNFAT-hrGFP-RBL703/21 cells were resuspended in medium containing same amount of calcium ionophore A23187 (1 μ g/ml) but different concentrations of calcium (0, 1.5, 3, 5, 10, 15, 20, 25 and 30 mM). IgE sensitised cells were then resuspended in medium containing the same amount of anti-IgE (2 μ g/ml) and different concentrations of calcium. All samples were loaded separately in fibronectin (10 μ g/ml) pre-coated plates (384-well plate, 3×10^4 cell/well) at 37 °C for 24 hours. After this incubation, the fluorescence signals were measured by Typhoon scanner at Ex/Em 488/520 nm, and quantitatively analysed by Image Quant software.

Preliminary test III – IgE titration

Cells (20 μ g/ml fibronectin pre-coated 384-well plate, 3×10^4 cell/well) were sensitised with series concentrations from 1, 0.5, 0.2, 0.125 to 0.1 μ g/ml (1:1000, 1:2000, 1:5000, 1:8000 and 1:10000 dilutions) of 1 mg/ml stock human-IgE (AbD Serotech, UK) overnight, next day stimulated by different concentration of 1mg/ml stock anti-IgE from 2, 1, 0.75 to 0.5 μ g/ml (1:500, 1:1000, 1:1500 and 1:2000 dilutions) for 24 hours in MR80/20 medium supplemented with 20 mM Ca^{2+} . Photos were taken by fluorescence microscopy (Leica DFC420, Leica Microsystems, Switzerland) and signal intensities were quantitatively measured by Typhoon scanner and Image Quant.

5.3 Results

5.3.1 Plasmid construction

The ligated plasmids pNFAT-DsRed (-pUB6/V5-His) was analysed by amplifying with primers to detect the specific target sequences. As shown in **Figure 5-3**, the amplification products (DsRed+EcoRI/XhoI and NFAT+BglII/EcoRI) generated strong bands containing DNA fragments at desired size on the agarose gel, which indicating the presence of the target (DsRed-678 bp and NFAT – 996 bp) sequences in the constructed plasmid.

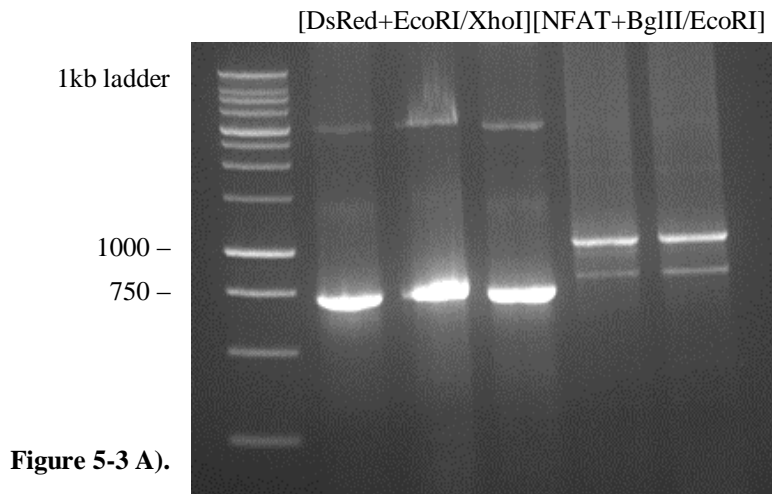


Figure 5-3 A).

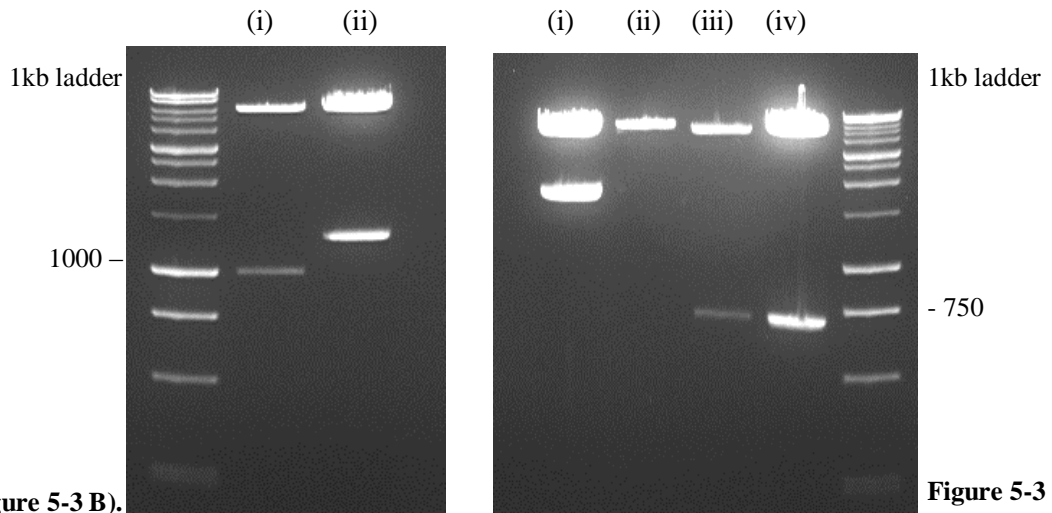


Figure 5-3 B).

Figure 5-3 C).

Figure 5-3. Analysis of ligation products on agarose gel. **A)** Amplifying primers (DsRed+EcoRI/XhoI and NFAT+BglII/EcoRI) with NFAT-DsRed -pUB6/V5-His. **B)** Comparison of original and NFAT-ligated pUB6/V5-His A by double digestion, (i) NFAT--pUB6/V5-His, (ii) Original pUB6/V5-His A. **C)** Comparison of NFAT-pUB6/V5-His A and NFAT-DsRed-pUB6/V5-His A by double digestion of EcoRI/XhoI sites. (i) NFAT-pUB6/V5-His A (ii) undigested pUB6/V5-His A (iii) & (iv) NFAT-DsRed (pUB6/V5-His A).

5.3.2 Transfection

5.3.2.1 Optimisation of transfection

The electroporation settings were optimised by using RBL-703/21 cells and pEGFP-Tub plasmid. Different voltages and capacitances were tested using the same quantity of cells and plasmid. The transfection efficiencies (**Table 5-1&5-2, Figure 5-4**) were compared to determine the optimal electroporation settings of the electroporator. The transfection efficiency was determined by the transfection rate in each condition: Transfection Rate (TR %) = No. of green cells/No. of total cells in the same area in each well.

Voltage & Capacitance	Total viable cells	Green cells	TR%	
250 V&250 μ F (control)	560	-	-	
250 V&250 μ F	205	83	40 %	Average: 37.5 %
	476	210	44 %	
	410	120	29 %	
	520	191	37 %	
250 V&500 μ F	406	-	-	

Table 5-1. TR% of pEGFP-Tub transfected into RBL-2H3 cells at different capacitance.

Voltage & Capacitance	Total viable cells	Green cells	TR%	
200 V& 250 μ F	99	10	10 %	Average: 6.20 %
	206	12	5.8 0%	
	208	7	3.40 %	
	320	18	5.60 %	
250V & 250 μ F	205	83	40 %	Average: 37.50 %
	476	210	44 %	
	410	120	29 %	
	520	191	37 %	
300 V& 250 μ F	431	21	4.90 %	Average: 3.60 %
	412	11	2.70 %	
	438	14	3.20%	
	890	33	3.70 %	

Table 5-2. TR% of pEGFP-Tub transfected into RBL-2H3 cells at different voltages.

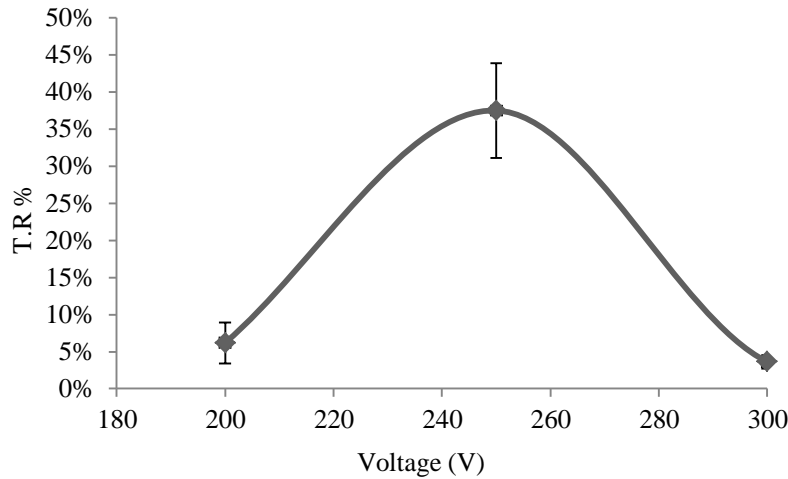


Figure 5-4. TR% of pEGFP-Tub plasmid transfected into RBL-2H3 cells at different voltages.

5.3.2.2 Transfection of plasmids and cell sorting

Both green and red fluorescence were seen after transfection of RBL-703/21 cells with constitutive GFP or DsRed reporter plasmid (**Figure 5-5**).

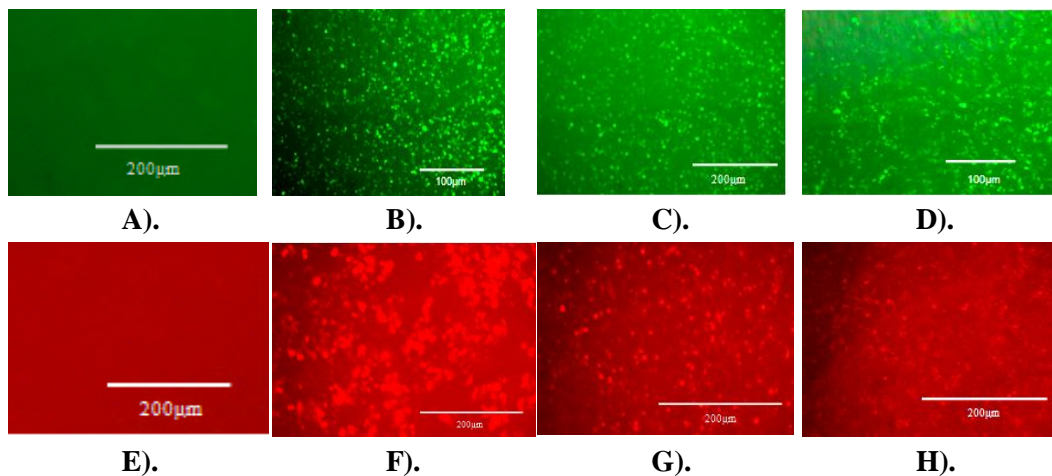
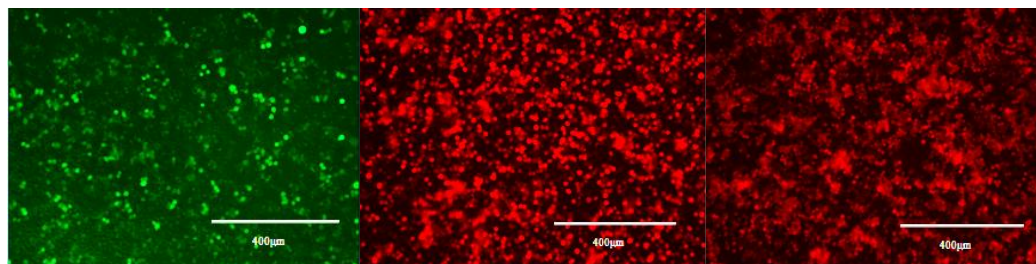


Figure 5-5. Transient transfection of RBL-703/21 with pNFAT-hrGFP or pNFAT-DsRed with different stimuli after 48 hours of electroporation. Stimuli were added after 24 hours of transfection and photos were taken after 24 hours stimulation by Leica DFC420 (Leica Microsystems, Switzerland) (bright field and RBL-SX38 not shown). Low proportion of both cell lines transfected with both responded by either ionophore A23187 or anti-IgE stimulation. **A)** Cell only without plasmid. **B)** Cell with pEGFP-Tub. **C)** Cell transiently transfected with pNFAT-hrGFP stimulated with ionophore A23187. **D)** Cells transiently transfected with pNFAT-hrGFP induced with IgE/anti-IgE. **E)** Cells only without plasmid. **F)** Cells with constitutive DsRed-Express 2-1. **G)** Cells transiently transfected with NFAT-DsRed stimulated with ionophore A23187. **H)** Cells transiently transfected with pNFAT-DsRed sensitised with IgE and induced with anti-IgE.

After 1 month's antibiotic selection of RBL-703/21 (or RBL-SX38) with NFAT-GFP and NFAT-DsRed, The cells were sorted by flow cytometer and the stable transfected cell lines were tested with anti-IgE and compared. **Figure 5-6** showed that pNFAT-DsRed-RBL-703/21 cells had the strongest signal intensity with high brightness and lower background than pNFAT-hrGFP-RBL703/21 and pNFAT-DsRed- RBL-SX38 cells, under the same stimulations and settings, therefore the pNFAT-DsRed- RBL-703/21 was employed for future system optimisation and real serum testing.



pNFAT-hrGFP-RBL703/21 pNFAT-DsRed- RBL-703/21 pNFAT-DsRed- RBL-SX38

Figure 5-6. Fluorescent intensity of RBL-703/21 and RBL SX38 transfected with NFAT-GFP or NFAT-DsRed after 1 month's antibiotic selection by anti-IgE (2 µg/ml) stimulation. pNFAT-hrGFP-RBL703/21: RBL-703/21 transfected with pNFAT-hrGFP. **pNFAT-DsRed-RBL-703/21:** RBL-703/21 transfected with NFAT-DsRed. **pNFAT-DsRed-RBL-SX38:** RBL-SX38 transfected with NFAT-DsRed. Photos taken by EVOS *fl* Digital Inverted microscope (AMG, Seattle, USA).

5.3.3 Initial optimisation tests

After cell sorting, a series of preliminary optimisation tests were carried out using pNFAT-hrGFP transfected RBL-703/21 as the DsRed plasmid was not available at the initial stage, some of the key tests and results are described here.

Preliminary test I – Time course

The fluorescence of cells induced by either ionophore A23187 or anti-IgE was detected about 8 hours after stimulation. **Figure 5-7** showed that with the presence of ionophore, intensity increased steadily and reached a peak at about 20 hours, then began to decrease; anti-IgE peaked at about 24-26 hours stimulation. Stimulation between 20-24 hours was considered the best period to detect the cell activation.

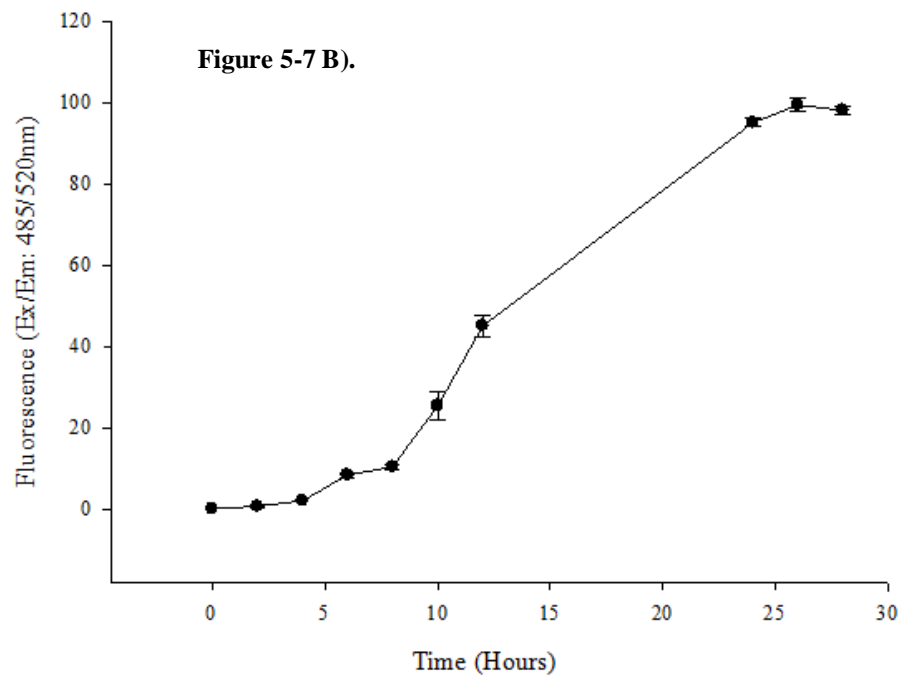
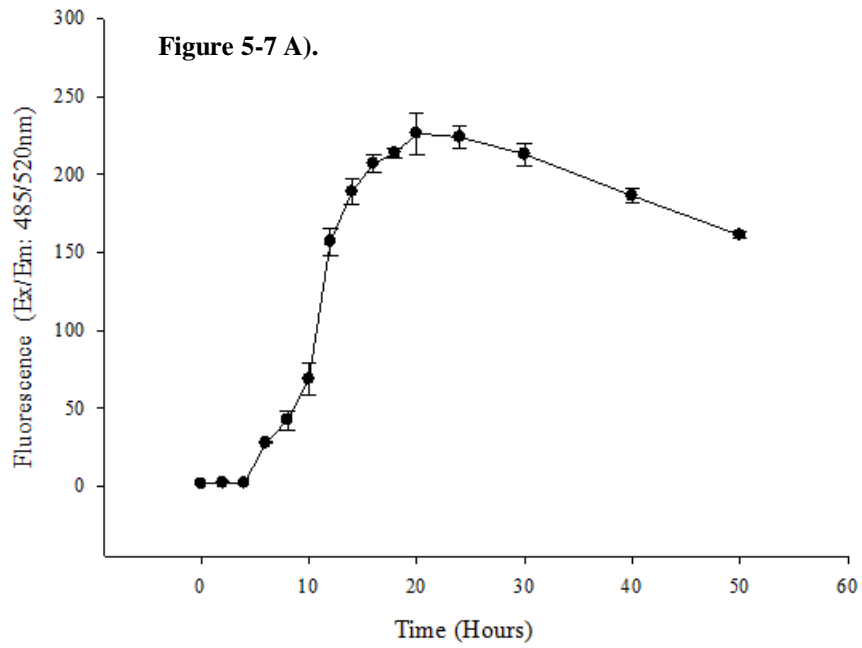


Figure 5-7. Fluorescence intensity time-course of pNFAT-hrGFP-RBL-703/21 cells by different stimulations in MR80/20 (1.5 mM Ca²⁺) at 37 °C/5 %CO₂ by FluoStar micro-well reader (background subtracted). A) 1 µg/ml ionophore A23187 stimulation. B) 2 µg/ml anti-IgE stimulation.

Preliminary test II – Calcium

As shown in **Figure 5-8**, background levels raised with increasing Ca^{2+} concentration. Fluorescence intensity of pNFAT-DsRed-RBL-703/21 cells induced by anti-IgE significantly increased and peaked at 20 mM. Cells stimulated by ionophore A23187 decreased steadily from low to higher calcium concentration, which means the activation of basophils by receptor-dependent and non-receptor dependent requires different extracellular calcium level. So 1 mM was chosen as optimal calcium concentration for future ionophore and 20 mM for IgE/anti-IgE stimulation.

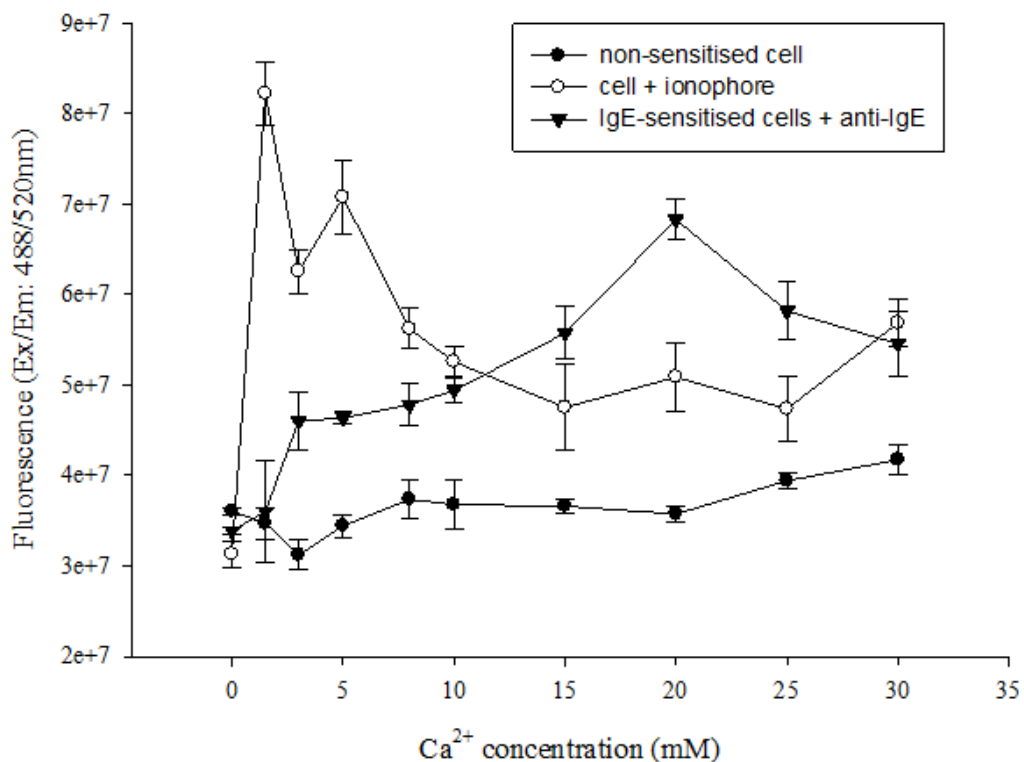


Figure 5-8. Calcium titration of pNFAT-hrGFP-RBL-703/21 under different stimulations. Fluorescence intensity detected by Typhoon.

Preliminary test III – IgE titration

Figure 5-9 showed that fluorescence intensity is IgE-dependent, which reflected that the cells' degranulation level is IgE-dependent. The signal intensity was significantly reduced from IgE 1, 0.5, 0.2, 0.125 to 0.1 $\mu\text{g}/\text{ml}$ (1:1000 to 1:10000 dilutions), and there were almost undetectable levels at IgE 1:10000. No significant differences were observed between 2, 1, 0.75 to 0.5 $\mu\text{g}/\text{ml}$ (1:500 to 1:2000) of anti-IgE with the same

concentration of IgE. So future tests were fixed on using combination of 1 μ g/ml IgE (1:1000 dilution) and 2 μ g/ml anti-IgE (1:500 dilution).

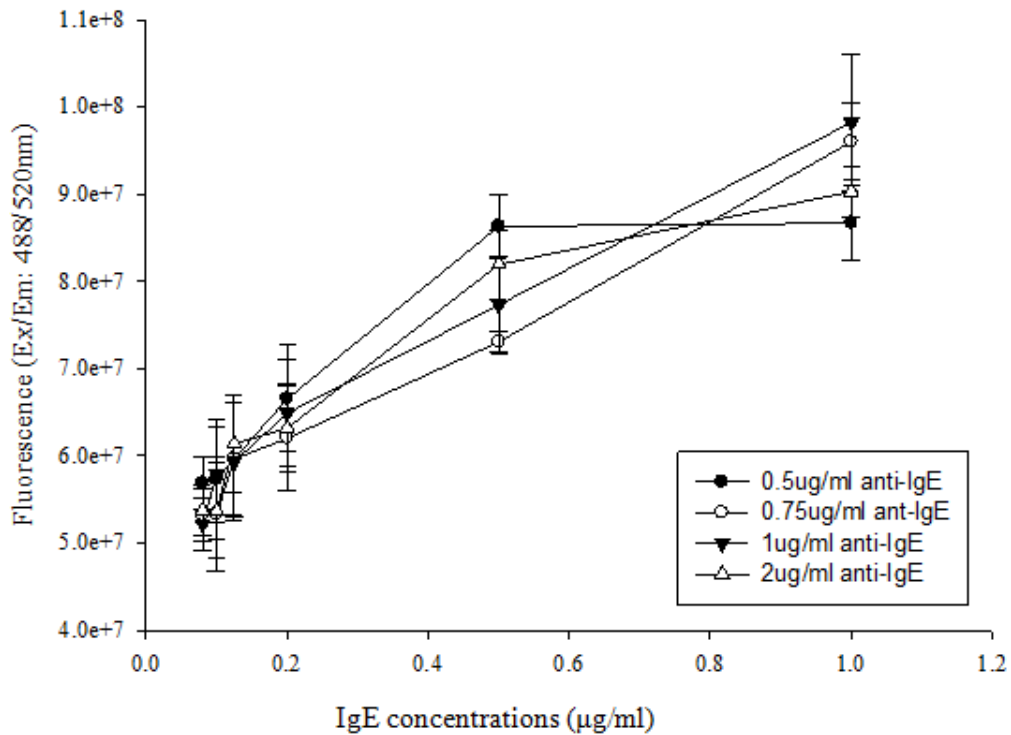


Figure 5-9. IgE/anti-IgE titration of pNFAT-hrGFP transfected RBL-703/21 cells after 24 hours stimulation in MR80/20 medium supplemented with 20 mM Ca²⁺. Fluorescence intensity detected by Typhoon scanner (Ex/Em 488/520, PMT 450, Normal sensitivity, pixel 10 μ M).

Although the initial series of the detailed optimisation experiments were carried out using the pNFAT-hrGFP transfected cells, once the NFAT-DsRed cells were available they have shown similar overall behaviour (results not shown). Due to their improved signal to background response, only the pNFAT-DsRed transfected RBL-703/21 system was used in the following experiments.

5.3.4 Time-lapse of activation of pNFAT-DsRed-RBL-703/21 cells

In the final stage of the project, an advanced microscope able to image time-lapse of living cells – Leica SP2 spectra confocal laser scanning microscope (Leica, Germany) was used. This machine is equipped with heating stage and CO₂ incubation which is particularly useful for imaging longer time-lapse and multi-channel of cultured/fluorescent cells. In order to test this microscope, a glass-bottomed multi-channel plate (Lab-Tek, NUNC, USA) was used to culture either non-stimulated and anti-IgE stimulated, photos were taken automatically by the camera equipped with the microscope every hour.

Figure 5-10 showed that, cells were activated at different timing, except a few the most auto-fluorescent cells, cells stimulated with 2 µg/ml anti-IgE start to produce signals after eight hours stimulation. Cells (**Figure 5-11**) that attached to each other were more likely to start to produce signals than the isolated ones, also it can be seen that, many cells intended to initiatively link with the fluorescent cells to activate themselves. Cell activity cannot be captured from time zero of adding stimuli, as the microscope required the cells to be firmly bound to the bottom of the plate before putting them into the chamber (which always took about 2 hours), also the setting of the microscope needed to be adjusted and optimised every time after loading cells, therefore normally the first 3-4 hours activities of stimulated cells cannot be observed, but this can be assumed as no signals from either photos taken in this part or from before.

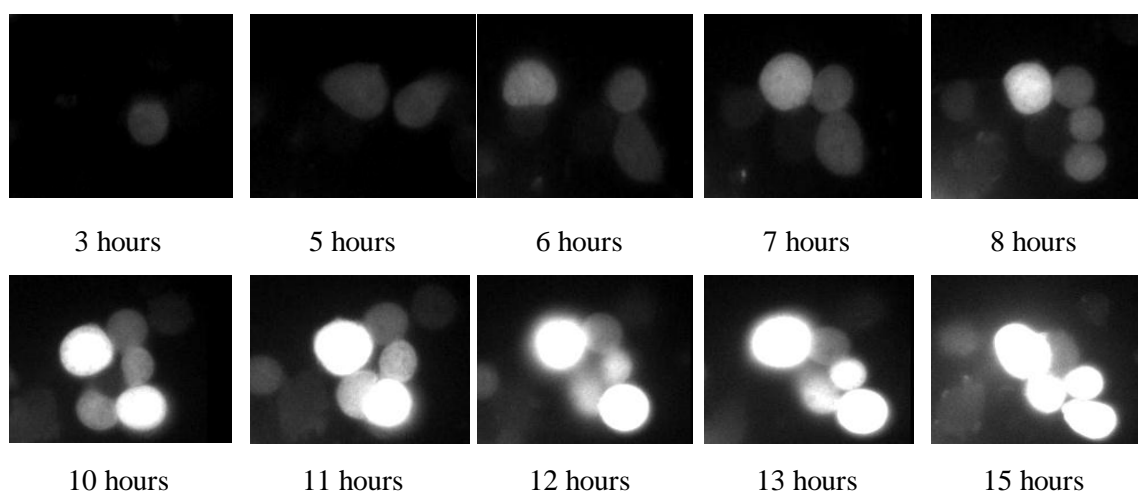


Figure 5-10. Time-lapse of anti-IgE induced pNFAT-DsRed transfected RBL-703/21 cells by Leica SP2.

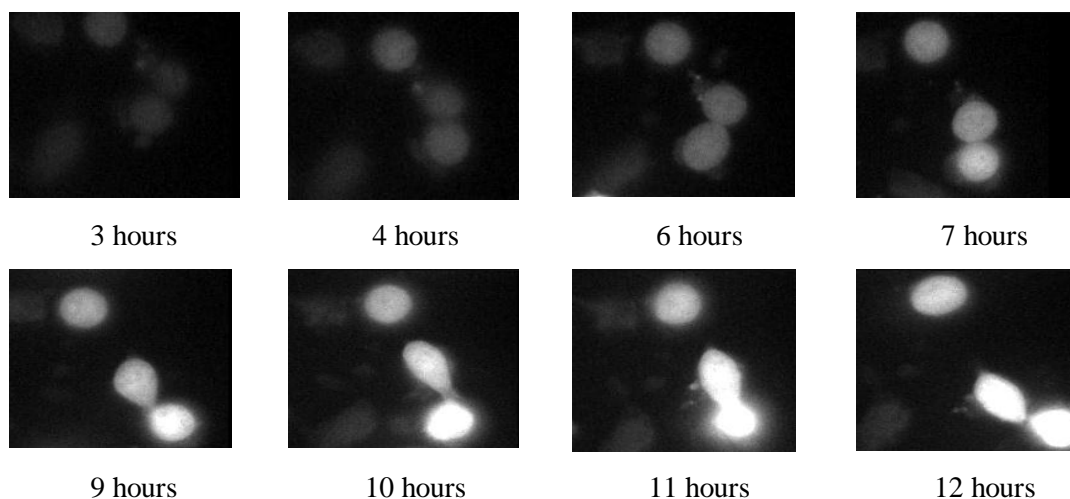


Figure 5-11. Time-lapse of anti-IgE induced pNFAT-DsRed transfected RBL-703/21 cells by Leica SP2.

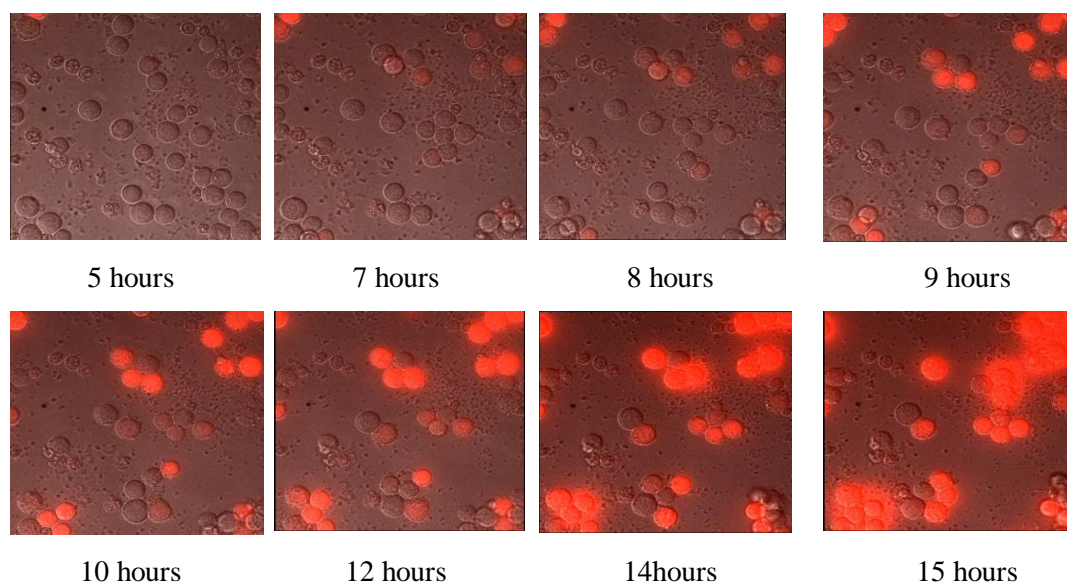


Figure 5-12. Overlay of fluorescent vs. bright field of time-lapse of anti-IgE induced pNFAT-DsRed transfected RBL-703/21 cells by Image J.

By using Leica SP2 and Image J, the activity of single cells can be more accurately observed and tracked, which was very helpful for us to understand the whole activation process of cells under different stimulations.

5.4 Discussion

The reporter systems described here, including four consecutive NFAT binding sites can be used efficiently to display RBL activation. Both GFP and DsRed humanised reporter cell lines showed the expected stable and efficient response to IgE/anti-IgE stimulation in micro-well format. A similar NFAT-luciferase reporter system has been recently reported by Nakamura *et al.* (2010) for diagnostic purpose. Highly sensitive the luciferase-based systems require cell lysis before measurement of luciferase activity. As our aim was to develop an automated detection system which can be used for array format, the luciferase system was not convenient as the lysis step will disconnect the signal from its exact position on the array. The fluorescent reporter system as reported here was much more suitable for the microarray system, as the fluorescent proteins produced are retained within intact cells without further incubation or processing and enable direct measurement by fluorescent scanners.

During the process of obtaining the fluorescent reported cells we observed that the quantities of both successfully transfected cells increased with ascending voltages, but so did the number of total dead cells resulted (data not shown), we therefore chose a compromise, 250V&250 μ F as the optimal electroporation settings.

According to Nakamura *et al.* (2010), with adding of deuterium oxide, the degranulations of RBLs were potentiated and the mediators released were increased. Our results showed that cells did not respond at all in ACB buffer containing deuterated water either induced by ionophore A23187 or anti -IgE after 24 hours stimulation. One possible reason for this might be the lack of essential nutrients in ACB buffer to support the longer incubation time (24 hour vs. 1 hour for biochemical test), therefore cells may not survive in ACB buffer for longer period of time exceeding 1 hour and no signals were produced. Cells incubated with mixtures of MR80/20 medium and ACB buffer (or D₂O alone) were tested, but generated much lower signals than using MR80/20 medium alone (data not shown). Therefore, although ACB buffer containing deuterated water was the most suitable medium for biochemical test, it is not suitable for our fluorescent reporter assay, as it needs longer incubation.

After the optimisation stage, some more tests were carried out using this cell line with human sera, but without much success. After further investigation it was clear

that the cells were too old to behaviour as well as before. This means that the condition of the cells needs to be monitored frequently and always use low passage number of the transfected cells, which generates more consistent results (passage <45) for all the tests (make large quantity of frozen stock).

5.5 Conclusion

The NFAT fluorescent reporter system was stable functional and generated detectable fluorescence after stimulation by anti-human IgE. These optimised conditions were used for testing of well characterised sera from allergic patients in the next chapter.

6 Real sera test

6.1 Introduction

In vitro diagnosis of allergy is usually performed by measuring levels of allergen-specific IgE (sIgE) in patients' serum. Traditionally each suspected allergen is tested individually in an expensive and time consuming protocol that requires large amounts of serum. More recently, technological advances have enabled the simultaneous assessment of specific IgE levels for hundreds allergens, either using multiplex flow cytometry (Pomponi *et al.*, 2012) or allergen arrays (Shreffler *et al.*, 2012; King *et al.*, 2007). While these new technologies in combination with recombinant or purified allergens allow component resolved diagnosis of allergic sensitization (De knop *et al.*, 2010), there are still unsolved issues regarding the clinical relevance of specific IgE measurements. The existence of specific IgE binding does not always correlate with clinical symptoms. False positive results obtained due to cross-reactivities with pan-allergens or IgE directed against cross reactive carbohydrate determinants (CCDs) may not have the ability to engage surface-bound IgE productively on mast cells and basophils and are thus often clinically irrelevant (Jin *et al.*, 2008; Altmann *et al.*, 2007).

A recent study described that the concordance between sIgE measurements and skin prick tests (SPT) in allergy to cow's milk and hen's egg is unexpectedly low (Mehl *et al.*, 2012). Similar inconsistencies between tests have also been reported for allergy to hymenoptera venom (Strum *et al.*, 2011). As a result, diagnosis of Type 1 Allergy is still best performed using a combination of *in vitro* specific IgE, SPT, clinical history, and, in the case of food allergy, oral challenge tests (Hamilton *et al.*, 2010).

Thus there is clearly a need for more clinically relevant diagnostic methods. In previous communications (Lin *et al.*, 2007) the Nottingham group had presented the proof of principle that combining the high throughput capacity of protein microarrays with the biological response of a cell system (basophil) might result in a significant improvement to allergy diagnosis.

In order to achieve this ultimate goal in the present study, the optimised pNFAT reporter system was tested with patients' sera against extracts or pure recombinant allergens in a micro-well format and the functionality and sensitivity of the system was evaluated.

6.2 Materials and methods

6.2.1 Sera characteristics and allergens

Human sera used in this chapter were selected samples obtained from several clinical studies carried out by collaborators in Rome and Copenhagen. Patients' sera from different suppliers were analysed by different methods with database of IgE levels. As shown in **Table 6-1**, skin prick test (SPT) of Arg#19 generated a high positive response to grass pollen; patients Adr-Ref (par j 2), Dan#7 and Dan#8 were all very allergic to the corresponding allergens*; the fluorescent intensity of protein-microarray obtained in the lab quantitatively reflects the IgE levels in Arg#19 and FW were very high to the allergens stated in the table.

Sera	Clinical database		
	SPT	ISAC IgE	Microarray
Arg#19	Grass pollen (3)	-	Grass pollen (41946)
Adr-Ref.	-	Bet v 1 (0) Bet v 2 (0) Par j 2 (55.59)	-
Adr # 54449	-	Par j 2 (42.59)	-
Dan#7	-	Bet v 1 (39.98) Phlp 1 (17.08)	-
Dan #18	-	Bet v 1 (6.92) Phlp 1 (10.81) Phlp 2 (19.11) Phlp 6 (9.22)	-
FW	-	-	House dust mite (37126)

Table 6-1. Clinical database data of sera tested. * IgE antibody results of ISAC standardised units (ISU) are indirectly linked to the WHO IRP 75/502 IgE, 1IU = 2.4ng IgE, the converted data that greater than 15 means very high IgE level.

Allergen	Suppliers
Ber e 1 (- control) (1 mg/ml)	purified in the lab
Bet v 1 & 2 (birch (<i>Betula verrucosa</i>) pollen) (1 mg/ml)	Biomay AG, Vienna, Austria
Phl p 1,2,6 (Phleum pollen (<i>Phleum pratense</i>)) (1 mg/ml)	
Par j 2 (<i>Parietaria judaica</i> pollen) (1 mg/ml)	Bial Industrial Farmacéutica S.A, Bilbao, Spain
<i>D. Pteronyssinus</i> (10 mg/ml)	GreerLab UK
<i>D. Farinae</i> (10 mg/ml)	
<i>Secale cereal</i> (10 mg/ml)	
<i>Sorghum halepense</i> (10 mg/ml)	

Table 6-2. Purified recombinant allergens and sources.

6.2.2 Methods

Initial and optimisation tests

Briefly, pNFAT-DsRed-RBL-703/21 or pNFAT-hrGFP-RBL/703/21 cells were resuspended to a final concentration of 1.5×10^6 cells/ml in MR80/20 medium, part of the cells were sensitised with 1 $\mu\text{g/ml}$ human IgE or different dilutions of patients' sera, 5×10^4 cells (30 μl) of non-sensitised and sensitised cells were loaded into 20 $\mu\text{g/ml}$ -fibronectin-coated 384-well plate (Nunc, Denmark) after washing and incubated at 37 °C/5 %CO₂ overnight. After 16 hours, the 384-well plate was washed and a series dilution of allergens (1 $\mu\text{g/ml}$ to 0.1 pg/ml) depend on the experiments in MR80/20 medium (w/o phenol red) supplemented with 20 mM Ca²⁺ were added into each well and incubated for 24 hours then scanned by Typhoon at Ex/Em 488/520 nm for GFP and 532/580 nm for DsRed with 600 PMT at normal sensitivity. β -hexosaminidase assay (described in chapter 2) was carried out in some experiments to monitor the biochemical degranulation ability of the tested cells. Alterations of individual experiments are indicated on the legend of the figures.

Time course during cytotoxicity reduction tests

RBL-2H3 cells were re-suspended in MR80/20 medium to a final concentration of 1.5×10^6 cells/ml, then loaded (500 μl cells) to individual 12-well plate to let them adherence to the bottom. Dan #19 serum (12.5 μl) was added to each well (1:40 dilution) and incubated for different period (0-24 hours) at 37 °C/5 %CO₂. Supernatant from each well was transferred to sterile eppendorfs and centrifuged at 500 g for 10 minutes, clear supernatant was then added to wells with pNFAT-hrGFP or pNFAT-DsRed-RBL-703/21 cells to start sensitisation.

Zeiss confocal microscope

A polypropylene flat bottom 96 well plates (Costar, UK) was coated with 20 $\mu\text{g/ml}$ fibronectin or 100 pg/ml Par j 2 in 20 $\mu\text{g/ml}$ fibronectin at 4°C overnight, pNFAT-DsRed cells were sensitised with 1:50 dilution of patient's serum at 37 °C/5 % CO₂ overnight. After 16 hours, all wells were washed 5 times by PBS and sterile air dried,

non-sensitised and serum-sensitised cells were resuspended in MR80/20 medium to a final concentration of 1×10^6 cells/ml, 100 μ l (1×10^5 cells/well) was added to each well and incubated for 20 hours. After that, cells were stained by 1 μ g/ml Hoechst 33342 (Life technology, UK) for 20 minutes in the dark, then measured by a Zeiss confocal microscope by Texas red and DAPI (LSM501uv META combi, Carl Zeiss AG, USA).

6.3 Results

As previously mentioned (Chapter 5) the pNFAT-DsRed (or -hrGFP) -RBL-703/21 cells were able to show activation in a synthetic IgE-anti-IgE system or in the presence of ionophore. In order to test whether these cells would be sensitive enough to detect real human sera against allergen mixtures, the following experiments were carried out.

6.3.1 Initial tests

At the initial stages, patients' sera (Arg#19 and FW) that showed high fluorescent intensity of IgE levels from protein microarray were tested against allergen extracts.

Initial test I

As shown in **Figure 6-1**, although a dose response curve of allergen extract concentration x fluorescence after 24-hour stimulation was observed, the differences between the allergen alone (-) and incubation with serum-sensitised cells for both grass pollen tested was small. The controls wells have clearly shown that the cells without the extracts possessed low fluorescence and that the cell endogenous fluorescence was able to be induced by IgE/anti IgE. Therefore the high fluorescence obtained with grass pollen treated cells was originated from the pollen autofluorescence (S.C. (-) and S.H. (-) in **Figure 6-1 A**). To confirm this, β -hexosaminidase assay was carried out with the same dilutions of serum and allergens. The results shown in **Figure 6-2** confirmed that there were little differences between non-sensitised and sensitised cells incubated with all dilutions of both grass pollen, hence the fluorescence observed was mainly correlated to the levels of allergen in the plate.

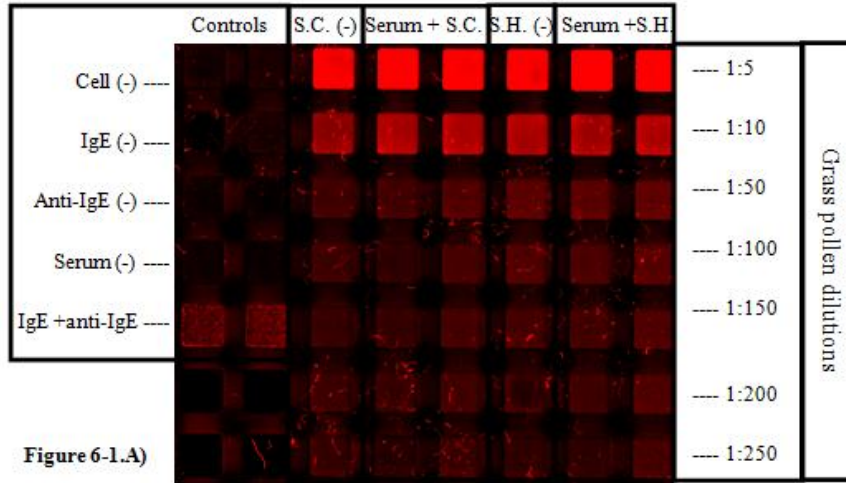


Figure 6-1.A)

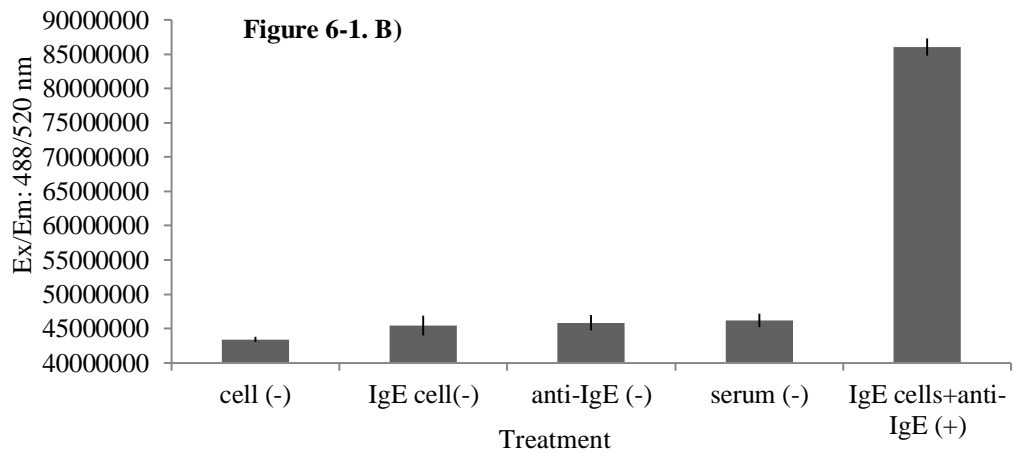


Figure 6-1. B)

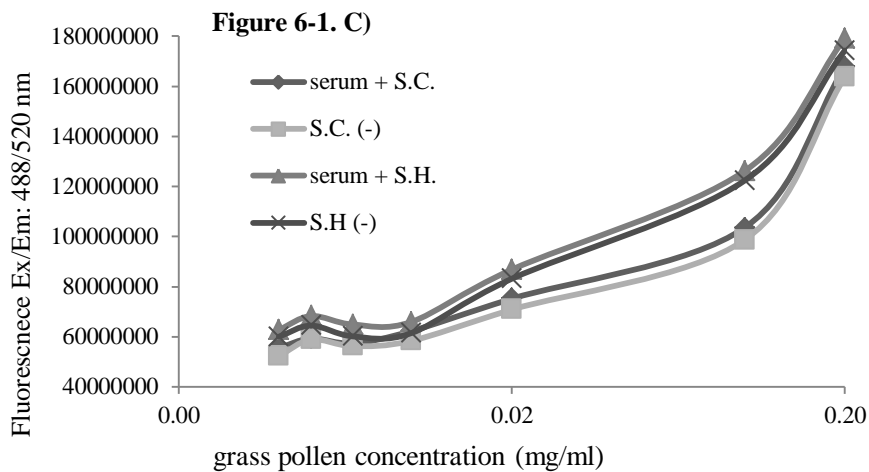


Figure 6-1. C)

Figure 6-1. Fluorescent intensity of serum Arg #19 (1:10 dilution) sensitised pNFAT-hrGFP-RBL-703/21 cells after 24-hour stimulation with Grass pollen (S.H.--*sorghum halepense* and S.C.—*secale cereale*) extracts. A) Typhoon image B) Reading of controls with unstimulated cells (cell (-)), cells sensitized with IgE but unstimulated (IgE (-)), unsensitized and anti-IgE stimulated cells (anti-IgE (-)), serum sensitized, unstimulated cells (serum (-)) and IgE-sensitized and anti IgE stimulated cells (IgE+ anti-IgE (+)). C) Reading of grass pollen between 0.004 mg/ml to 0.2 mg/ml (1:5 to 1:250 dilutions) alone (S.C./S.H. (-)) or with serum-sensitized cells (serum + S.C./S.H.).

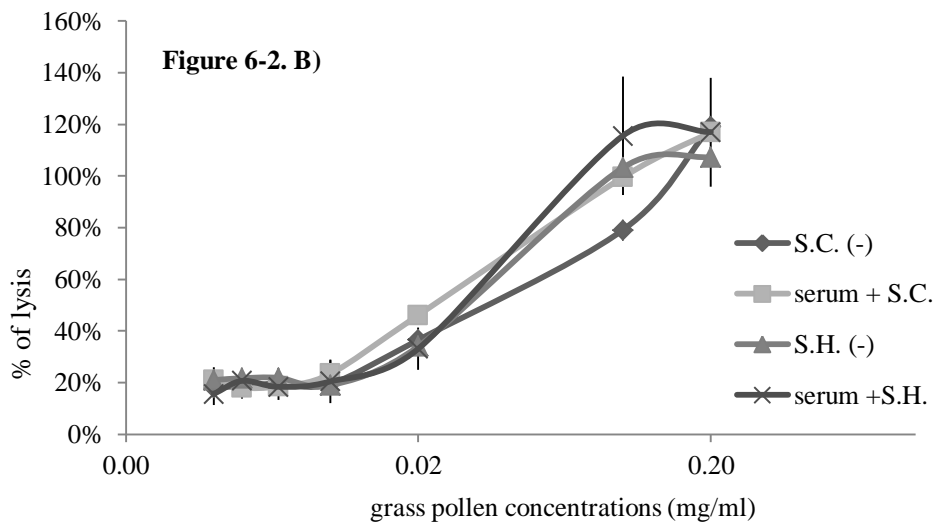
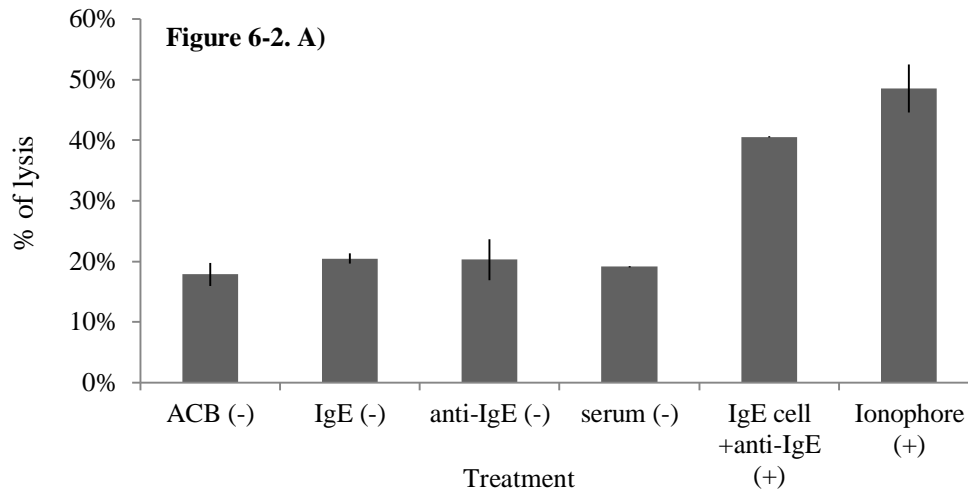
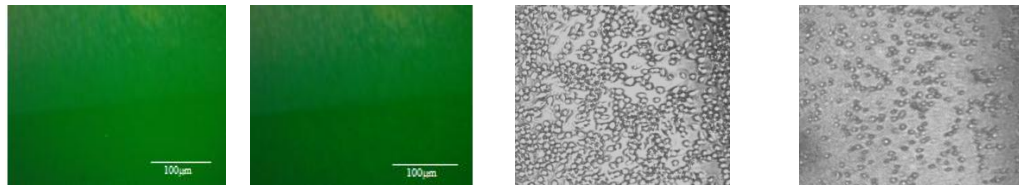


Figure 6-2. β -hexosaminidase assay of serum Arg #19 sensitised pNFAT-hrGFP-RBL-703/21 cells induced by grass pollen. A) Controls. B) Grass pollen between 0.004 mg/ml to 0.2 mg/ml (1:5 to 1:250 dilutions) alone or with serum-sensitised cells.

When cells containing the grass pollen extracts were observed under the microscope (**Figure 6-3**), it clearly showed that with the presence of both types of pollen, almost no fluorescence signals (**B**) of induced cells could be observed. This meant that there was almost no activation of this patient's serum sensitised cells stimulated by either type of grass pollen. Furthermore, cells died (**D**) after 24-hour incubation, which suggested that these allergen extracts are toxic to cells at high concentrations.



A) S.C./S.H. (-) B) sensitised cells + S.C./S.H. C) Cells in medium D) Cells with S.C./S.H.

Figure 6-3. Fluorescent and morphology of pNFAT-hrGFP-RBL-703/21 cells with grass pollen extract at 1:5 dilution after 24-hour stimulation (magnification 100x). A) Grass pollen with un-sensitised cells. **B)** Grass pollen with serum-sensitised cells. **C)** Non-sensitised cells alone in medium. **D)** Un-sensitised cells incubated with grass pollen.

Initial test II

Due to their high content of carotene and fluorescence compounds pollen the autofluorescence of pollen was to be expected. In order to confirm whether other common extracts will show the same level of interference, a well characterised house dust mite serum FW was then employed. Firstly, the serum was titrated with 2 µg/ml anti-IgE using pNFAT-hrGFP-RBL-703/21 cells and scanned by Typhoon. **Figure 6-4** showed the fluorescence signal peaked at 1:40 dilutions, which was used as optimal serum concentration for following test.

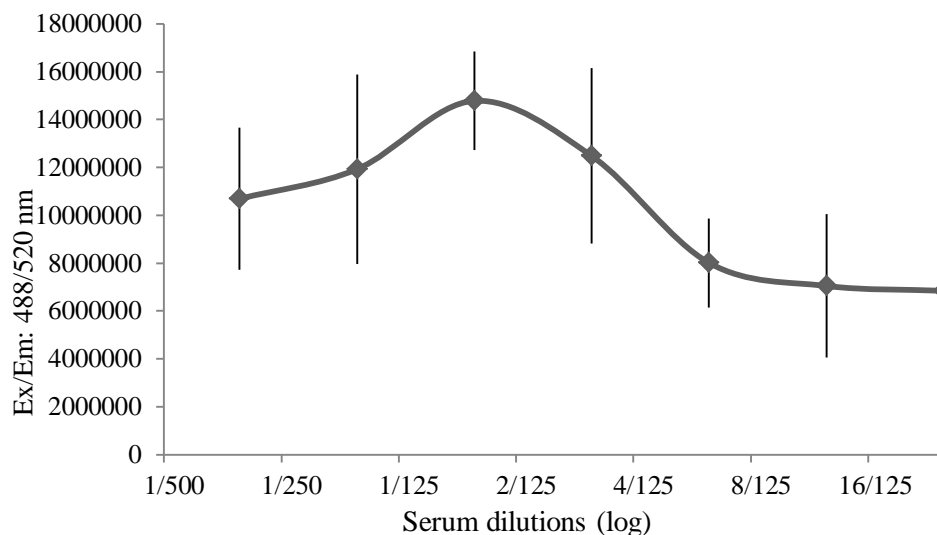
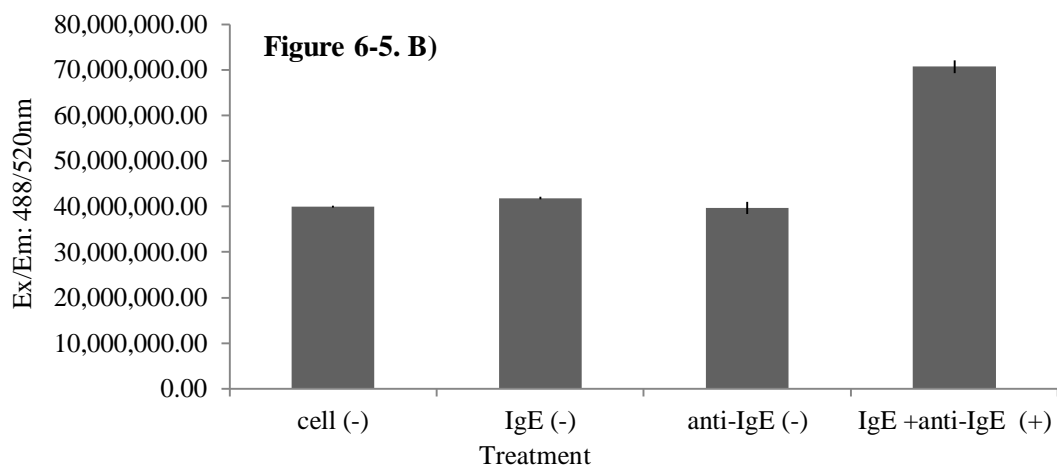
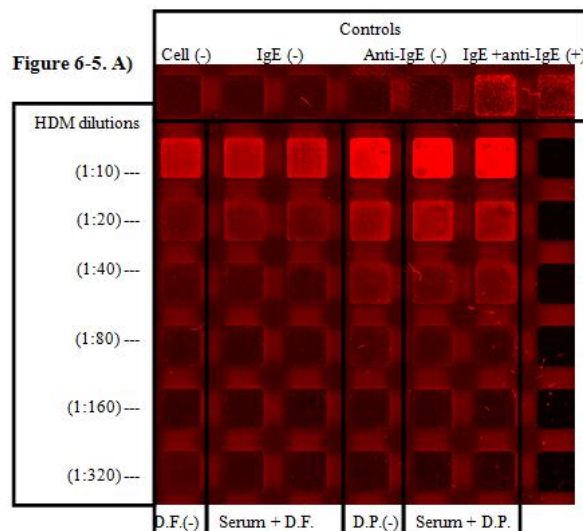


Figure 6-4. Fluorescence intensity of FW's serum sensitised pNFAT-hrGFP-RBL-703/21 cells stimulated by 2 µg/ml anti-IgE (subtracted by background). FW's serum in 1:10, 1:20, 1:30, 1:40, 1:80, 1:160 and 1:320 dilutions. **A)** Typhoon image. **B)** Readings of fluorescent intensity.

This patient was characterised as clinically allergic to house dust mites (HDM), 1:40 dilution of the serum was tested against with a series dilutions of two types of HDM: *D. Pteronyssinus* and *D. Farinae*. **Figure 6-5 & 6-6** showed very similar results to Arg#19 (**Figure 6-1**). From both biochemical and fluorescent intensity, very little differences between non-sensitised and sensitised incubated with all dilutions of both HDM were observed, which meant that there was almost no activation of patient's serum sensitised cells stimulated by either *D. Pteronyssinus* (D.P.) or *D. Farinae* (D.F.). Also these allergen extracts were auto-fluorescent and shown possess a β -hexosaminidase activity without the presence of sera. Very few faint fluorescent cells in the wells with high concentration of HDM were observed after 24-hour incubation under microscope, which meant that the fluorescent intensity imaged by typhoon was from the allergen extracts.



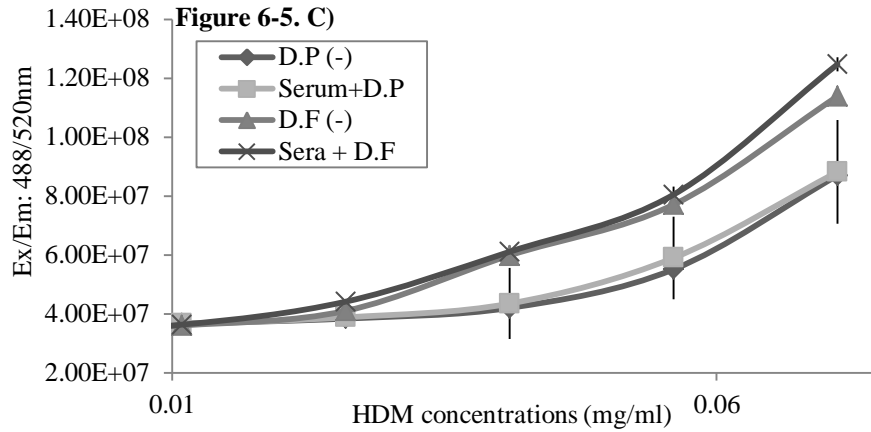


Figure 6-5. Fluorescence intensity of FW's serum (1:40 dilution) sensitised pNFAT-hrGFP-RBL-703/21 cells induced by HDM. A) Typhoon image. B) Reading of controls. C) Reading of HDM from 0.0625 mg/ml to 0.1 mg/ml (1:10, 1:20, 1:40, 1:80, 1:160 and 1:320 dilutions) alone or with serum-sensitised cells.

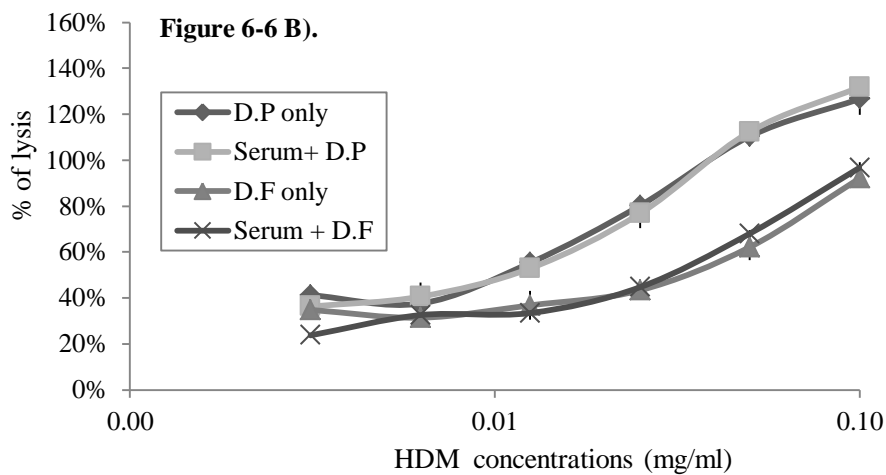
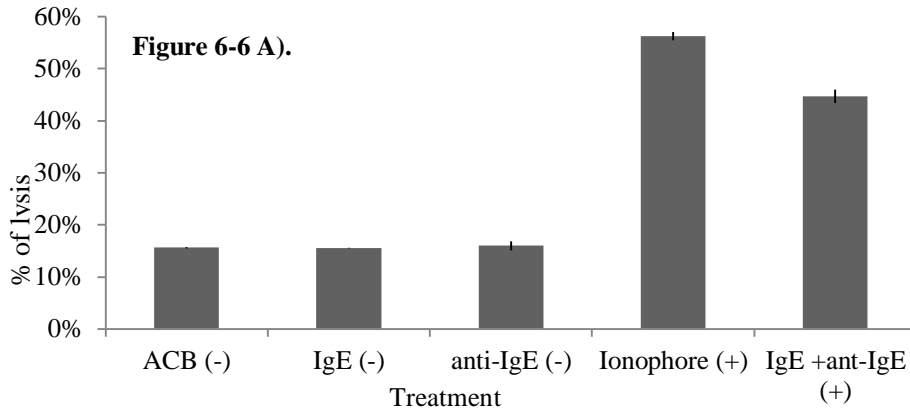


Figure 6-6. β -hexosaminidase assay of FW's serum sensitised pNFAT-hrGFP-RBL-703/21 cells induced by HDM. A) Controls. B) HDM 0.0625 mg/ml to 0.1 mg/ml (1:10, 1:20, 1:40, 1:80, 1:160 and 1:320 dilutions) alone or with serum-sensitised cells.

Hence the initial results have shown that allergen extracts are auto-fluorescent and might possess an intrinsic β -hexosaminidase activity. Thus results obtained from Typhoon or biochemical using allergen extracts needs to be further scrutinised and purified recombinant allergen should then be employed for the optimisation stage.

6.3.2 Optimisation tests

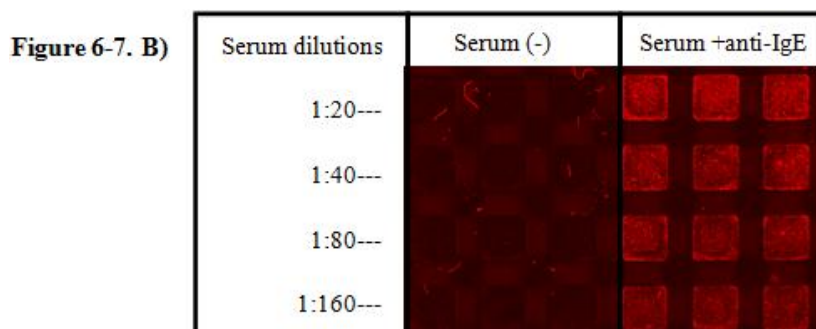
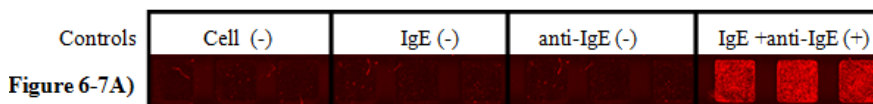
In this stage, purified recombinant allergens were employed to test with patients' sera (Adr-Ref, Adr #54449, Dan#7 and Dan#18) with high ISAC reactivity as shown in **Table 6-1.A**) using pNFAT-DsRed-RBL-703/21 cells

Optimisation test I

A serum (Adr-Ref) which is known mono-specific allergic to Par j 2 was used to test series dilutions of recombinant Par j 2 with pNFAT-DsRed-RBL-703/21 cells.

Titration of Adr-Ref serum

Adr-Ref serum was firstly titrated with 2 μ g/ml anti-human IgE to determine the optimal experimental concentration. Both fluorescent (**Figure 6-7**) and biochemical (**Figure 6-8**) results showed that, the signals produced by activated cells increased as the serum concentration ascending, cells incubated with serum at 1:20 dilution were observed as health as normal cells (data not shown), so 1:20 dilution of the serum was used to test against allergens in following experiments.



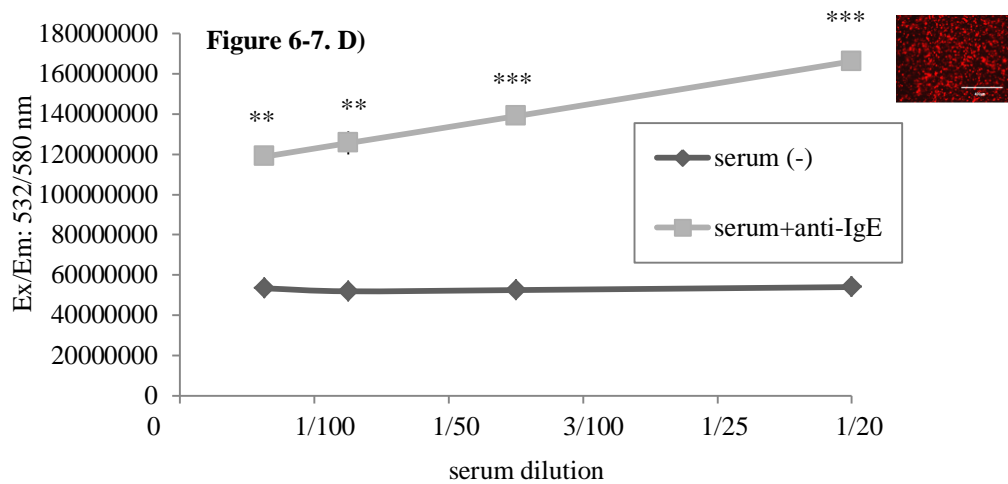
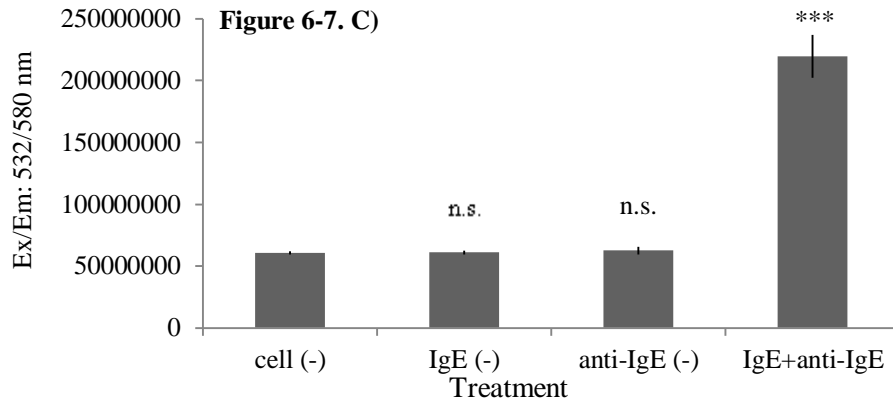
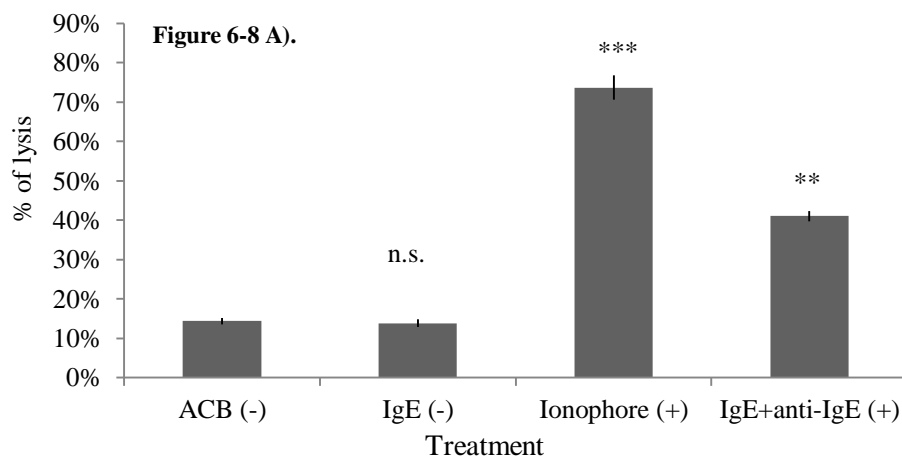


Figure 6-7. Fluorescence intensity of pNFAT-DsRed-RBL-703/21 cells sensitised by serious dilutions of Adr-Ref serum and stimulated by anti-IgE. A) Typhoon image (controls). B) Typhoon image (samples). C) Fluorescent intensity of controls. D) Fluorescent intensity of samples. Asterisks show results of two-tailed t-test against the negative control, n. s.: not significant, * $P < 0.05$, ** $P < 0.01$, * $P < 0.001$.**



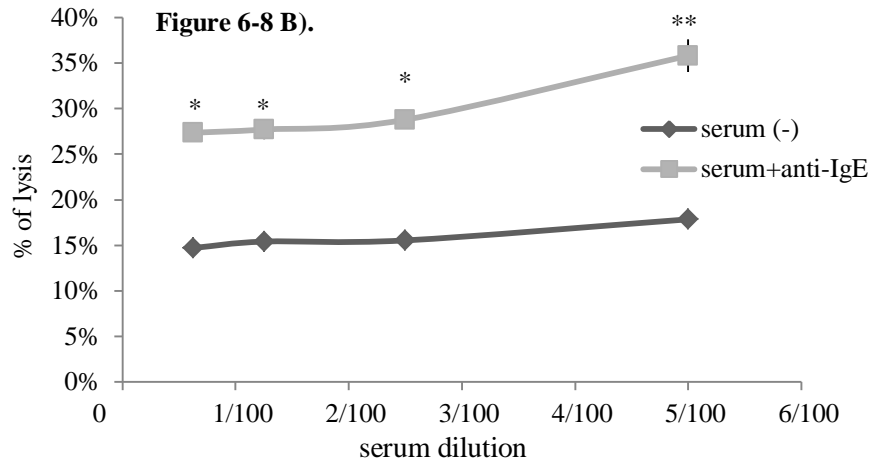


Figure 6-8. β -hexosaminidase assay of pNFAT-DsRed-RBL-703/21 cells. A) Controls. B) Cells sensitised by serious dilutions of Adr-Ref's serum and stimulated by anti-IgE. Asterisks show results of two-tailed t-test against the negative control, n. s.: not significant, * P<0.05, ** P<0.01, * P<0.001.**

Titration of Par j 2

Adr-Ref Serum at 1:20 dilution was then used to titrate purified recombinant Par j 2. Both fluorescent intensity (**Figure 6-9**) and biochemical (**Figure 6-10**) results showed a dose-dependent bell-shaped curve with a broad optimum, which clearly showed that the activation of Adr-Ref serum (1:20) sensitised pNFAT-DsRed-RBL-703/21 cells induced by purified Par j 2 in all dilutions. High concentrations of Par j 2 between 0.01 mg/ml to 0.1 μ g/ml (1:100 to 1: 10,000 dilutions) caused supraoptimal stimulation and lead to lower fluorescent intensity and β -hexosaminidase released than 10ng/ml (1:100,000 dilution), both curves peaked between the dilution of 10 ng/ml to 1 ng/ml (1:100,000 and 1:1,000,000), so 10 ng/ml (1:100,000 dilution) was chosen as the optimal Par j 2 dilution to stimulate Adr-Ref serum-sensitised cells.

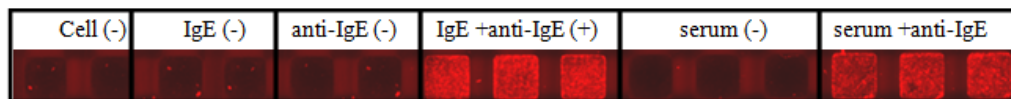


Figure 6-9 A).

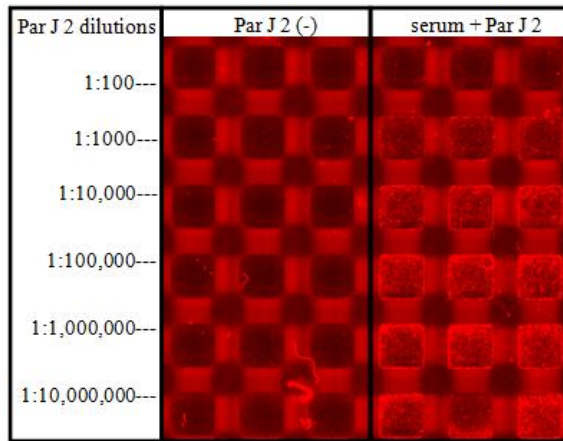


Figure 6-9 B).

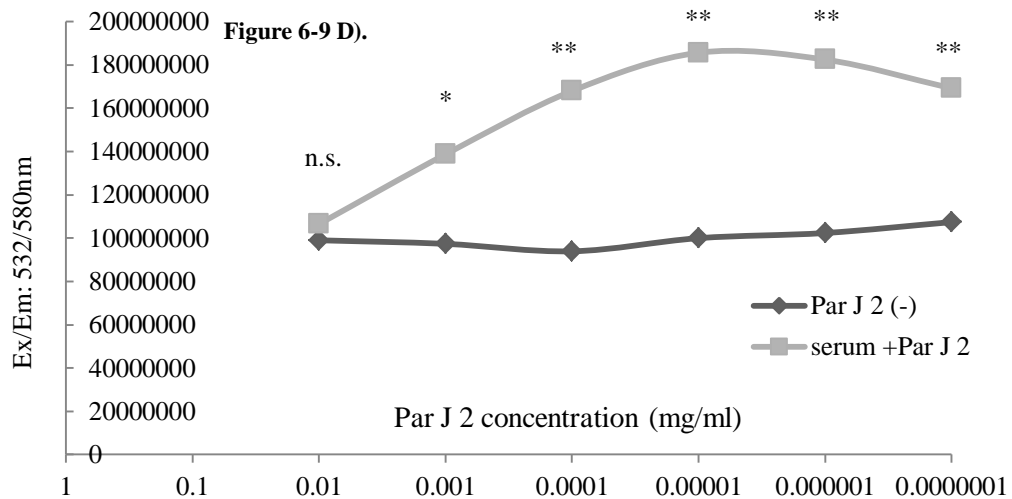
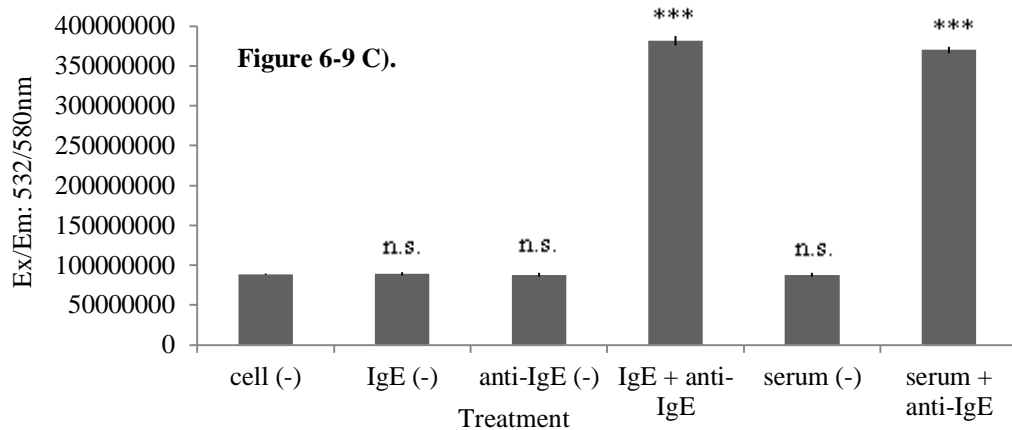


Figure 6-9. Fluorescence intensity of Adr-Rref's serum (1:20) sensitised pNFAT-DsRed-RBL-703/21 cells induced by a series dilution of Par j 2 (log scale). A) Typhoon view (controls). B) Typhoon view (samples). C) Fluorescence intensity of pNFAT-DsRed-RBL-703/21 cells (controls). D) Fluorescence intensity of cells sensitised by serum and stimulated by 0.01 mg/ml to 0.1 ng/ml (1:100, 1:1000, 1:10,000, 1:100,000, 1:1,000,000 and 1:10,000,000 dilutions) of Par j 2. Asterisks show results of two-tailed t-test against the negative control, n. s.: not significant, * P<0.05, ** P<0.01, * P<0.001.**

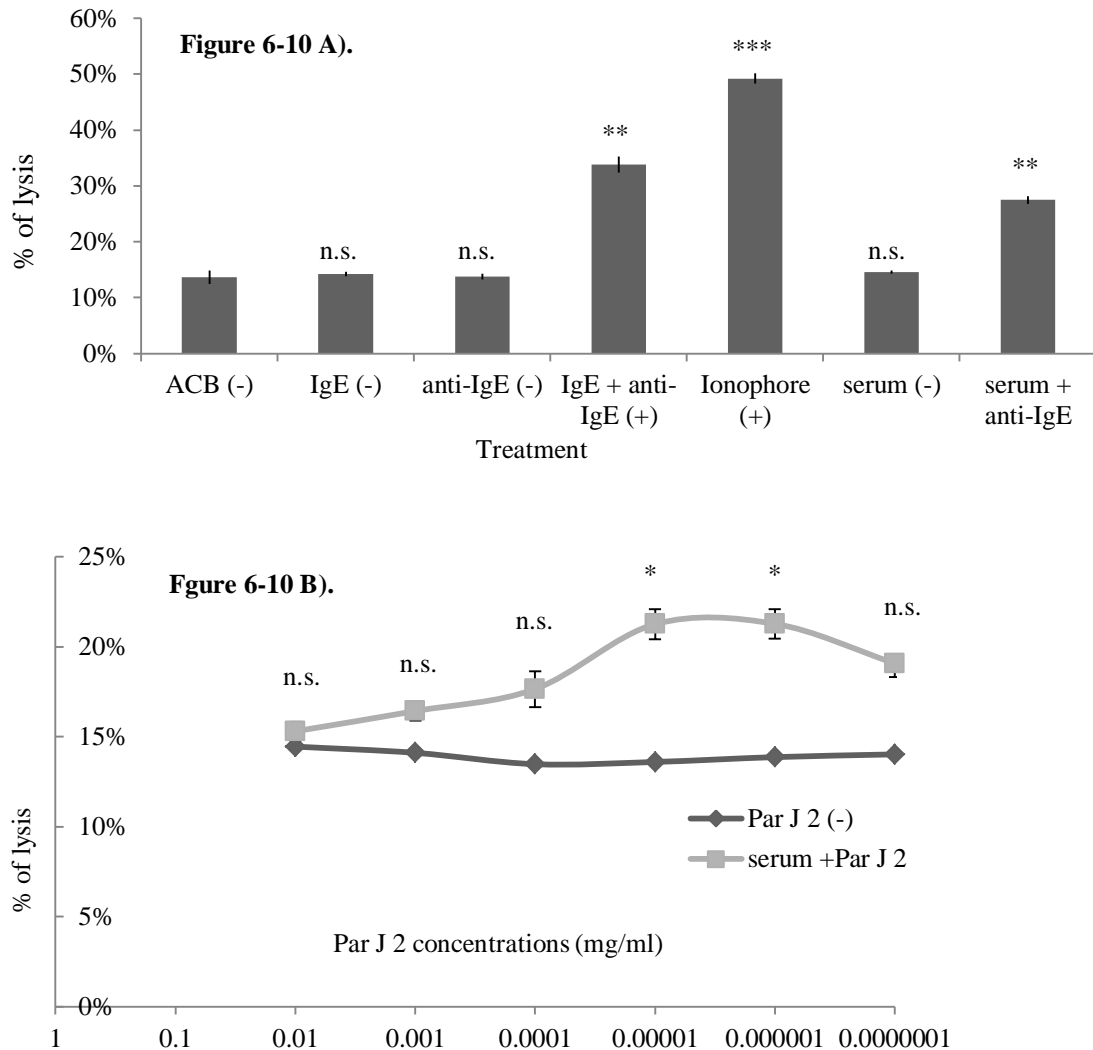


Figure 6-10. β -hexosaminidase assay of pNFAT-DsRed-RBL-703/21 cells sensitised by Adr-Ref serum (1:20) and induced by a series dilution from 0.01 mg/ml to 0.1 ng/ml of Par j 2 (log scale). A) Controls. B) Samples. Asterisks show results of two-tailed t-test against the negative control, n. s.: not significant, * P<0.05, ** P<0.01, * P<0.001.**

Specificity of the test against different allergens

Adr-Ref serum was described as mono-specific to Par j 2. In order to test the specificity, different allergens - Par j 2, Bet v 1, Bet v 2 and Ber e 1 were used to stimulate Adr-Ref serum sensitised cells and the fluorescent intensities were measured by Typhoon. Results (**Figure 6-11**) showed that the activation of pNFAT-DsRed- RBL-703/21 cells sensitised with Adr-Ref's serum was specific to Par j 2 in 10 ng/ml to 0.01 ng/ml (1:100,000, 1:1,000,000, 1:10,000,000 and 1:100,000,000 dilutions), there was no activation with stimulation of the other allergens, which made this system more reliable and sensible to be used for detecting cross-linking of patients' sera and specific allergens induced cell activation in micro-wells.

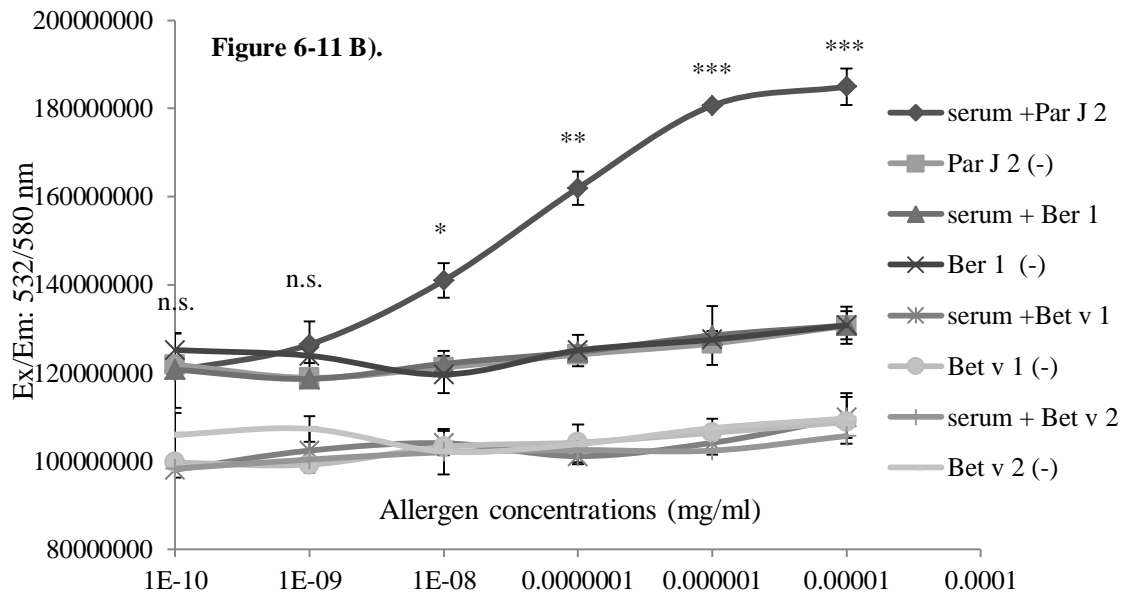
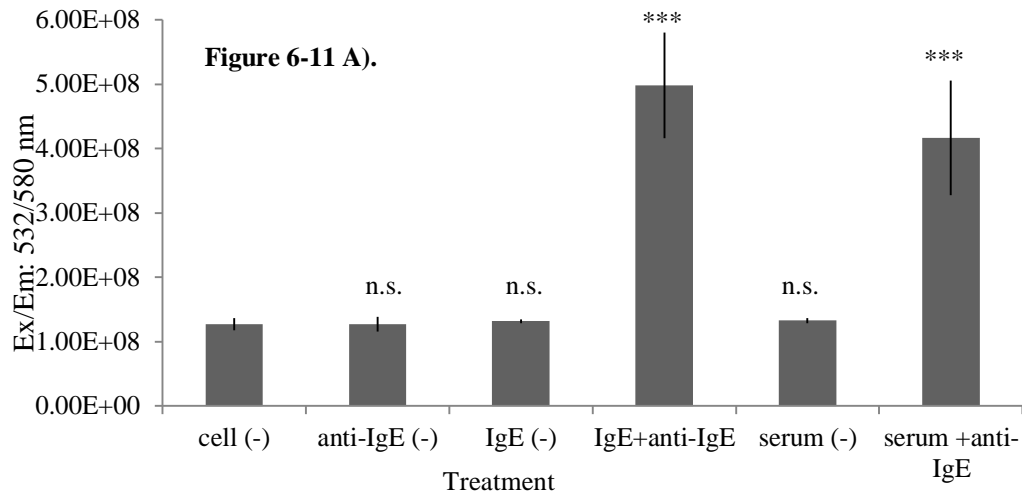


Figure 6-11. Fluorescent intensity of pNFAT-DsRed- RBL-703/21 cells sensitised with Adr-Ref⁷ serum and induced by different allergens (log scale). A) Controls. B) Cells sensitised with serum and induced by Par j 2, Bet v 1, Bet v 2 and Ber e 1 separately with concentrations between 10 ng/ml to 0.1 pg/ml (1:100,000 to 1:10,000,000,000 dilutions). Asterisks show results of two-tailed t-test against the negative control, n. s.: not significant, * P<0.05, ** P<0.01, * P<0.001.**

Optimisation test II- Test of Dan #7 serum against different allergens

A serum (Dan #7) that was known allergic to Phl p 1 and Bet v 1 was tested against with series dilutions of these recombinants allergens using pNFAT-hrGFP-RBL-703/21. **Figure 6-12** showed that both purified bet v 1a and phl p 1 were capable of degranulating Dan #7 serum-sensitised pNFAT-hrGFP-RBL-703/21 cells in all dilutions, with optimal concentration peaked at around 0.1 µg/ml (1:10,000 dilution).

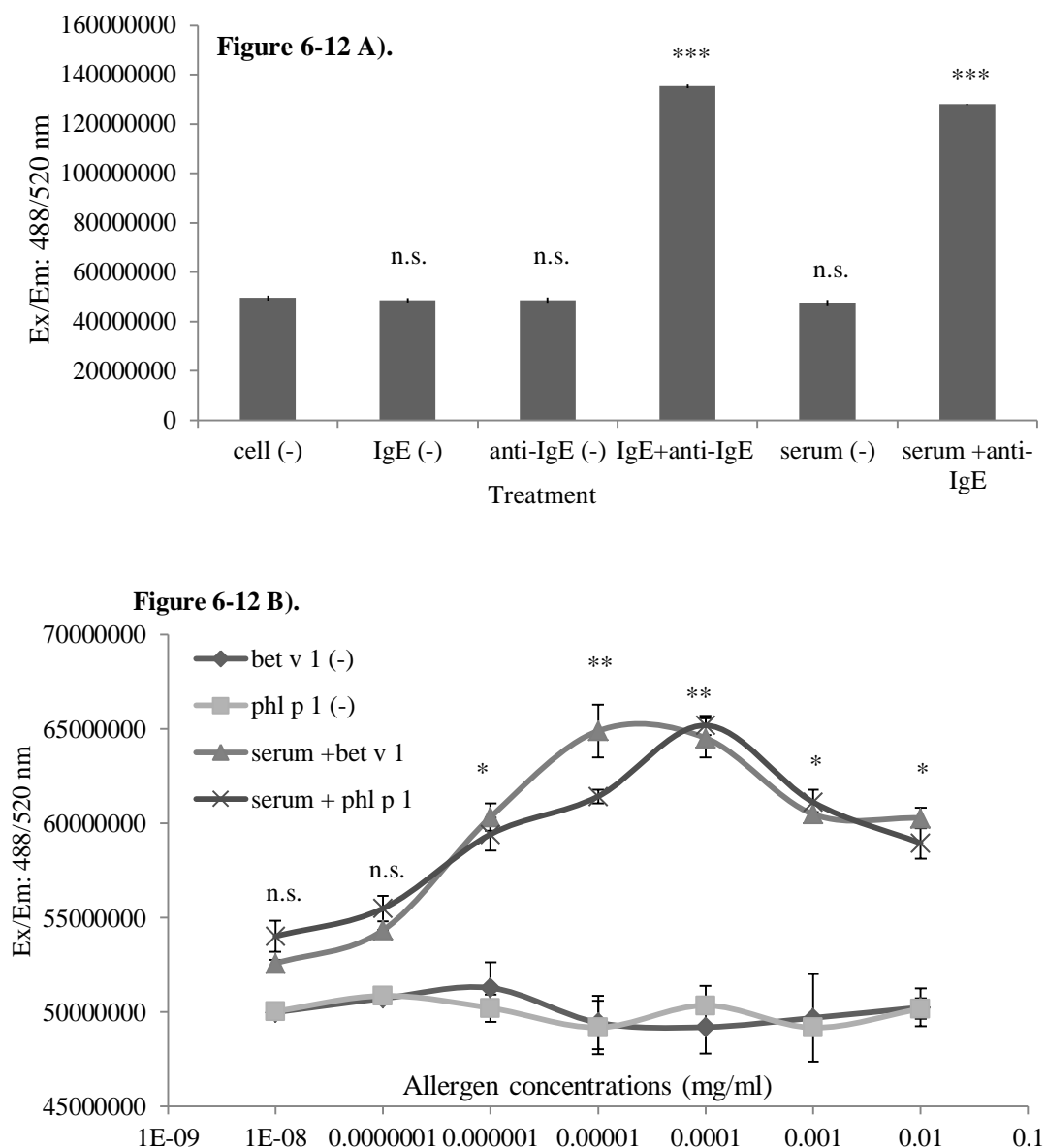


Figure 6-12. Fluorescent intensity of pNFAT-hr-GFP-RBL-703/21 cells sensitised by Dan #7 and induced with Bet v 1a and Phl p 1. A) Controls. B) Allergens diluted in 1:100, 1:1000, 1: 10,000, 1:100,000, 1:1,000,000, 1: 10,000,000 and 1: 100,000,000. Asterisks show results of two-tailed t-test against the negative control, n. s.: not significant, * P<0.05, ** P<0.01, * P<0.001.**

Optimisation test III - Test of Adr#54449 against different allergens

A serum sample (Adr#54449) was clinically proven to allergic to Par j 2. To test these sera's ability and specificity to degranulate basophils, pNFAT-DsRed-RBL-703/21 cells were used to test against this serum with three allergens - Par j 2, Bet v 1, Ber e 1 with three concentrations from 1 µg/ml, 10 ng/ml to 100 pg/ml (1:1000, 1:100,000 and 1:10,000,000 dilutions). Firstly, the serum was titrated with 2 µg/ml anti-IgE, **Figure 6-13 A)** showed that the fluorescent intensity decreased with the serum concentration descending, 1:10 was chosen as the optimal dilution for following experiments. **B)** showed that proper dilutions of recombinant Par j 2 was capable of degranulating serum Adr#54449-sensitised pNFAT-DsRed-RBL-703/21 cells. No reaction was observed with cells stimulated by either Bet v 1 or Ber e 1, which demonstrated the functionality and reliability of the system.

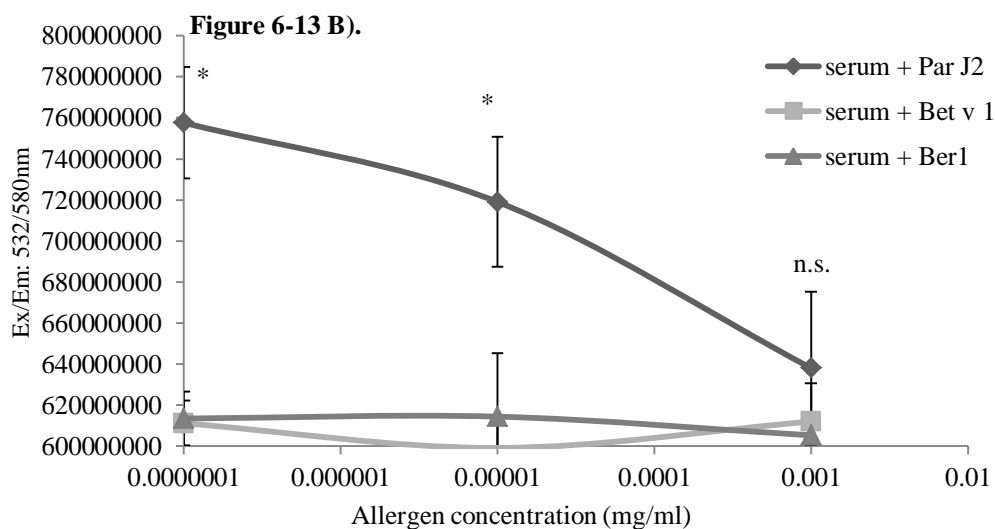
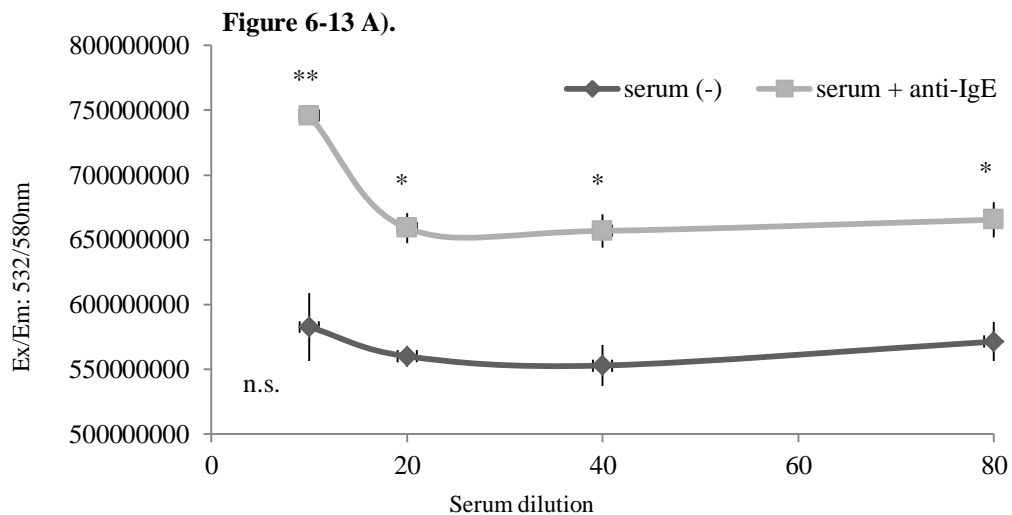


Figure 6-13. Test of serum Adr #54449 with anti-IgE and recombinant allergens. A) Titration of serum (1:10, 1:20, 1:40 and 1:80) by 2 µg/ml anti-IgE. **B)** Adr#54449 sensitised pNFAT-DsRed-RBL-703/21 cells induced with different allergens separately. Allergen concentrations from 1 µg/ml, 10 ng/ml to 100 pg/ml (1:1000, 1:100,000 and 1: 10,000,000 dilutions). Asterisks show results of two-tailed t-test against the negative control, n. s.: not significant, * P<0.05, ** P<0.01, *** P<0.001.

These results in optimisation stage showed that an increase in DsRed fluorescence is only obtained when IgE or patients' sera sensitised cells are activated by cross-linking agents (either anti-IgE antibodies or allergens). DsRed as reporter fluorescent proteins generated approximately 5-fold for the positive controls (monoclonal IgE sensitized anti-IgE stimulated or serum sensitized, anti-IgE stimulated) and almost 2-fold for the experimental samples at optimum allergen concentration, the DsRed reporter showed a sharp, pronounced bell-shaped activation curve upon stimulation with a serial dilution of the allergen. Reproducibility between experiments was also good.

6.3.3 Contrast test

In order to evaluate the sensitivity of the NFAT-reporter system, contrast tests were carried out using serum from allergic Dan patient #18 before and after one-year vaccination treatment, the first (before vaccine) and last time point (after vaccine) of the same patient's serum were used (1:20 dilution, sera titration data not shown) to test against concentration from 1 µg/ml, 10 ng/ml to 100 pg/ml (1:1000, 1:100,000 and 1:10,000,000 dilutions) of specific recombinant allergens - Phl p 2, Phlp 2, Phlp 6 and Bet v 1. Results showed that, fluorescent signals of vaccinated-serum-sensitised-cells induced by both anti-IgE controls (**Figure 6-14**) and allergens (**Figure 6-15**) significantly reduced with proper dilutions compared to the non-vaccinated ones, which reflected that the IgE levels in the treated sera reduced and lead to less cross-linking with allergens and degranulation of cells. Results from contrast tests showed agreement with the clinical record and demonstrated the sensitivity and functionality of the NFAT-DsRed reporter system as a reliable technique compared to clinical allergy diagnostic methods.

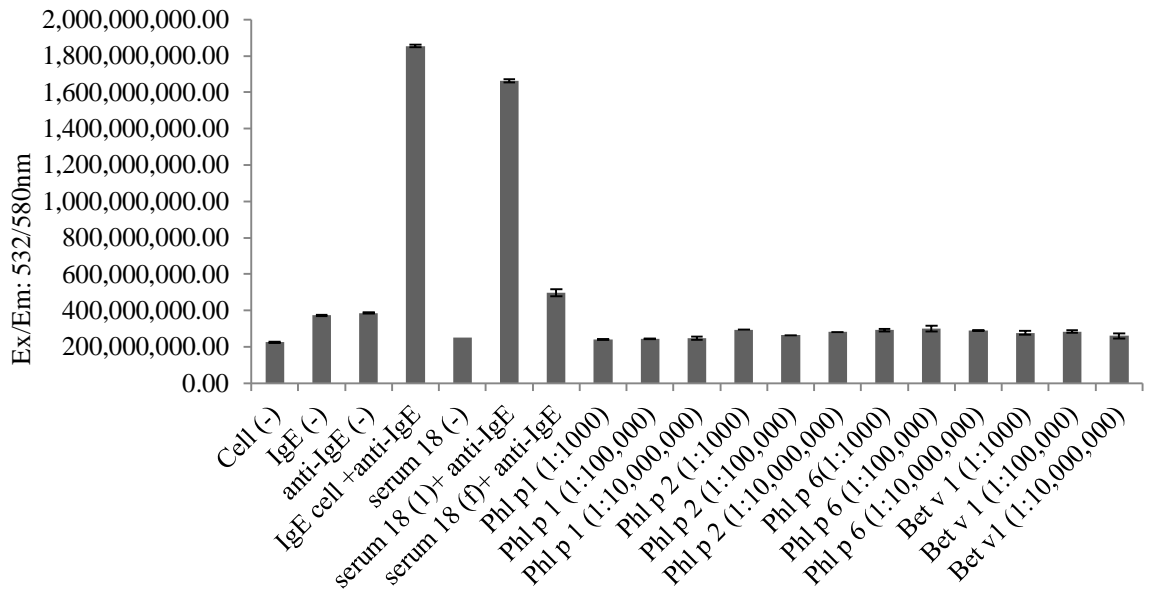


Figure 6-14. Fluorescent intensity of pNFAT-DsRed-RBL-703/21 cells sensitised by Dan #18 serum and induced by anti-IgE (controls).

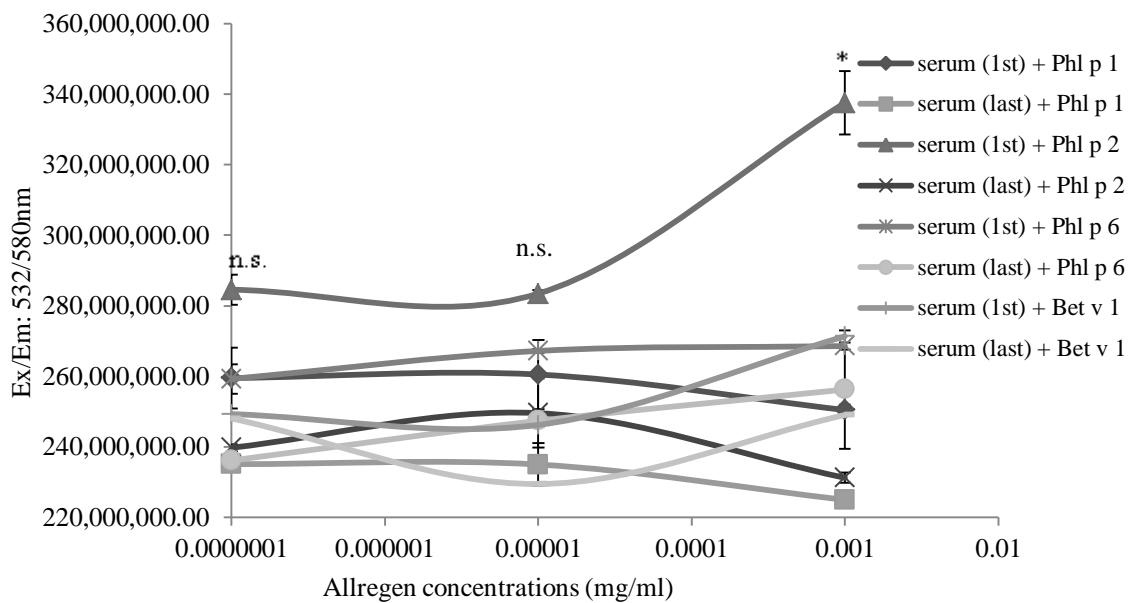


Figure 6-15. Fluorescent intensity of pNFAT-DsRed-RBL-703/21. Cells were sensitised with Dan #18 and induced by Phl p 1 phl p 2, phl p 6 and Bet v 1 with concentration from 1 μ g/ml, 10 ng/ml to 100 pg/ml (1:1000, 1:100,000 and 1:10,000,000 dilutions). Asterisks show results of two-tailed t-test against the negative control, n. s.: not significant, * $P < 0.05$, ** $P < 0.01$, *** $P < 0.001$.

6.3.4 Time course during cytotoxicity reduction tests

It was observed that, some patients' sera at high dilutions (from 1:5 to 1:50) were toxic to cells and can cause cell dead and detached from the micro-well surface after several-hour incubation. As IgE is heat labile, common heat inactivation of sera is not applicable. Nakamura *et al.* (2010) suggested that by cross-absorbing the sera against wild-type RBL-2H3 cells prior sensitisation will remove the cytotoxic factors. Before sensitisation with cells, sera were incubated with RBL-2H3 cells for a period. **Figure 16** showed that without pre-incubation (0 hour) with RBL-2H3 cells, most of the Dan #19 serum sensitised cells dead and detached after washing, no signals were observed by Typhoon, after hours (2-24 hours) pre-absorbing with RBL-2H3 cells, more quantity of cells alive and start to produce fluorescent signals just like normal healthy cells. As it was concerned that the incubation with RBL-2H3 cells can affect the IgE level in patients' sera, to compromise this, the optimal pre-incubation time with RBL-2H3 cells was chosen to be four hours before sensitisation.

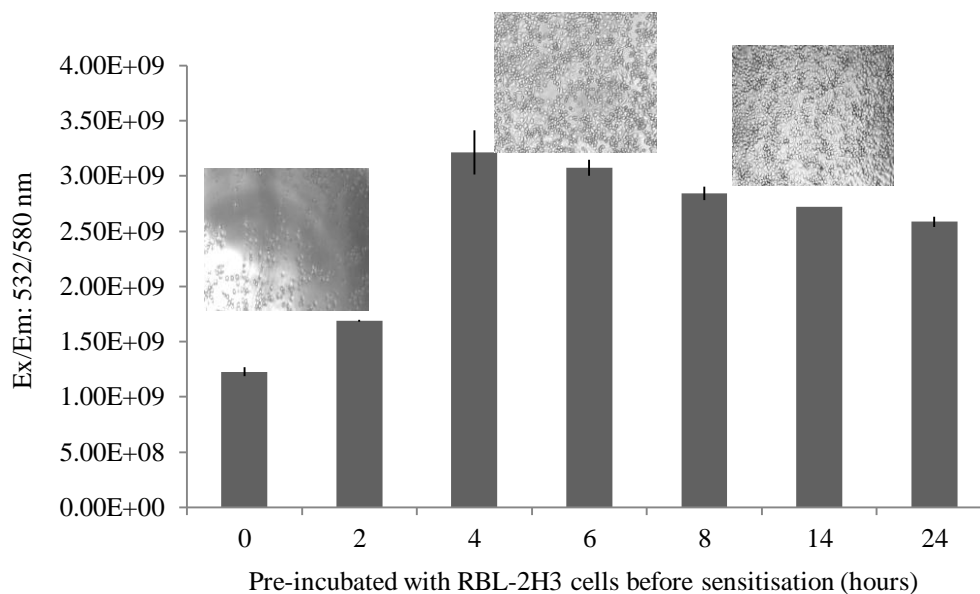


Figure 6-16. Pre-incubation of Dan #19 serum with RBL-2H3 cells before sensitisation pNFAT-DsRed-RBL-703/21cells. Images: Bright field of treated-serum-sensitised cells after washing. **Data:** Fluorescent intensity of treated-serum-sensitised cells induced with 2 µg/ml anti-IgE.

6.3.5 Preparation of applying the system onto microarray format

Before applying the pNFAT-DsRed onto real microarray format, a micro plate was used as a dried solid surface to simulate the cells activation on real slides. Instead of adding stimuli into the wells containing cell suspension, stimuli were pre-coated onto the surface of each well, and air-dried before adding cells. **Figure 6-17 and 6-18** showed a dose-dependent fluorescent intensity of both anti-IgE and cell number in the plate pre-coated with stimuli. **Figure 6-19** showed that, wells coated with anti-IgE with less efficient of stimulation than coated together with fibronectin. The patient's serum sensitised cells can be induced by surface-printed anti-IgE. Results obtained in this part clearly showed that either activating IgE-sensitised cells on stimuli pre-coated surface or adding stimuli into cell suspension can both degranulate RBL-703/21 cells, which demonstrated that the system is suitable for future applying on array format.

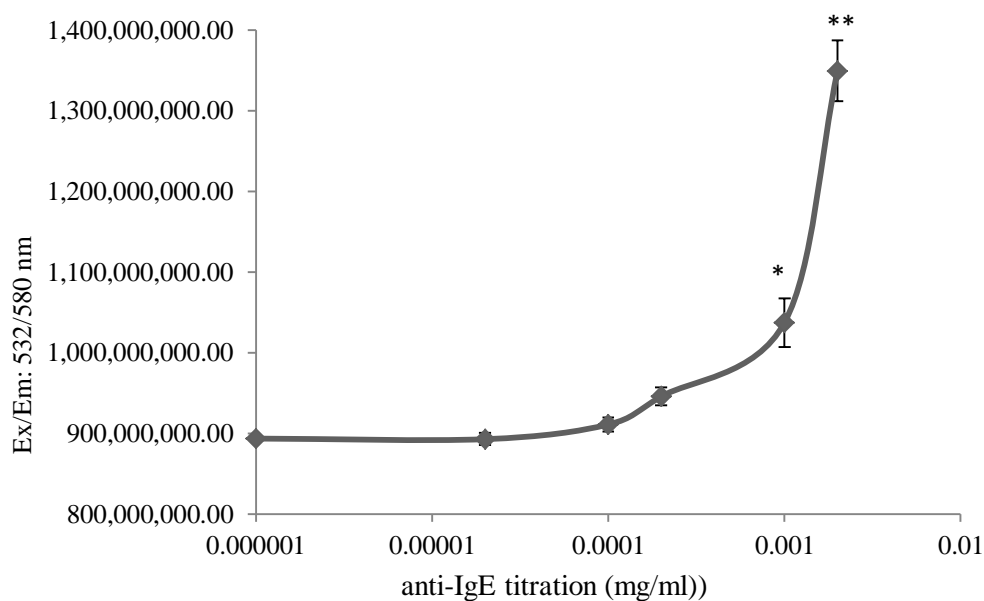


Figure 6-17. Anti-IgE titration of the pNFAT-DsRed-RBL-703-21 cells in 384-well plate pre-coated with fn + anti-IgE. A series dilution of anti-IgE (1:500, 1:1000, 1:5000, 1:10000, 1:50000 and 1:1000000) were used to coat the plate overnight and air-dried before loading IgE-sensitised cells, the fluorescent in each well was detected by Typhoon. Asterisks show results of two-tailed t-test against the negative control, n. s.: not significant, * P<0.05, ** P<0.01, *** P<0.001.

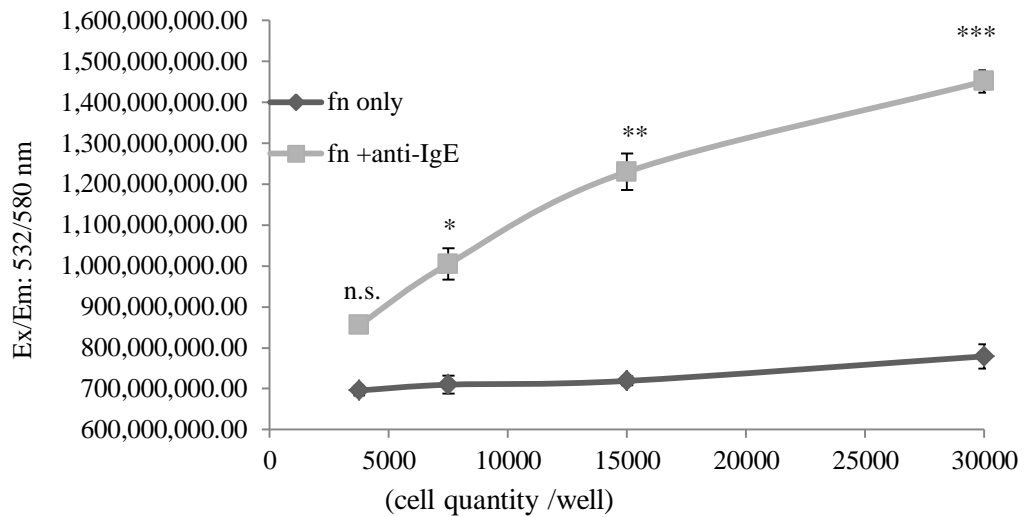


Figure 6-18. pNFAT-DsRed RBL 703/21 cell density dilutions in dried 384-well plate. A series dilution of non-sensitised and IgE-sensitised cells were added into fn/fn + anti-IgE pre-coated plate. Results showed that, with the same concentration of anti-IgE, signal intensity was direct regulated by the quantity of cells in each well. Asterisks show results of two-tailed t-test against the negative control, n. s.: not significant, * P<0.05, ** P<0.01, *** P<0.001.

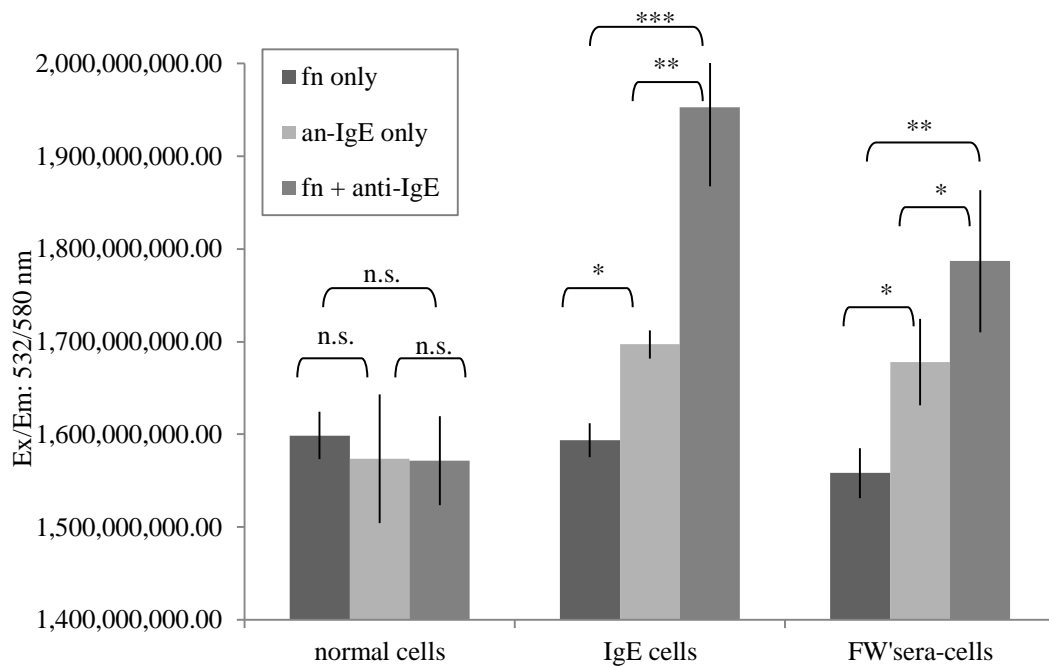


Figure 6-19. Test IgE and patient's serum (FW) sensitised pNFAT-DsRed- RBL-703/21 cells on anti-IgE pre-coated 384-well plate. Plate was coated with 20 µg/ml fibronectin alone (fn only), 2 µg/ml anti-IgE alone (anti-IgE only) and fibronectin + anti-IgE. Non-sensitised, IgE-sensitised and FW's serum-sensitised cells were loaded into each well and incubated for 24 hours and scanned by Typhoon. Asterisks show results of two-tailed t-test against the negative control, n. s.: not significant, * P<0.05, ** P<0.01, *** P<0.001.

The correlation between the NFAT reporter system and the traditional β -hexosaminidase assay was determined by testing in parallel using the same sera/allergen and IgE/anti-IgE positive controls as separate method to analyse the early and late stage of cells activation for individual test, **Figure 6-20** showed a strong linear relationship between these two methods, which demonstrated the high efficiency of the NFAT system is constant and reliable for detection RBLs activation in the microplate format.

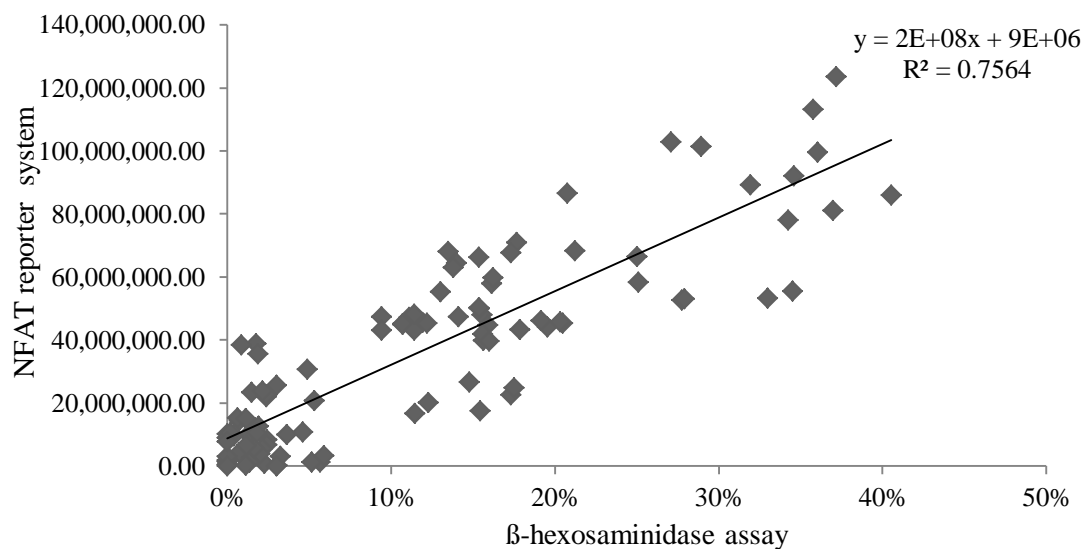


Figure 6-20. Relationship between NFAT reporter system and β -hexosaminidase assay.

6.3.6 Zeiss confocal microscope

An advanced Zeiss confocal microscope (LSM501uv META combi) which can be used to accurately detect fluorescent intensity of activated pNFAT-DsRed-RBL-703/21 cells with resolutions in cellular level. By using nuclei staining, the number of fluorescent cells yields total cells can be accurately detected and differentiate by high resolution laser. Percent of positive cells in each well can be quantified automatically by the lined Mata Xpress software. **Figure 6-21** clearly showed that, the pre-coated/spotted and sterile air-dried allergen (Par j 2, 100 pg/ml) maintained the function to degranulate IgE/patient's serum sensitised pNFAT-DsRed-RBL-703-21 cells properly. The work done with the Zeiss confocal microscope supplied not only image but more sensitive and accurate in depth data than the other methods used (e.g.

Typhoon), which was considered to be a very useful system in future experiments. Though with less efficiency than adding stimuli into cell suspension, by using patient's sera sensitised cells in allergen-pre-coated micro-well format made us closer to the final microarray stage.

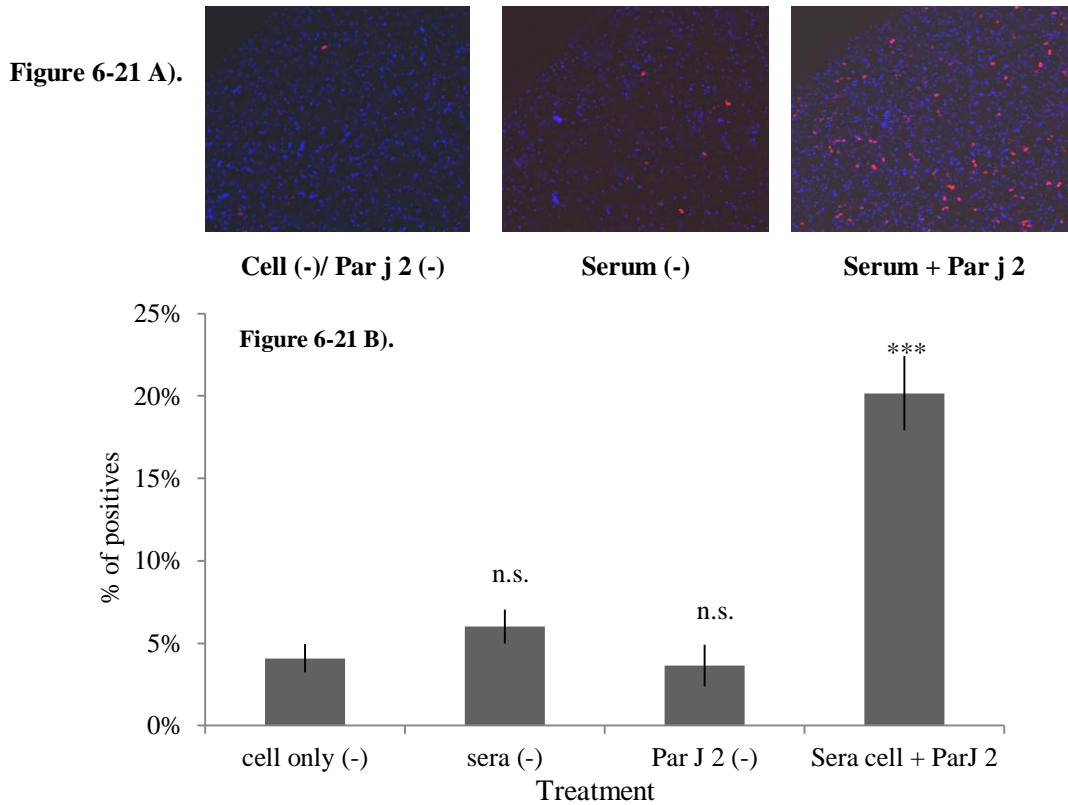


Figure 6-21. Fluorescent intensity of pNFAT-DsRed -RBL-703/21 cells in stimuli-pre-coated 96-well plate. A) Image from Zeiss confocal microscope after 24 hours of stimulation. Non-sensitised cells loaded into wells coated with fn alone (cell (-)), or coated with fn + Par j 2 (Par j 2 (-)), Adr-Ref serum-sensitised cells loaded into wells coated with fn alone (serum (-)), or coated with fn + Par j 2 (serum + Par j 2). **B)** Percentage of fluorescent pNFAT-DsRed -RBL-703/21 cells each well. Data were obtained and calculated by MataXpress. Asterisks show results of two-tailed t-test against the negative control (cell only), n. s.: not significant, * P<0.05, ** P<0.01, *** P<0.001.

6.4 Discussion

In initial tests, results from Typhoon showed that cells produced high signals at highest dilution of allergen extracts with all dilutions of serum. However, the image from the fluorescent microscopy showed that no fluorescent signals were observed in all the wells, which meant that the signals caught by Typhoon were the auto-fluorescent of the grass pollen extract. The auto-fluorescent properties of pollens were previously demonstrated by different reports (Mitsumoto K *et al.*, 2008; Roshchina *et al.*, 1999) and in most of them it was used to differentiate types of pollens. Therefore, the allergen extracts alone are possibly auto-fluorescent and can have β -hexosaminidase activity of their own. The β -hexosaminidase release with high dilution of grass pollen extracts (1:5) was higher than 100% of total lysed cells, which meant that there's some substances exists in these allergen extracts that can interact with substrate solution and interfere detection. From the image of bright field, with the presence of high concentration of pollen (1:5 -1:100), the majority of both non-sensitised and sensitised cells were died after 24 hours incubation, but the sera sensitised cells (1:10 dilution) alone and the pollens at low (1:500) dilutions induced cells were observed as healthy as normal cell, which means pollens are toxic to cells at high concentrations. Therefore results obtained from Typhoon or biochemical cannot be reliable by using allergen extracts, purified recombinant allergen (no observed auto-fluorescent) were used instead of in future tests. Also, one of the disadvantages of Typhoon was that, it cannot differentiate the fluorescent signals either from cells or backgrounds, so the fluorescent microscopy needs to be employed throughout the project to monitor and compare the results of each experiment.

Results from optimisation stages showed that, all the tested purified recombinant allergens at most of the dilutions were capable of degranulating the allergenic specific serum-sensitised pNFAT-hrGFP-RBL-703/21/pNFAT-DsRed-703/21 cells. According to Gibbs *et al.* (2006), the dose-response curve for Fc ϵ RI activation of primary human basophils were bell shaped, with supraoptimal stimulating leading to reduced mediator release. In agreement with literature, results showed the expected bell-shaped dose-dependent response, with allergen concentrations peaked between 0.1 μ g/ml and 1 ng/ml. High concentrations of allergens cause supraoptimal stimulation and lead to lower fluorescent intensity and β -hexosaminidase released

than proper lower dilutions. RBLs were reported has a high density of FcεRI on cell surface, so it can respond to very low level of antigen with obvious response (Qu *et al.*, 2013). The NFAT-reporter system generated approximately 5-fold for the positive controls (monoclonal IgE sensitized anti-IgE stimulated or serum sensitized, anti-IgE stimulated) and 3-4 fold for the experimental samples at optimum allergen concentration. Results of Adr-Ref's serum with different allergens also showed that the system enables test the specificity of allergens and sera.

Literally the β-hexosaminidase release of RBLs was used to determine the total IgE concentrations of sera from allergenic patients (Takagi K *et al.*, 2003), and the allergenic activity of specific allergens, good release was normally indicated between 30 %-60 % (Ladics GS *et al.*, 2008). The results from β-hexosaminidase assay of allergen-induced cells generated maximum 22 % release, which was not as good as compared to literature.

6.5 Conclusion

Results from this chapter showed agreement with the database supplied from ISAC which demonstrated that the system is reliable and sensitive to be used for detecting cross-linking of patients' sera and specific allergens induced cell activation compared to clinical allergy diagnostic methods.

7 General discussion

Activation basophils by cross-linking of FcεRI- IgE complexes results in two phase of effector function, the early phase involves cell degranulation and released of pre-formed mediators present in the granules immediately into the surrounding tissues such as histamine and serotonin, which occurs very quick – within minutes of FcεRI cross-linking. The late phase involves synthesis and secretion of new mediators such as cytokines and chemokines, which normally take hours (Blayne A *et al.*, 2008). A suitable method of quantifying degranulation of RBLs must be able to measure the significant differences before and after cells' activation. Current available methods are mainly classified as measuring the mediators released by cells' immediate degranulation, e.g. histamine; measuring surface marker up-regulation, e.g. CD63; or using reporter systems to analyse FcεRI cross-linking and gene induction (Ana *et al.*, 2009).

β-hexosaminidase assay is a well-established method to measure the mediator released by immediate degranulation of cells. The assay was originally optimised for the humanised RBL-2H3 cells (encoding human FcεRI) therefore cells are expected to degranulate after cross-linking of receptor-bound human IgE by the allergens (Vogel *et al.*, 2005). Our results clearly demonstrated that humanised RBL cell lines (either RBL-703/21 or pNFAT-hrGFP-703/21 cells) do degranulate by the stimulation with anti-human IgE or allergens as described by Vogel *et al.* (2005). Although this method can be used to diagnose allergic reactions in micro-well format, due to the solubility of the substrate, the hexosaminidase activity is not suitable for the microarray format. Therefore β-hexosaminidase assay was employed as a standard routine control to monitor cell behaviour throughout the project.

Ionophore A23187, a lipid soluble molecule, was previously reported to induce histamine secretion, and acts as calcium ion carrier that increases permeability of biological membranes to transfer Ca²⁺ ions across the cell membrane, hence increase the intracellular calcium concentration and inducing cell activation (Tedeschi *et al.*, 1994). It was used as positive inducer throughout the project, and results from all chapters showed that ionophore A23187 generates stimulation effect on RBL-703/21 cells, with maximum activation at 1 µg/ml. However, according to the adhesion assay, the addition of calcium ionophore A23187 caused marked cell detachment

from FN within the 2-hour incubation period, which indicated that ionophore A23187 is an unsuitable positive control for microarray due to a fast down-regulation of surface expression of VLA-4 and subsequent detachment of cells.

The inclusion of fibronectin on solid surface greatly reduced cell losses during the washing steps. Activation with anti-human IgE antibody enhanced cell adhesion compared with IgE alone. There are several reports describing an increased attachment of mast cells and basophils (Thompson *et al.*, 1990; Dastych *et al.*, 2001) to ECM proteins after activation. In such reports, attachment of primary mast cells to ECM proteins was found to depend on pre-activation, as in the case of bone marrow-derived murine or peritoneal rat mast cells, via PMA (Dastych *et al.*, 1991). However, such pre-activation is not necessary for RBL cells (Hamawy *et al.*, 1992), which are able to attach spontaneously.

RBL-703/21 cells express only the α -chain of human Fc ϵ RI, whereas RBL-SX38 cells express the α - and γ -chain of the human Fc ϵ RI. It has been described that, human α -chain can interact with the rat β - and γ -chain to form the functional high affinity IgE receptor complexes and activate the downstream signalling cascades (Taudou *et al.*, 1993), so RBL-703/21 cells are capable of activation by IgE crosslinking. Whether the human γ -chain is associated with the rat α -chain or not in SX-38 cells remains to be shown. According to the results described in chapter 5, results from RBL-703/21 was more stable than RBL-SX38, especially when using the NFAT-reporter system. This is in contrast with the luciferase system reported by Nakamura *et al.* (2010) that described better results with the SX-38 clones. Whether the differences are in the short time (4-6 hours) necessary for the expression of the luciferase protein against the time necessary for accumulations of the DsRed reporter protein remains to be shown. Moreover, as fluorescent proteins produced are retained within the cells that allow the measurements by scanners, the fluorescent system is considered much more suitable for use in microarray format. Compared to fluorescence, though luciferase assays possess intrinsically better signal to noise efficiency, this system is not suitable for use in microarray format as it requires cell lysis, which can only be carried out in microplate format.

It has been reported that IgE alone was able to activate several signalling pathways that lead to synthesis of cytokines in the absence of cross-linking by multivalent allergens (Kalesnikoff *et al.*, 2001). It has been also demonstrated that monomeric

IgE alone elicits RBL-2H3 cells' degranulation and transduction pathways for cytokine synthesis, including phospholipases C and D, a rise in cytosol Ca^{2+} and low-level NFAT translocation; high calcium concentrations persist for hours as long as IgE is present resulting in the maintained translocation of NFAT to the nucleus (Pandey *et al.*, 2004). The results from all chapters are in agreement with literatures, IgE/sera alone treated but non-stimulated cells generate a higher background signal than non-sensitised cells.

Calcium is vital for IgE-dependent basophil activation and degranulation (Lin *et al.*, 2007). In agreement with the literature, in this study, investigations on the effects of Ca^{2+} on cell activation showed that Ca^{2+} has an enhancing effect on basophil degranulation and activation in the presence of anti-IgE /antigens. Adhesion assay confirmed that cell attachment to fibronectin was dependent upon the presence of calcium. Results from the fluorescent reporter system showed that cell activation increased with ascending concentrations of Ca^{2+} in the presence of anti-IgE.

A possible issue with using RBL could be the cytotoxicity of human sera, as the cells would not respond during the sensitisation stage with human sera, producing false positive signals. As IgE is heat labile, common heat inactivation of sera is not applicable. Nakamura *et al.* (2010) suggested that by cross-absorbing the sera against wild-type RBL-2H3 cells prior sensitisation the cytotoxic effect would be removed. Sufficiently diluted sera before sensitisation was demonstrated as a suitable alternative, which significantly reduced cytotoxicity of patient's sera without affecting IgE level. Cross-absorbing treated cells were observed to produce fluorescent signals at the same intensity as healthy cells.

One of the main obstacles faced by the use of fluorochromes as final read out are the impurities in allergen extracts with the appearance of auto-fluorescence that leads to inaccurate results. As described in Chapter 6 the use of extracts had to be abandoned in favour of purified allergens.

The newly developed NFAT fluorescent reporter system was stably functional, and generated detectable fluorescence after stimulation by either anti-human IgE or recombinant allergens. DsRed reporter cell lines showed the expected bell-shaped dose-dependent response with specific sera. A longer incubation of the reporter cells (24 hours) is needed in comparison with the NF-AT-Luciferase system, with optimal

activation described after 3 hours (Nakamura *et al.*, 2010). While increases in fluorescence as early as 8 hours post stimulation was detected, these changes increased steadily for at least 20 hours. Whether this reflects an issue of sensitivity of detection or differences in the rate of synthesis or folding of the different reporter proteins remains to be shown. However, the main problem here was the low signal-to-noise ratio due to the high background, ranging from 2 to 5-fold even under the best stimulation conditions. Our final aim was to employ the reporter cell lines using allergen arrays with several hundreds of recombinant allergens or food extracts in parallel with immunoglobulin determination. However, the use of conventional laser array scanners is not compatible with the use of cells growing in medium, and commercially available laser microscopes do not have the necessary width of field of view to record the patterns of cellular activation at the array level. Thus the experiments with the fluorescent reporter cell lines were performed using 384-well plates and a Typhoon scanner, which could be used with cells immersed in aqueous culture medium. This type of scanner does not have the necessary resolution at the cellular level and the plastic materials used in 384-well cell culture plates have unacceptably high background fluorescence for this application. Part of the work needs to be repeated to produce more reliable results to support statistical evidence of all the findings.

8 Conclusion

In conclusion, fibronectin was shown to be more efficient than collagen type I and laminin in binding to RBL-703/21, with optimal concentration at 20 $\mu\text{g/ml}$ and with 2-hour incubation. The use of fibronectin will greatly avoid cell losses up activation during the washing steps. A23187 is an unsuitable positive control in this format due to a fast down regulation of VLA-4 and subsequent detachment of cells. β -hexosaminidase assay demonstrated that humanised RBL cell lines do degranulate by the stimulation with anti-human IgE or allergens. This assay was employed as a standard control to routinely monitor the cells' batch-to-batch consistency in micro-well format. Fluo-4 AM can efficiently detect the intracellular calcium flux for anti-IgE activated basophil. Due to lack of detection equipment, the system cannot be applied onto a microarray format. Using these optimized conditions, both GFP and DsRed humanized reporter cell lines were able to detect the presence of allergen-specific IgE in the sera of patients and showed the expected bell-shaped dose response. Results showed agreement with clinical diagnostic methods, which confirmed the functionality and reliability of the reporter system for detecting cross-linking of patients' sera and specific allergens induced basophil activation.

Our long term aim is to develop a fully automated basophil microarray. The findings described above, especially the optimised fluorescent system using the reporter genes, were significant and available for the next stage – to be used in high throughput platforms such as a protein microarray, providing a further biological readout.

References

- Aas, K., A. Backman, *et al.* (1978). "Standardization of Allergen Extracts with Appropriate Methods - Combined Use of Skin Prick Testing and Radio-Allergosorbent Tests." Allergy **33** (3): 130-137.
- Ahmed, N., *et al.* (2013). "Identification and characterisation of IL-4 and IL-4 receptor as novel intervention targets for allergy treatment." Allergy **68**: 470-470.
- Benhamou, M., N. J. P. Ryba, *et al.* (1993). "protein-tyrosine kinase p72(syk) inbinding integrins on rat mast-cells." International Immunology **7** (2): 251-258.
- Blackley, C. (1959). "Experimental Researches on the Causes and nature of Cartarrhus Aestivus (Hayfever or Hay-Asthma)." Dawson's of Pall Mall.
- Blank U, Ra C, Miller L, White K, Metzger H, Kinet JP (1989). Complete structure and expression in transfected cells of high affinity igereceptor. Nature **337**:187-189.
- Butterfield JH, Weiler D, Dewald G, Gleich GJ (1988). Establishment of an immature mast cell line from a patient with mast cell leukemia. Leuk Res **12**:345-355.
- Craig, L., P. C. Sanschagrín, *et al.* (1998). "The role of structure in antibody cross-reactivity between peptides and folded proteins." Journal of Molecular Biology **281** (1): 183-201.
- Dastych, J., J. J. Costa, *et al.* (1991). "Mast-cell adhesion to fibronectin." Immunology **73** (4): 478-484.
- Dastych, J., J. Wyczolkowska, *et al.* (2001). "Characterization of alpha 5-integrin-dependent mast cell adhesion following Fc epsilon RI aggregation." International Archives of Allergy and Immunology **125** (2): 152-159.
- Debjit bhowmik, K. P Sampath Kumar, M Umadevi (2012). "Allergy - Symptoms, Diagnosis, Treatment and Management" Pharma Innovation **1** (3) 16-29.
- Deinhofer, K., H. Sevcik, *et al.* (2004). "Microarrayed allergens for IgE profiling." Methods **32** (3): 249-254.
- De Knop, K. J., *et al.* (2010). Component-resolved allergy diagnosis by microarray: potential, pitfalls, and prospects. Advances in Clinical Chemistry, Vol 50. G. S. Makowski. **50**: 87-101.
- Englund, P., *et al.* (2000). "Investigation into the effects of amyloid (1-42) beta-peptide upon basal and antigen-stimulated hexosaminidase and serotonin release

from rat RBL-2H3 basophilic leukemia cells." Methods and Findings in Experimental and Clinical Pharmacology **22** (9): 657-661.

Falcone, F. H., H. Haas, *et al.* (2000). "The human basophil: a new appreciation of its role in immune responses." Blood **96** (13): 4028-4038.

Franco H. Falcone, D. Z. B. F. G. (2006). "The 21st century renaissance of the basophil? Current insights into its role in allergic responses and innate immunity." Experimental Dermatology **15** (11): 855-864.

Falcone, F. H., E. F. Knol, *et al.* (2011). "The role of basophils in the pathogenesis of allergic disease." Clinical and Experimental Allergy **41** (7): 939-947.

George Pinchuk (2002). Schaum's Outline of Immunology. Edition 01. McGraw-Hill.

Gibbs, B. F., A. Rathling, *et al.* (2006). "Initial Fc epsilon RI-mediated signal strength plays a key role in regulating basophil signaling and deactivation." Journal of Allergy and Clinical Immunology **118** (5): 1060-1067.

Gilfillan, A. M. and C. Tkaczyk (2006). "Integrated signalling pathways for mast-cell activation." Nature Reviews Immunology **6** (3): 218-230.

Gillespi.E and Lichtens.Lm (1972). "Potentiation by deuterium-oxide (d2o) of allergic histamine-release - evidence for microtubule involvement." Federation Proceedings **31** (2): A748

Gonzalez-Buitrago JM, Ferreira L, Isidoro-Garcia M, Sanz C, Lorente F, Davila I (2007). Proteomic approaches for identifying new allergens and diagnosing allergic diseases. ClinChim Act **385** (1-2):21-7.

Grodzki, A. C. G., K. D. Moon, *et al.* (2009). "Fc epsilon RI-induced activation by low antigen concentrations results in nuclear signals in the absence of degranulation." Molecular Immunology **46** (13): 2539-2547.

Grundstrom, J., *et al.* (2012). "Human Cord Blood Derived Immature Basophils Show Dual Characteristics, Expressing Both Basophil and Eosinophil Associated Proteins." Plos One **7** (10).

Guerti, K., *et al.* (2010). "TRENDS IN SENSITISATION TO BIRCH POLLEN: AN INCONVENIENT TRUTH!" Acta Clinica Belgica **65**(3): 220-220.

Hamawy, M. M., C. Oliver, *et al.* (1992). "Adherence of rat basophilic leukemia (rbl-2h3) cells to fibronectin-coated surfaces enhances secretion." Journal of Immunology **149** (2): 615-621.

Hamawy, M. M., S. E. Mergenhagen, *et al.* (1993). "Aggregating the high-affinity ige receptors (fc-epsilon-ri) and adherence to fibronectin synergistically regulate

tyrosine phosphorylation of pp125(fak) in rat basophilic leukemia (rbl-2h3) cells." Journal of Immunology **150** (8): A250-A250.

Hamilton, R. G. (2010). "Clinical laboratory assessment of immediate-type hypersensitivity." Journal of Allergy and Clinical Immunology **125** (2): S284-S296.

Harwanegg, C., S. Laffer, *et al.* (2003). "Microarrayed recombinant allergens for diagnosis of allergy." Clinical and Experimental Allergy **33** (1): 7-13.

Harwanegg, C. and R. Hiller (2005). "Protein microarrays for the diagnosis of allergic diseases: state-of-the-art and future development." Clinical Chemistry and Laboratory Medicine **43** (12): 1321-1326.

Ishizaka, K. And T. Ishizaka (1967). "Identification of Gammae-Antibodies as a Carrier of Reaginic Activity." Journal of Immunology **99** (6): 1187-1198.

Jolly, P. S., *et al.* (2005). "Expression of SphK1 impairs degranulation and motility of RBL-2H3 mast cells by desensitizing S1P receptors." Blood **105** (12): 4736-4742.

Jung, I. D., H. S. Lee, *et al.* (2009). "Fc epsilon RI-mediated mast cell migration: Signaling pathways and dependence on cytosolic free Ca²⁺ concentration." Cellular Signalling **21** (11): 1698-1705.

Kalesnikoff, J., M. Huber, *et al.* (2001). "Monomeric IgE stimulates signaling pathways in mast cells that lead to cytokine production and cell survival." Immunity **14** (6): 801-811.

Kawasugi, K., P. W. French, *et al.* (1995). "focal adhesion formation is associated with secretion of allergic mediators." Cell Motility and the Cytoskeleton **31**(3): 215-224.

Kaul, S., S. Scheurer, *et al.* (2003). "Monoclonal IgE antibodies against birch pollen allergens: Novel tools for biological characterization and standardization of allergens." Journal of Allergy and Clinical Immunology **111**(6): 1262-1268.

Khan FM, Ueno-Yamanouchi A, Serushago B, Bowen T, Lyon AW, Lu C, Storek J. (2012). Basophil activation test compared to skin prick test and fluorescence enzyme immunoassay for aeroallergen-specific Immunoglobulin-E. Allergy Asthma and Clinical Immunology **8** (1):1

King, E. M., *et al.* (2007). "Simultaneous detection of total and allergenspecific IgE by using purified allergens in a fluorescent multiplex array." Journal of Allergy and Clinical Immunology **120** (5): 1126-1131.

Kobayashi, S., Yokoyama, S , Maruta, T. , Muroyama, A. , Yoshikawa, H. and Mitsumoto, Y. (2013) Attenuation of nicotine-evoked Ca²⁺ influx by antibody to the

nicotinic acetylcholine receptor $\alpha 3$ subunits in human embryonic kidney cells. *Advances in Bioscience and Biotechnology*, **4**, 9-14.

Kopec, A., *et al.* (2006). "Intracellular signaling pathways in IgE-dependent mast cell activation." *Archivum Immunologiae Et Therapiae Experimentalis* **54** (6): 393-401.

Kraft, S, Fleming, T, Billingsley, JM, Lin, SY, Jouvin, MH, Storz, P, Kinet, JP. (2005) Anti-CD63 antibodies suppress IgE-dependent allergic reactions in vitro and *in vivo* *faseb journal* 19, (5): A1447-A1447.

Kraft, S. and J. P. Kinet (2007). "New developments in Fc epsilon RI regulation, function and inhibition." *Nature Reviews Immunology* **7**(5): 365-378.

Kruger-Krasagakes, S., A. Grutzkau, *et al.* (1996). "Interactions of Immature Human Mast Cells with Extracellular Matrix: Expression of Specific Adhesion Receptors and Their Role in Cell Binding to Matrix Proteins." *Journal of Investigative Dermatology* **106** (3): 538-543.

Kukar, T., S. Eckenrode, *et al.* (2002). "Protein microarrays to detect protein-protein interactions using red and green fluorescent proteins." *Analytical Biochemistry* **306** (1): 50-54.

Ladics, G. S., J. H. M. van Bilsen, *et al.* (2008). "Assessment of three human Fc[epsilon]RI-transfected RBL cell-lines for identifying IgE induced degranulation utilizing peanut-allergic patient sera and peanut protein extract." *Regulatory Toxicology and Pharmacology* **51**(3): 288-294.

Laidlaw, T. M., *et al.* (2011). "Characterization of a novel human mast cell line that responds to stem cell factor and expresses functional Fc is an element of RI." *Journal of Allergy and Clinical Immunology* **127** (3): 815-U499.

Law, M. Morales, J. L. Mottram, L. F. Iyer, A. Peterson, B. R. August, A. (2011) Structural requirements for the inhibition of calcium mobilization and mast cell activation by the pyrazole derivative BTP2. *International Journal of Biochemistry & Cell Biology* **43**, (8): 1228-1239.

Lebrun, S. J., W. N. Petchpud, *et al.* (2005). "Development of a sensitive, colorimetric microarray assay for allergen-responsive human Ige." *Journal of Immunological Methods* **300** (1-2): 24-31.

Lin, J., N. Renault, *et al.* (2007). "A novel tool for the detection of allergic sensitization combining protein microarrays with human basophils." *Clinical and Experimental Allergy* **37**: 1854-1862.

MacGlashan, D. and S. Lavens-Phillips (2001). "Characteristics of the free cytosolic calcium timelag following IgE-mediated stimulation of human basophils:

significance for the nonreleasing basophil phenotype." Journal of Leukocyte Biology **69** (2): 224-232.

MacGlashan Donald (2008). "IgE receptor and signal transduction in mast cells and basophils." Current opinion in immunology **20**, (6): 717-723

Madsen, C. (2005). "Prevalence of food allergy: an overview." Proceedings of the Nutrition Society **64** (4): 413-417.

Mari A, Iacovacci P, Afferni C, Barletta B, Tinghino R, Di Felice G *et al* (1999). Specific IgE to cross-reactive carbohydrate determinants strongly affect the in vitro diagnosis of allergic diseases. Journal of Allergy and Clinical Immunology **103**:1005–1011.

Mari, A., *et al.* (2012). "Allergen micro-bead array for IgE detection: a new flexible multiplex system." Allergy **67**: 631-632.

Masahiko Yasuda, *et al.* (1994). "Expression and function of fibronectin binding integrins on rat mast cells." International immunology **7**(2): 251-258.

Masuda, E. S., *et al.* (1998). "Signalling into the T-cell nucleus: NFAT regulation." Cellular Signalling **10** (9): 599-611.

Mehl, A., *et al.* (2012). "Skin prick test and specific serum IgE in the diagnostic evaluation of suspected cow's milk and hen's egg allergy in children: does one replace the other?" Clinical and Experimental Allergy **42**(8): 1266-1272.

Middleton's Allergy Principles and Practice Textbook 6th edition (2003). Edited by N. Franklin Adkinson, Jr., MD, William W. Busse, MD, Bruce S. Bochner, MD, Stephen T. Holgate, MD, DSc, FRCP, FRCPE, MRC, F. Estelle R. Simons, MD, FRCPC and Robert F. Lemanske, Jr., MD. Mosby, Inc.

Murphy, K., P. Travers, *et al.* (2008). "Janeway's Immuno Biology." Garland Science **7th Edition**.

Nakamura R, Ishida S, Ozawa S, Saito Y, Okunuki H, Teshima R *et al* (2002). Gene expression profiling of Ca²⁺-atpase inhibitor DTBHQ and antigen-stimulated RBL-2H3 mast cells. Inflammation Research **51**:611–618.

Nakamura R, Uchida Y, Higuchi M, Nakamura R, Tsuge I, Urisu A, Teshima R. (2010) A convenient and sensitive allergy test: IgE crosslinking–induced luciferase expression in cultured mast cells. Allergy **65**: 1266–1273.

Nilsson, G., *et al.* (1994). "Phenotypic characterization of the human mast-cell line hmc-1." Scandinavian Journal of Immunology **39**(5): 489-498.

- Novak, N., S. Kraft, *et al.* (2001). "IgE receptors." Current Opinion in Immunology **13**(6): 721-726.
- Oka, T., M. Hori, *et al.* (2005). "Microtubule disruption suppresses allergic response through the inhibition of calcium influx in the mast cell degranulation pathway." Journal of Immunology **174**(8): 4584-4589.
- Pandey, V., S. Mihara, *et al.* (2004). "Monomeric IgE stimulates NFAT translocation into the nucleus, a rise in cytosol Ca(2+), degranulation, and membrane ruffling in the cultured rat basophilic leukemia-2H3 mast cell line." Journal of Immunology **172** (7): 4048-4058.
- Pierschbacher, M. D., *et al.* (1984). "Cell attachment to fibronectin and the extracellular-matrix." In Vitro-Journal of the Tissue Culture Association **20** (3): 255-255.
- Qu, M. S., *et al.* (2013). "A Rat Basophilic Leukaemia cell sensor for the detection of pathogenic viruses." Biosensors & Bioelectronics **43**: 412-418.
- Ra, C. S., M. Yasuda, *et al.* (1994). "Fibronectin receptor integrins are involved in mast-cell activation." Journal of Allergy and Clinical Immunology **94** (3): 625-628.
- Renault, N. K., S. R. Gaddipati, *et al.* (2011). "Multiple protein extract microarray for profiling human food-specific immunoglobulins A, M, G and E." Journal of Immunological Methods **364** (1-2): 21-32.
- Roshchina, V. V. and V. N. Karnaukhov (1999). "Changes in pollen autofluorescence induced by ozone." Biologia Plantarum **42** (2): 273-278.
- Sahara, N., R. P. Siraganian, *et al.* (1990). "Morphological-changes induced by the calcium ionophore-a23187 in rat basophilic leukemia (2h3) cells." Journal of Histochemistry & Cytochemistry **38**(7): 975-983.
- Sainte-Laudy, J., A. Boumediene, *et al.* (2007). "Use of both CD63 up regulation and IgE down regulation for the flow cytometric analysis of allergen induced basophil activation. Definition of an activation index." Inflammation Research **56** (7): 291-296.
- Sarratt, K. L., *et al.* (2004). "Platelet receptor glycoprotein VI-mediated adhesion to type I collagen under hydrodynamic flow." Annals of Biomedical Engineering **32**(7): 970-976.
- Schneider, M., *et al.* (2012). "Evaluation of natural purified peanut allergens for the use in diagnosis with basophil activation test." Allergy **67**: 542-542.
- Seltzer, J. M., G. M. Halpern, *et al.* (1984). "Correlation of Allergy Test-Results Obtained by IgE Fast, Rast, and Prick-Puncture Methods." Annals of Allergy **52**(3): 240-240.

Siraganian, R. P., A. McGivney, *et al.* (1982). "Variants of the rat basophilic leukemia-cell line for the study of histamine-release." Federation Proceedings **41**(1): 30-34.

Siraganian, RP (2003) Mast cell signal transduction from the high-affinity IgE receptor Current opinion in immunology **15** (6): 639-646.

Siraganian, R. P. De Castro, R. O. Barbu, E. A. Zhang, J. A. (2010) Mast cell signaling: The role of protein tyrosine kinase Syk, its activation and screening methods for new pathway participants. Febs Letters **584** (24):4933-4940.

Springer, T. A. (1990). "The sensation and regulation of interactions with the extracellular environment - the cell biology of lymphocyte adhesion receptors." Annual Review of Cell Biology **6**: 359-402.

Sturm, G., *et al.* (2008). "Double sensitisation in Hymenoptera venom allergy: comparison of western blot IgE binding patterns with results from skin testing, serum IgE determination, and basophil activation test." Allergy **63**: 12-13.

Sturm, G. J., *et al.* (2011). "Inconsistent Results of Diagnostic Tools Hamper the Differentiation between Bee and Vespid Venom Allergy." Plos One **6** (6).

Takagi, K., R. Nakamura, *et al.* (2003). "Application of Human Fc ϵ RI α -Chain-Transfected RBL-2H3 Cells for Estimation of Active Serum IgE." Biological & Pharmaceutical Bulletin **26** (2): 252-255.

Takahashi, A., *et al.* (1999). "Measurement of intracellular calcium." Physiological Reviews **79** (4): 1089-1125.

Taudou, G., N. Varinblank, *et al.* (1993). "Expression of the alpha-chain of human fc-epsilon-ri in transfected rat basophilic leukemia-cells - functional activation after sensitization with human mite-specific ige." International Archives of Allergy and Immunology **100** (4): 344-350.

Tedeschi, A., M. Palella, *et al.* (1994). "Ionic regulation of human basophil releasability .3. effects of na⁺ and ca²⁺ on histamine-release induced by different stimuli." Pharmacological Research **30** (3): 229-241.

Teshima R, Onose J, Okunuki H, Sawada J. (2000). Effect of Ca²⁺atpaseinhibitors on MCP-1 release from bone marrow-derived mast cells and the involvement of p38 MAP kinase activation. International Archives of Allergy and Immunology **121**:34-43.

Thomas WR, Stewart GA, Simpson RJ, Chua KY, Plozza TM, Dilworth RJ, *et al.* (1988). Cloning and expression of DNA coding for the major house dust mite allergen der p 1 in escherichia coli. International Archives of Allergy And immunology **85** (1):127-129.

Thompson, H. L., P. D. Burbelo, *et al.* (1990). "Regulation of adhesion of mouse bone marrow-derived mast-cells to laminin." Journal of Immunology **145** (10): 3425-3431.

Tomoko Horiguchi, Nahoko Ishiguro, Kazuyasu Chihara, Kazuhiro Ogi, Kenji

Nakashima, Kiyonao Sada, and Naoko Hori-Tamura (2011). Inhibitory Effect of Ac-a1' (Euterpeoleraea Mart.) Pulp on IgE-Mediated Mast Cell Activation Journal of Agricultural and Food Chemistry 59:5595–5601.

Tomoko Horiguchi, Nahoko Ishiguro, Kazuyasu Chihara, Kazuhiro Ogi, Kenji

Nakashima, Wide, L., H. Bennich, *et al.* (1967). "Diagnosis of Allergy by an in-Vitro Test for Allergen Antibodies." Lancet **2** (7526): 1105-1179.

Vinita, M. B. A. and B. A. Macher (2004). "Development of methodology to identify cell-surface glycoproteins." Glycobiology **14** (11): 1194-1195.

Vogel, L., D. Luttkopf, *et al.* (2005). "Development of a functional in vitro assay as a novel tool for the standardization of allergen extracts in the human system." Allergy **60** (8): 1021-1028.

Von Bubnoff, D., N. Novak, *et al.* (2003). "The central role of Fc epsilon RI in allergy." Clinical and Experimental Dermatology **28** (2): 184-187.

Wide, L., H. Bennich, *et al.* (1967). "Diagnosis of Allergy by an in-Vitro Test for Allergen Antibodies." Lancet **2** (7526): 1105-1107.

Yasuda M, Hasunuma Y, Adachi H, Sekine C, Sakanishi T, Hashimoto H, Ra C, Yagita H, Okumura K. (1995). "expression and function of fibronectin binding integrins on rat mast cells International Immunology **7** (2):251-8

Appendix I

Reagent	Amount
Sodium chloride (NaCl)	40g
Potassium chloride (KCl)	1g
Sodium phosphate monobasic monohydrate (NaH ₂ PO ₄ ·2H ₂ O)	325mg
Magnesium chloride hexahydrate (MgCl ₂ ·6H ₂ O)	500mg
Calcium chloride dihydrate (CaCl ₂ ·2H ₂ O)	2g
HEPES (C ₈ H ₁₈ N ₂ O ₄ S)	12g
Distilled water (H ₂ O)	To 500ml

Table 1. Composition of 500ml Tyrode's buffer stock solution (10x). All reagents were from Sigma, UK. The made up solution was stored at 4°C for at least six months.

Reagent	Amount
Tyrode's buffer stock solution (10x)	50ml
D-Glucose (C ₆ H ₁₂ O ₆)	500mg
Distilled water (H ₂ O)	200ml
3M Sodium hydroxide (NaOH)	To pH 7.45
Bovine serum albumin (BSA)	500mg
Distilled water (H ₂ O)	To 500ml

Table 2. Composition of 500ml 1x Tyrode's wash buffer (TWB). Reagents all from Sigma UK. The made-up buffer was filtered using sterile Plastipak syringes (BD, UK) and Minisart Higher Flow 0.2µm syringe filters (Sartorius Stedim Biotech, UK), aliquots were frozen stored at -20°C for up to six months (4°C for 1 week).

Reagent	Percentage (v/v)
Triton-X100	1%
Phosphate buffered saline (PBS)	99%

Table 3. Composition of Lysis buffer. Reagents all from Sigma UK. The made-up buffer was sterile filtered as in Table 2, and kept at 4°C for up to six months.

Reagent	Amount
Citric acid monohydrate (C ₆ H ₈ O ₇ ·H ₂ O)	42.5g
Distilled water (H ₂ O)	400ml
10% v/v hydrochloride acid (HCl)	To pH 1.75
Distilled water (H ₂ O)	To 500ml

Table 4. Composition of 500ml 0.4M citric acid solution. Reagents all from Fisher UK. The made up solution was stored at -20°C for up to one year (4°C for 2 weeks).

Reagent	Amount
Sodium phosphate dibasic dihydrate ($\text{Na}_2\text{HPO}_4 \cdot 2\text{H}_2\text{O}$)	8.9g
p-Nitro-N-acetyl- β -D-glucosaminide	650ml
Distilled water (H_2O)	To 400ml
0.4M citric acid ($\text{C}_6\text{H}_8\text{O}_7$)	To pH 4.5
Distilled water (H_2O)	To 500ml

Table 5. Composition of 500ml substrate solution. All reagents from Sigma UK. The made-up solution was filtered as in Table 2, and stored at -20°C for up to six months (4°C for 1 week).

Reagent	Amount
Glycine ($\text{C}_2\text{H}_5\text{NO}_2$)	15.02g
Distilled water (H_2O)	To 900ml
3M sodium hydroxide (NaOH)	To pH 10.7
Distilled water (H_2O)	To 1L

Table 6. Composition of 1L stop solution. All reagents from Sigma, UK. The made-up solution was sterile filtered as in Table 2, and frozen stored at -20°C for up to one year (4°C for 2 weeks).

Appendix II

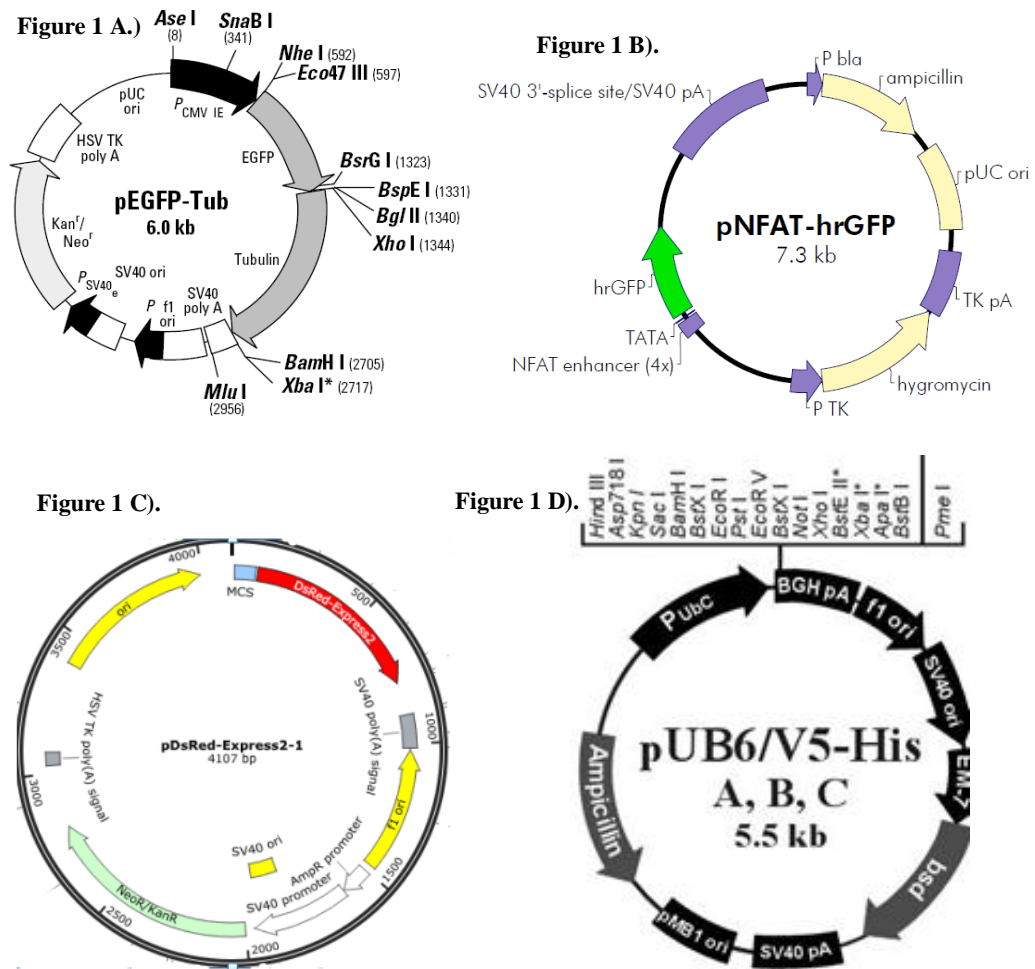


Figure 1. Plasmid maps. A) pEGFP-Tub (Stratagene, USA). B) pNFAT-hrGFP (Stratagene, USA). C) pDsRed-Express2-1 (Clontech, USA). D) pUB6/V5-His A (Invitrogen, Paisley, UK), plasmid encodes blasticidin S resistance was used as a base vector for the construction of the new plasmid.

Appendix III

Oligo Name	Sequence (5'-3')
DsRed + EcoRI(F)	ATATAATAGAATTCACCATGGATAGCACTGAGAACGTCATCAAG
DsRed + XhoI(R)	ATATTTAATCTCGAGCTACTGGAACAGGTGGTGGCGG
NFAT + BglII(F)	ATAATTAAGATCTGCAGAACTGTGAATGCGCAAACC
NFAT + EcoRI(R)	ATAATTAATGAATTCGAGCTCGGTACCCGG

Table 7. Primers for synthesis of pNFAT-DsRed.

Reagent		Concentration	Volume (µl)	Final concentration
PCR Gold buffer		10x	10	x 1
MgCl ₂ solution		25mM	18	4.5 mM
dNTP		10mM	2	0.2 mM
Forward primer		10µM	3.2	0.32µM
Reverse primer		10µM	3.2	0.32µM
DNA template	pNFAT-hrGFP	1.6µg/µl	1.2	0.02µg/µl
	pDsRed Express2-1	2.8µg/µl		0.04µg/µl
Ampli Tag Gol		5U/ml	0.8	40U/µl
H ₂ O (RNase/Dnase free)		-	61.6	-

Table 8. PCR reaction components. A master mix of the constituents minus the DNA templates was made up for both reactions including control, and all reagents were from Promega UK.

Reagent		Concentration	Volume (µl)	Final concentration
H buffer		10x	20	1x
Acetylated BSA		1mg/ml	20	100ng/µl
H ₂ O (RNase/Dnase free)		-	116	-
NFAT-PCR products		118.8ng/µl	40	24ng/µl
DsRed-PCR products		187.6ng/µl	40	38ng/µl
Enzymes for NFAT	BglII	10U/ µl*	2	100mU/µl
	EcoRI	12U/ µl	2	120mU/µl
Enzymes for DsRed	EcoRI	12U/ µl	2	120mU/µl
	XhoI	10U/ µl	2	100mU/µl

Table 9. Setting up restriction sites for inserts. Restriction reactions were carried out in 200µl of each in PCR tubes, 1U (unit) of each restriction enzyme is capable of digesting 1µg of DNA at 37°C for 1 hour.

Reagent		Concentration	Volume (µl)	Final concentration
Ligase buffer		10x	2µl	1x
T4 DNA ligase		3U/µl	0.5	75mU/µl
pUB6/V5-His A+BglII/EcoRI		36ng/µl	8	14ng/µl
NFAT + BglII/EcoRI		118.8ng/µl	6	36ng/µl
H ₂ O (RNase/Dnase free)		-	3.5	-

Table 10. Reaction in 20µl in PCR tubes.

Reagent	Concentration	Volume (μ l)	Final concentration
D buffer	10x	10	1x
NFAT-pUB6/V5-His A	567.4 ng/ μ l	6	34 ng/ μ l
XhoI	10 U/ μ l	0.5	250 mU/ μ l
EcoRI	12 U/ μ l	0.5	300 mU/ μ l
Acetylated BSA	10mg/ml	5	500 g/ μ l
H ₂ O (RNase/Dnase free)	-	78	-

Table 11. Restriction digestion of NFAT- pUB6/V5-His A in 100 μ l in PCR tubes.

Reagent	Concentration	Volume (μ l)	Final concentration
Ligase buffer	10x	2 μ l	1x
T4 DNA ligase	3U/ μ l	0.5	75mU/ μ l
NFAT-pUB6/V5-His A +EcoRI/XhoI	43.2ng/ μ l	9.2	20ng/ μ l
DsRed +EcoRI/XhoI	36ng/ μ l	4.8	9ng/ μ l
H ₂ O (RNase/Dnase free)	-	3.5	-

Table 12. Ligation of DsRed insert and NFAT-pUB6/V5-His A vector in 20 μ l in PCR tubes.

